BEHAVIOUR OF DEMOUNTABLE SHEAR CONNECTORS IN COMPOSITE STRUCTURES

By

Naveed Ur REHMAN

Submitted for the Degree of
Doctor of Philosophy

Faculty of Engineering and Informatics
University of Bradford

2017

ABSTRACT

NAVEED UR REHAMAN

BEHAVIOUR OF DEMOUNTABLE SHEAR CONNECTORS IN COMPOSITE STRUCTURES

Keywords: Demountable shear connectors, Push off tests, Shear capacity, Ductility, Stiffness

The research presented in this thesis is to evaluate the feasibility of demountable shear connectors as an alternative to welded shear connectors in composite structures through push off tests and composite beam tests. Push off tests were conducted to examine the shear strength, stiffness and ductility of demountable shear connectors in composite structures. The experimental results showed that demountable shear connectors in composite structures have very similar shear capacity to welded shear connectors.

The shear capacity was compared against the prediction methods used for the welded shear connections given in Eurocode 4 and AISC 360-10 and the methods used for bolted connections in Eurocode 3 and ACI 318-08. It was found that the AISC 360-10 and ACI 318-08 methods overestimated the shear capacity in some cases. The Eurocode method is conservative and can be utilised to predict the shear capacity of demountable connectors in composite structures.

The experimental studies of two identical composite beams using demountable shear connectors and welded shear connectors showed very similar moment capacity. However, the specimen with demountable shear connectors was more ductile compared to the welded specimen. The

experimental study suggests that the methods available in Eurocode 4 and BS 5950 for predicting moment capacity and mid span deflection can be adopted for composite beam with demountable shear connectors.

In addition, a finite element analysis of push off test and beam test with demountable shear connectors was also conducted for parametric studies and results are used to evaluate the behaviour of composite structures.

ACKNOWLEDGMENTS

It is a pleasure to thank those who made this thesis possible. First and foremost, I would like to thank **Allah**; our Lord, the All-Knowing, the Almighty, the most Merciful and the most Compassionate.

I would like to express my sincere appreciation and special thanks to my supervisors **Prof. Dennis Lam, Dr. Xianghe Dai and Prof. Ashraf Ashour,** for their excellent supervision, constant encouragement and approachability throughout the period of this work. I deeply appreciate **Prof. Lam** and **Dr. Dai** for their great support, help and guidance.

Special thanks go to the **Laboratory staff** who were always ready to help in times of needs. I would like to particularly thank **Steve Robinson**, **Owen Baines** and **Michael Procter** for their expert advice and help during the experimental investigation.

I am forever deeply grateful to my dear family, **my parents, my wife and my daughters and my sisters** for their moral support, help and understanding during the whole period of this work.

I take the chance to thank and express my gratitude to all **my friends** for their encouragement, advice and understanding.

I do appreciate the grant and financial support provided by the EPSRC and the University of Bradford to finish this research.

Finally, I would like to thank everybody who was involved in this work as well as expressing my apology to those I did not mention in this acknowledgment.

Declaration

I declare that this thesis is the result of my own work. No part of this thesis has been submitted to any other University or other educational establishment for a Degree, Diploma or other qualification.

Naveed UR Rehman

Contents

List of Figures

List of tables

Chapter 1
Introduction

1.1 Background

Steel-concrete composite structures have been used in the construction industry since the early 1920s. They are a cost-effective construction system for multi-storey buildings and bridges owing to the composite action between steel beams and concrete slabs. Initially, solid concrete slabs and steel beams were used to construct these composite structures. A temporary formwork is required for casting the solid concrete slabs, which is a time-consuming process, however, the invention of profiled metal decking has replaced the need of temporary formwork.

In the present time, profiled metal decking is very common in construction practice and used as a permanent formwork during concrete casting. This method of construction is very economical and allows speedy construction. Once the concrete has been casted, the profiled metal decking acts compositely to form a composite concrete slab and provides an additional tensile reinforcement in the composite concrete slab. The profiled metal decking reduces the weight of the concrete in composite floor system due to its geometry and thus there is less load on the foundations.

The profiled metal decking is laid down on the steel beam before the casting of concrete. It is attached to the steel beam through welded shear connectors to achieve the composite action between the steel beam and the composite concrete slab as shown in Figure 1-1. The shear connectors are welded to the flange of a steel beam through the profiled metal decking and embedded

in the concrete slab. These welded shear connectors in composite beams transfer the longitudinal shear forces between the composite concrete slab and the steel beam. Besides transferring shear forces these shear connectors also resist the uplift forces across the interface of the composite concrete slab and steel beam due to the bending action.

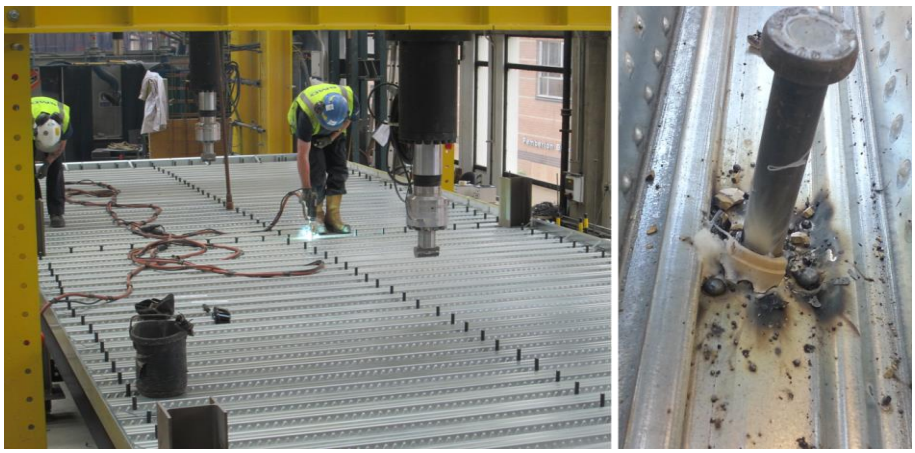

Figure 1-1 Composite construction with welded shear connectors

Although welded shear connectors are quicker to install during construction but a problem arises when this type of composite structure comes to the end of their design life. These welded shear connectors make it almost impossible to separate the composite concrete slab and steel beam. Therefore, composite structures are demolished completely using traditional methods of demolition. This demolition process costs a huge amount of energy, produces a carbon footprint and generates waste. This method of demolition does not allow the re-use of the structural parts especially the steel beam and composite concrete slabs unless the material is recycled to make a new product. The recycling process again consumes a lot of energy and produces a carbon footprint too. This process of demolishing and recycling is not very environment friendly.

There is a need to develop a system of demolition which enables to separate the structural components and re-use them without going into recycling process. Therefore, demountable shear connectors are considered as an alternative to welded shear connectors in this research. Experiments are conducted to investigate the structural behaviour and demountability of composite structures using demountable shear connectors through push off tests and full scale composite beam tests.

The research presented in this thesis highlights the future of these demountable shear connectors as an alternative to welded shear connectors as these experiments provide strong evidence that demountable shear connectors can be installed and demounted easily before and after experimental testing. The steel beam can then be reused without going into the recycling process to achieve a sustainable construction.

1.2 Research significance

The increasing rate of carbon emissions in the environment has highlighted the issue of sustainability during the last few decades. The main emphasis has been placed on environmental issues such as carbon emissions, sustainability, energy, deconstruction and waste management by re-using the used materials as much as possible.

During the present period, sustainability is a priority for the government as is lowering carbon emissions into the environment and the re-use of materials effectively. This will enable future generations to have a greener environment and the resources to fulfil their needs. The government has a policy to reduce greenhouse gases by 2050 by up to 50-85% (Allwood et al. 2010) and is

trying to encourage industries to adopt sustainable policies. The Government also has taken some measures like, landfill tax, climate change levy and thermal performance requirement of buildings to make the environment more sustainable and avoid any dangerous climate change.

The construction industry has a great impact on the environment, especially in consuming resources and generating waste by demolition of structures. The construction industry in Europe consumes over 70,000 million tonnes of material each year and generates 250 million tonnes of waste every year through demolition.

More sustainable building techniques are being considered in the construction industry to reduce waste and use material more efficiently without the need for recycling. Therefore demount-ability or deconstruct-ability of the structural parts especially in composite flooring systems is very important as it make it possible to reuse the structural parts without going into the recycling process.

It is very difficult to repair or replace a damaged composite concrete slab or a steel beam if the shear connectors are welded to the steel beam. The welded shear connectors used in composite structures make it impossible to reuse the steel beam without the input of significant energy for its recycling (structural modification) process.

In current practice the steel beams are recycled. The dismantling and recycling process requires a significant amount of energy and produces carbon emissions into the environment. Its environmental and economic impacts have led to research for possible reuse of steel beams and

deconstruction techniques. Therefore, demountable shear connectors are considered and tested to see if they are a viable alternative to welded shear connectors.

Demountable shear connectors have received very little attention in the published literature and in the construction industry as they are rarely used. This might be due to the lack of detailed research and design specification rules compared to welded shear connectors. There is some research on single and double nut bolt systems using high strength friction grip (HSFG) bolts (Dedic and Klaiber, 1984) and (Kwon et al. 2010), that is carried out using a solid concrete slab for rehabilitation of old non-composite structures, however HSFG bolted connectors are not very cost effective. Therefore, in this research a new form of demountable shear connector without an embedded nut is proposed as an alternative to welded shear connectors in a composite structure with profiled metal decking.

Currently, there has been no research carried out to investigate the ductility, strength and stiffness of this type of demountable shear connector without an embedded nut in the profiled metal decking composite concrete slab. Therefore, to understand the behaviour of demountable shear connectors in composite structures, there is a need to carry out experimental and numerical studies. This will help to establish an accurate behaviour of demountable shear connectors in composite structures.

1.3 Applications of demountable shear connectors

The design of demountable shear connectors has emerged to facilitate the future re-use of steel beams without going into the recycling process, as at

present the steel beams are usually recycled. The steel beams do not degrade with use unless they have major damage and can be used after dismantling the composite structure.

The replacement of welded shear connectors by demountable shear connectors has the major advantage of being easy to separate the steel beam from the composite concrete slab as shown in Figure 1-2. The use of demountable shear connectors will make the construction more sustainable with the effective re-use of the steel beam and concrete slabs. This type of construction will help us to reduce the carbon emissions, energy and time consumed in the process of demolition, disposal and recycling (Akinade et al. 2016).

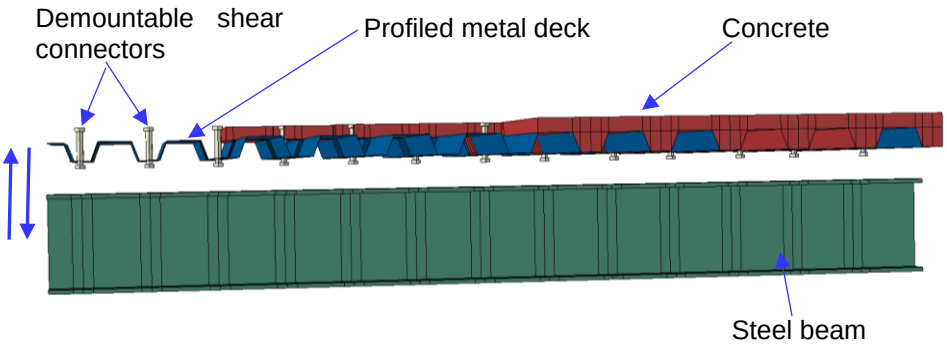

Figure 1-2 Application of demountable shear connectors

Faster construction methods can be developed by using demountable shear connectors. Demountable shear connectors can be installed into the pre-drilled hole in the top flange of a steel beam and profiled metal decking. The construction cost of using demountable shear connectors might be higher at the construction stage compared to welded shear connectors but in terms of

faster construction and longer life cycle may prove more economically and sustainable.

The main application and reason of using demountable shear connectors is to promote sustainability in composite structures by allowing the structural components (especially steel beam) to be reused at the end of its structural design life without recycling. The demountable shear connectors will also make it possible to make any change to the design for other uses (adaptability) of the structure. These demountable shears will also help to replace the damaged structural parts easily.

1.4 Aims and objectives of the research

The main aim of this research is to investigate the behaviour of demountable shear connectors in composite structures and to check the viability and feasibility of demountable shear connectors without an embedded nut in a composite concrete slab with a steel beam. The objectives are as follow;

- To develop a system which allows the demountability of a composite concrete slab from a steel beam.
- To check the ductility, stiffness and shear capacity of the demountable shear connectors in a composite beam with a profiled metal decking slab through push-off tests.
- To carry out simply supported composite beam tests with demountable and welded shear connectors in a profiled metal decking composite concrete slab for a direct comparison of moment capacities, slip capacities between the steel beam and profiled metal deck composite concrete slab and mid span deflections.

- To develop a FE model to carry out parametric studies.

1.5 Research Methodology

Three different methods were used to evaluate the structural behaviour of demountable composite structures i.e., experimental study, finite element analysis and design method analysis.

In the experiments two different techniques were adopted, push off tests and full scale composite beam tests. The Push off test technique as described in Eurocode 4 for welded shear connectors was used to perform the experimental work and establish a load slip behaviour of demountable shear connectors in composite structures. Full scale composite beam tests were carried out using demountable shear connectors and welded shear connectors.

Advanced 3D finite element models of the push off tests and the demountable composite beam were developed to conduct a parametric study using the validated FE models for push off tests and beam tests.

1.6 Scope of the Thesis

The scope of this research is limited to the behaviour of demountable shear connectors in a composite beam with profiled metal decking slab.

Chapter 2 presents the review of previous research related to composite beams with profiled sheeting. The literature review focuses on experimental and numerical studies of bolted shear connectors in composite structures along with some discussion of standard push off test arrangements and design equations to calculate the shear connector resistance.

Chapter 3 is about the experimental results of the push off tests. It also presents the push test set up, instrumentation, loading procedure, material tests, failure patterns and summary of push test results.

A discussion of the push off test results and the effect of different parameters on the behaviour of a demountable shear connector is discussed in chapter 4.

Chapter 5 presents the experimental investigation of a full scale composite beam and companion push off tests and their results.

Chapter 6 presents a finite element model (FEM) of the push off tests and composite beam test with profiled sheeting using ABAQUS. After selecting a suitable modelling approach, the developed FEM is validated against the experimental test results conducted in this study, in terms of the strength, ductility and failure modes of the shear connectors. A parametric study using validated FEM of push off test and composite beam test is also reported in this chapter.

Chapter 7 presents the design coded methods for composite structures. A comparison between the push off tests and different strength prediction code equations is presented in this chapter. A comparison and calculations of moment capacity and deflection are also presented in this chapter.

Finally, Chapter 8 presents conclusions drawn from experimental and numerical studies and gives recommendations and suggestions for future work.

Chapter 2
Literature Review

2.1 Introduction

This chapter summarises the leading research that has been conducted on the behaviour of welded and demountable shear connectors in composite structures. The focus however is on demountable shear connectors, as they are the main subject of this thesis. At present, there are no design rules available for demountable shear connectors in any design code. Therefore, design equations for welded shear connectors available in different design codes are discussed in this chapter and later used to evaluate the shear strength of demountable shear connectors.

2.2 Composite beams

Composite construction started in the early 1920s utilising steel and concrete, in the 1950s and 1960s composite construction technique was commonly adopted for bridges and in multi-storey buildings (Ollgaard et al 1971). A steel beam, shear connectors and reinforced concrete slabs are the major components of a composite beam. Traditionally, solid concrete slabs have been used with steel beams to construct a composite beam. But after the invention of profile metal decking, that became more popular in modern composite construction.

Composite construction with profiled metal decking is more cost effective in terms of saving labour costs and construction time as it reduces the amount of concrete required for the concrete slab and minimises the self-weight of the concrete slab. Therefore, these days composite beams are constructed with profile metal decking in the construction industry. This is a new

development in the construction industry and is used as permanent formwork for concrete. This enhances the tensile strength of the concrete slab after the curing period of concrete. Profiled metal decking can be placed either parallel or perpendicular to the steel beam according to the requirement of the buildings as shown in Figures 2-1 and 2-2. Shear connectors are then used to attach the profiled metal decking to the steel beam which are welded through the profiled metal decking to steel flange.

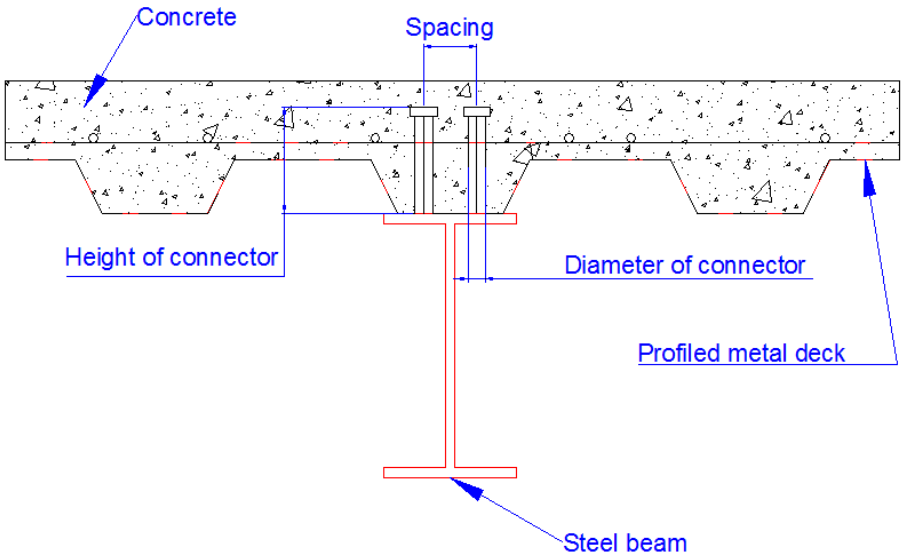

Figure 2-1 Composite beam with profiled metal deck (oriented parallel to steel beam)

Concrete and steel perform much better when they act together compared to the performance of each individual one. The fact that each material is used to take advantage of its positive attributes makes composite steel-concrete construction very efficient and economical. Concrete is good for resisting compression and steel is good for resisting tension (Hegger and Goralski 2006). So their composite action is developed by the use of welded shear connectors to transfer the longitudinal shear forces at the interface of a steel beam and composite concrete slab.

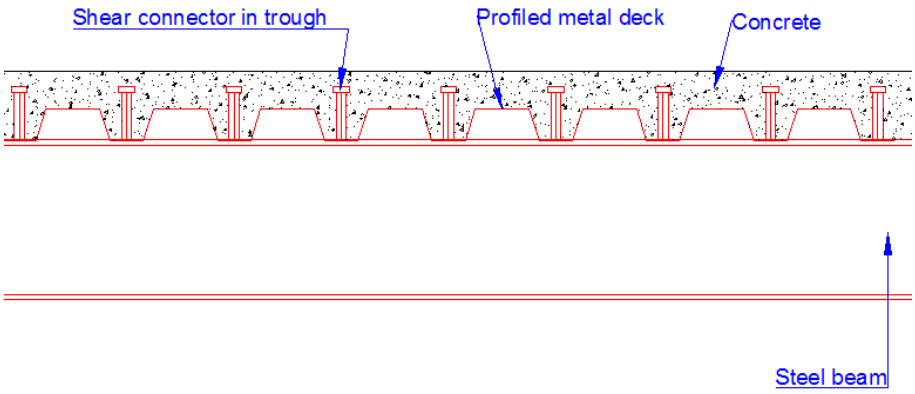

Figure 2-2 Composite beam with profiled metal decking (oriented perpendicular to steel beam)

2.2.1 Welded shear Connectors

There have been a number of different types of mechanical shear connectors developed to replace welded headed studs since the 1930s including the bar, spiral, T section, perfobond rib shear connectors, H shape and channel connectors. Before the invention of profiled metal decking, the channels shear connectors were used to a large extent in composite beams.

However, the headed shear connectors are the most popular and commonly used in today's construction industry due to the through deck welding process and available design rules for welded headed shear connectors. Also, they prevent the uplifting of the composite slab and resists the shear force equally in all directions due to its circular shape. A typical head shear connector can be seen in Figures 2-3 it is welded to the top flange of the steel beam with profiled metal decking.

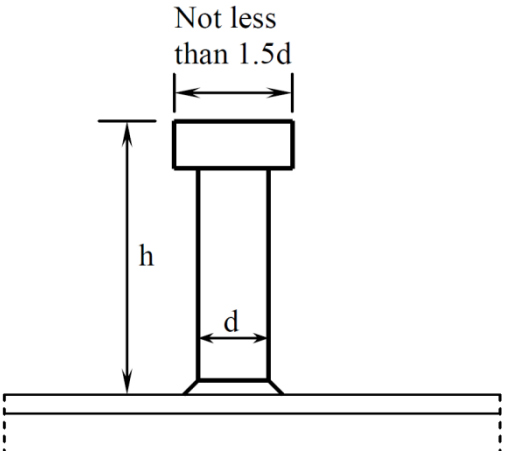

Figure 2-3 Welded headed shear connector

These headed shear connectors are available in different diameters ranging from 13-25 mm and lengths ranging from 50-250 mm. According to Eurocode 4, the minimum ultimate tensile strength should be 450 MPa, they should have an elongation of 15% and the head diameter should be 1.5 times the shank diameter (d).

2.3 Push test technique

Most of the research carried out on welded shear connectors using the technique of push tests. Eurocode 4 (2004) provides a simple procedure for push tests and equations to predict the shear capacity of welded shear connectors in composite beams. However, the push test details provided in Eurocode 4 are for welded shear connectors in solid concrete slabs. Mottram and Johnson (1990) suggested a geometric adjustment to the standard push-off test for welded headed shear connectors in profiled metal decking composite concrete slabs.

The push test technique is well established and used to determine the shear capacity of a shear connector. It is used as a substitute for a full scale composite beam test to reduce the time and cost related to a full scale test. A

standard push test is described in Eurocode 4 (2004) for welded shear connectors and its layout is presented in Figure 2-4. The push test specimen consists of two identical concrete slabs attached to a steel beam. The slabs should be casted in a horizontal position and cured in open air. The specimen is loaded vertically downward until it fails.

However, this standard push test is not designed for specimens with a profiled metal decking and there is no guidance available in any code of practice for testing composite concrete slabs with demountable shear connectors. The performance of composite concrete slabs with profiled metal decking is checked by using empirical equations as described in Eurocode 4. The comparability of the push test and beam test is also a debatable issue and generally, it is considered that the push test results are conservative compared to the beam test (Hick 2009). The characteristic resistance P_{RK} can be taken as the minimum failure load per shear connector from three nominal identical push tests and reduced by 10% according to EC4.

Ductility is another major factor in composite construction. The ductility of a shear connector can also be determined from push tests, this depends on the slip capacity at the interface of the steel beam and the composite concrete slab. The slip capacity is the maximum slip measured at the characteristic load level as shown in Figure 2-5. Shear connectors are considered to be ductile if the connectors have sufficient deformation capacity.

According to Eurocode 4, the shear connector will be considered to be ductile if the slip reaches 6 mm. A large plastic deformation of the headed shear connector is characterized as good ductile behaviour. On the other hand if

the shear connector does not fulfil the limit of 6mm it is characterized as brittle behaviour of the headed shear connector with very little plastic deformation.

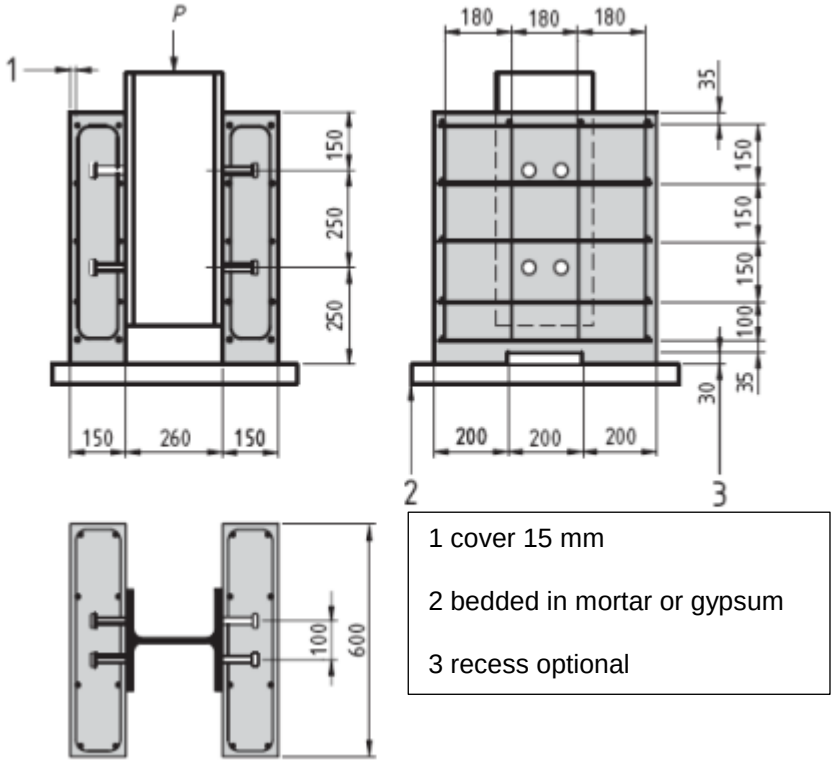

Figure 2-4 General Arrangements of standard push test in Eurocode 4

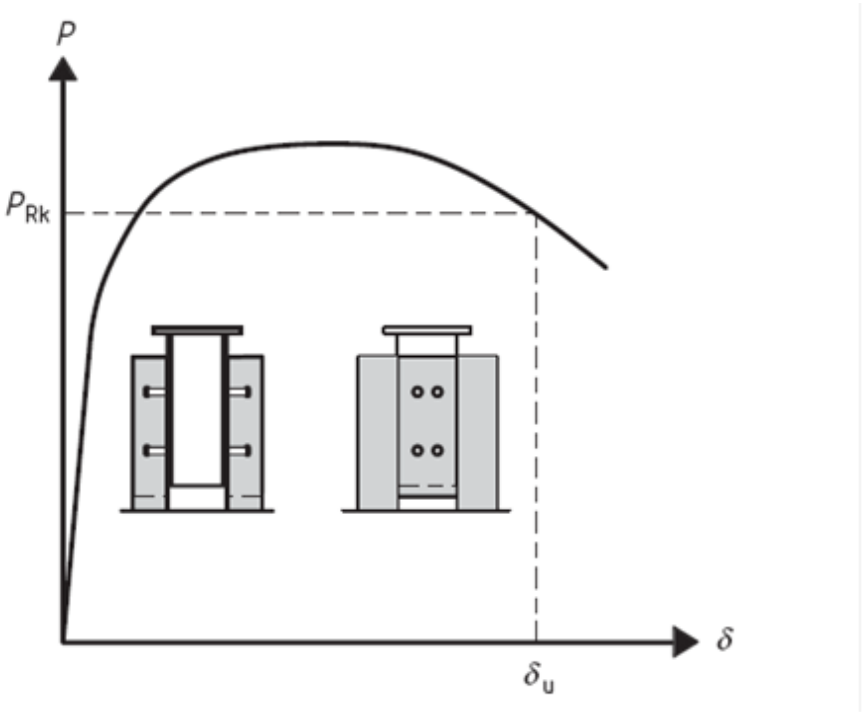

Figure 2-5 Determination of slip capacity according to Eurocode 4

2.4 Design equations for shear strength

There is no design guide available for demountable shear connectors in a composite construction. Therefore, the design equations available for welded shear connectors are considered for demountable shear connectors. A short overview of some of the available design codes for the shear strength of welded shear connectors in composite construction is presented in this section.

The strength of the shear connection is mainly influenced by shank diameter, height and tensile strength of the connector, compressive strength and the elastic modulus of concrete. The shear forces are resisted by bending, tension or shearing at the root of the shear connection. The connector's root transmits the horizontal shear forces acting at the interface, while the head prevents the uplifting of the slab. The plastic deformation occurs after reaching the ultimate strength of the stud.

2.4.1 AISC 360-10

In America, the AISC 360-10 (2010) specification has included provisions for composite construction since 1936. In 1961, the shear capacity of headed shear connectors in solid slabs appears in the AISC 360-10 specification as a function of stud diameter and concrete strength. In 1978, a new provision was added for profiled metal decking in composite construction.

AISC 360-10 adopted the Ollgaard's proposed equation to work out the shear strength of headed welded shear connectors. The strength of a shear connection in a solid slab is a function of concrete strength and the cross-sectional area of a connector. The upper limit in this equation is the tensile strength of the connector as shown in equation 2-1. In AISC 360-10, the shear connector position and group factors were also considered to determine the nominal shear capacity (Q_n).

$$Q_n = 0.5\, A_{sc}\sqrt{f_c^{/} E_c} \quad < \quad R_g R_p A_{sc}\, F_u \qquad (2\text{-}1)$$

In these expressions

R_g = is group effect factor and

R_p = is position effect factor.

A_{sc} = is the cross sectional area of a connector

F_u = is minimum tensile strength of a shear connector respectively.

$f_c^{/}$ = is the compressive cylinder strength and modulus of elasticity of the concrete (Psi).

E_c = is the modulus of elasticity

2.4.2 Eurocode 4

Eurocode 4 provides two different equations one for solid concrete slab and one equation for using metal profiled decking.

Equations for solid slab

In Europe, the provisions for composite construction as part of Eurocode were included in the1990s and followed by the issuing of Euro-code 4 more recently. BS EN 1994-1-1:2004 Eurocode 4 clause 6.6.3.1, provides two equations as described in equations 2-2 and 2-3 for shear resistance of welded headed shear connectors in solid slabs. The design resistance (P_{Rd}) should be determined from the minimum value from these two equations. These two equations are related to two main failure modes, concrete cone failure and shear connector failure.

$$P_{Rd} = \frac{0.29\alpha d^2 \sqrt{f_{ck} E_c}}{\gamma_v} \quad (2\text{-}2)$$

$$P_{Rd} = 0.8 f_u \frac{\pi d^2}{4} \frac{1}{\gamma_v} \quad (2\text{-}3)$$

Where $\alpha = 0.2\left(\frac{h_{sc}}{d} + 1\right) \leq 1.0$, for $3 \leq \frac{h_{sc}}{d} \leq d$ and $\alpha = 1$, for $\frac{h_{sc}}{d} > 4$

d = is the shear connector shank diameter in mm

h_{sc} = is the shear connector height

f_u = is the shear connector ultimate tensile strength

f_{ck} = is the characteristic cylinder compressive

E_c = is modulus of elasticity of concrete

γ_v = is the partial safety factor for shear resistance (γ_v = 1.25)

Equations for profiled metal Deck

The shear strength of a shear connector embedded in a profiled metal deck composite concrete slab is based on a reduction factor (K_t) and used with the shear strength of a shear connector in a solid concrete slab as presented in equation 2.4.

$$P_r = K_t \ P_{Rd} \tag{2-4}$$

$$K_t = \frac{0.6}{\sqrt{n_r}} \frac{b_o}{h_p}\left[\frac{h_{sc}}{h_p} - 1\right] \leq 1.0 \tag{2-5}$$

$$K_t = \frac{0.7}{\sqrt{n_r}} \frac{b_o}{h_p}\left[\frac{h_{sc}}{h_p} - 1\right] \leq 1.0 \tag{2-6}$$

The reduction factor (K_t,) depends on the direction of metal profile decking laydown at the steel flange. Either it is parallel or transverse to the direction of the steel beam as illustrated in Figures 2-6 and 2-7 and in equations 2-5 and 2-6 respectively.

bo = is effective width of the slab
nr = is the number of stud per rib
hp = is the height of the metal profiled decking
hsc = is the height of the shear connector

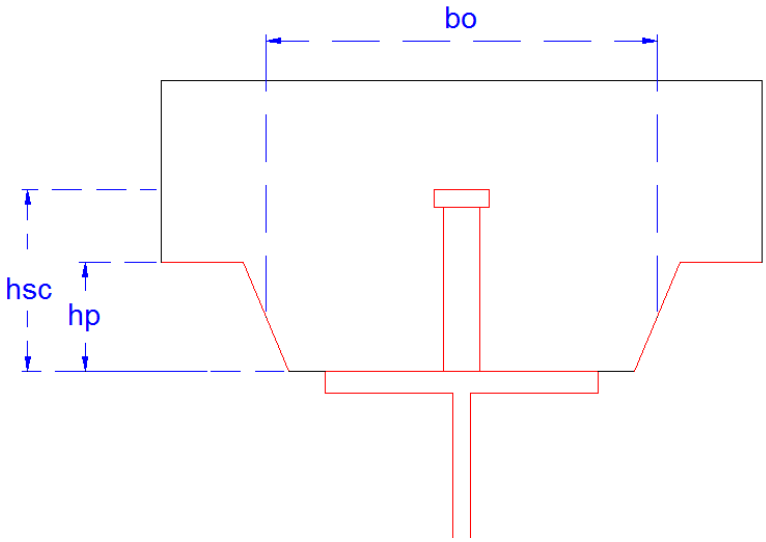

Figure 2-6 Composite beam with metal profile decking parallel to steel beam (EC4)

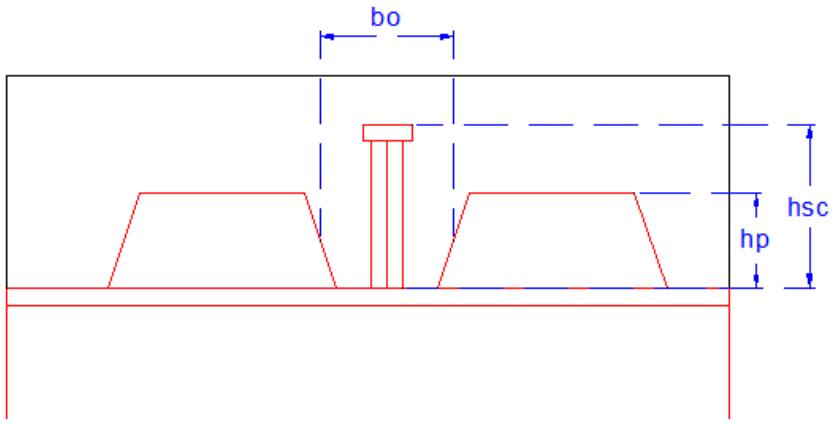

Figure 2-7 Composite beam with metal profile decking transverse to steel beam (EC4)

2.5 Previous studies on welded shear connector

A comprehensive experimental study was carried out using push test and composite beam tests techniques by Ollgaard et al (1971) and Grant et al (1977) to investigate the behaviour of welded shear connectors in composite structures. Ollgaard et al (1971) investigated the behaviour of welded shear connectors in solid concrete slabs. Whereas, Grant et al (1977) adopted the profiled metal deck in their extensive research studies and made a modification to the equation proposed by Fisher (1970) by including the height of the shear connector.

In 1984, Hawkins and Mitchell (1984) examined the effect of reverse loading and monotonic loading on the behaviour of welded shear connectors in composite structures through push tests and observed that the shear capacity was 17% lower than monotonic loading. Similar push tests were conducted by Jayas and Hosain (1988) in 1988 using the same profiled metal decking height to examine the shear resistance of welded shear connector in composite structures under monotonic loading. The authors of later studies modified the equation propose by former authors and propose two new equations depending on the factor for density and different deck's heights.

A comparison of push test results and full scale beam test results was carried out by Hicks (2009) in 2009. Six push out tests and two full scale composite beam tests using composite concrete slabs with profiled metal decking were performed. It has been observed that the load-slip performance measured in the push tests were well below the beam test results.

The research carried out on welded shear connectors using the push test technique from the past few decades is well summarised by Pallares and Hajjar (2010) in 2010. In present era, most of the research on welded shear connectors is often being conducted using finite element analysis (FEA). Lam and Ellobody (2005) developed the finite element model to study the behaviour of welded shear connectors in solid concrete slabs with different connector's height and different concrete strengths. Whereas Ellobody and Young (2006) and Mirza and Uy (2010) developed the FE model for composite beam profiled metal decking.

A 3D finite element model was developed by Qureshi and Lam (2012) for composite structure to study the post failure behaviour of welded shear connectors in a trapezoidal deck and FE results were compared with experimental push tests. It was concluded that the shear connection is highly influenced by concrete strength and the maximum stresses in the concrete are near the bottom half of the connector which causes concrete failure around the connector. It has been noted that as the load increases the steel deck tends to separate from the concrete and become deformed eventually as the load approaches the failure load.

2.6 Previous studies on bolted shear connectors

Literature shows that the research on demountable shear connectors is very limited. Although, the research on the use of bolted shear connectors started in 1960s, 1970s and 1980s by Dallam (1968), Marshall et al. (1971), Dedic, Klaiber (1984) and Hawkins (1987). In the previous mentioned research works, high strength friction grip bolts in solid concrete slabs were investigated by using the push out technique and a full scale composite beam test. These bolts were often placed inside the concrete slab through the post installation method after casting the concrete slab. However, the post installation method is a time-consuming technique.

The push test technique as shown in Figure 2-8 was used by Dallam to investigate the behaviour of high strength grip bolts ASTM A325 and A449 in composite structures with three different diameters of 12.7, 15.9 and 19.9 mm and a height of 102mm. The formwork of installing the bolts was not very clear. The zero slip was reported at the serviceability limit stage and the

ultimate shear strength was almost double compared to welded studs. Ultimate shear resistance and slip capacity could have been affected by using this unusual way of casting the concrete slab and holding the bolts.

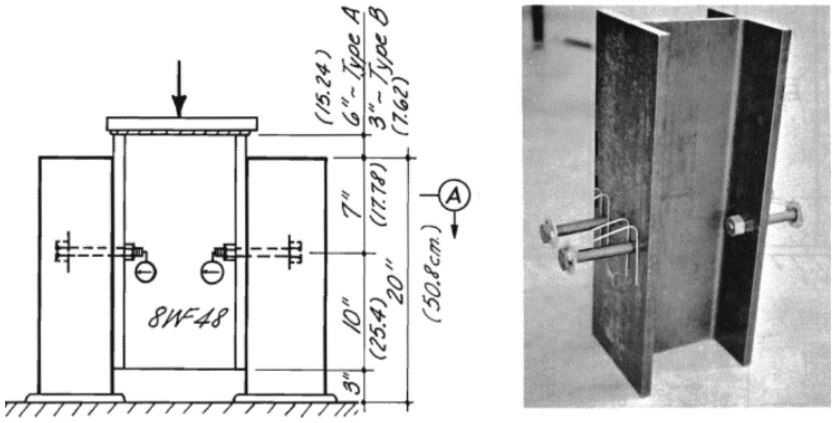

Figure 2-8 Friction grip bolt push out tests (Dallam, 1968)

The push test as presented in Figure 2-9 and a full scale composite beam technique with solid concrete slabs was adopted by Marshall et al (1971) to investigate the behaviour of friction grip bolts. Bolts were preloaded before testing the specimen to achieve the friction coefficient of 0.45. It was reported that only one out of eleven tests push test specimens failed due to the concrete and the slip can be restricted to zero by using the friction coefficient of 0.45 at the working load and using adequate partial shear connection. But the calculation of friction coefficient was not very clear to follow.

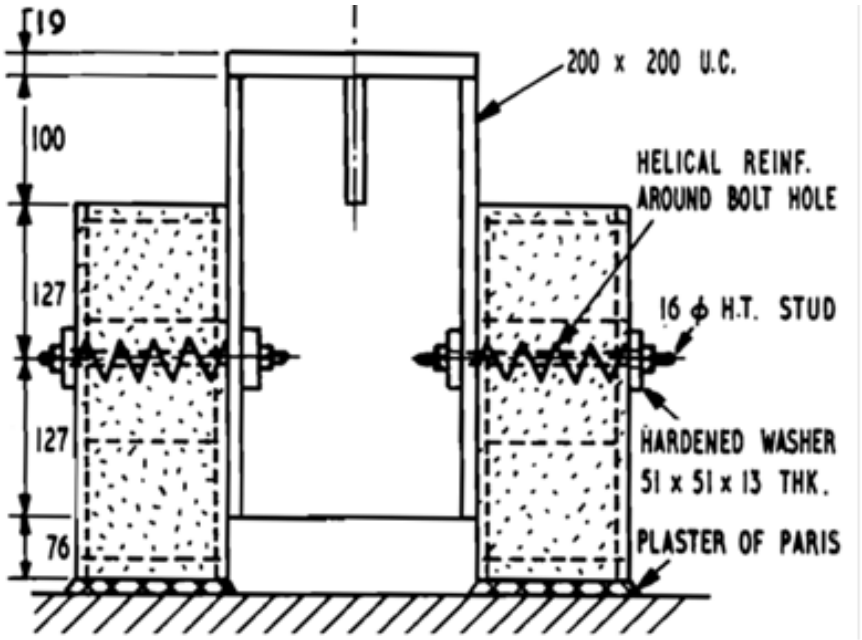

Figure 2-9 Push test technique (Marshall et al, 1971)

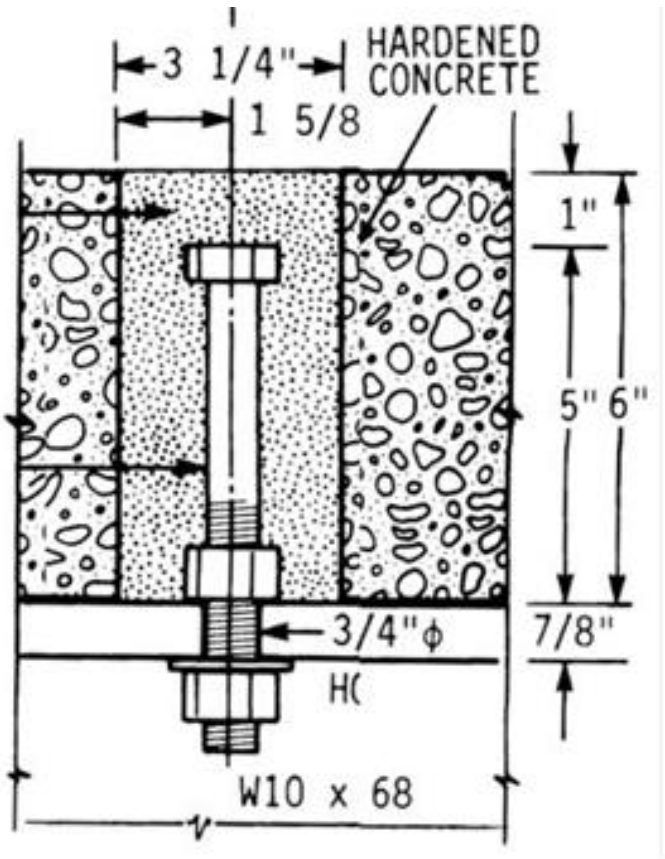

Figure 2-10 Bolted shear connector with embedded nut (Dedic and Klaiber, 1984)

The research carried out by Dedic, and Klaiber [1984] was mainly focused on the rehabilitation work using post installed high strength bolts to strengthen

the non-composite old structures as illustrated in Figure 2-10. Push test technique was used to study the behaviour of high strength bolts (A325) with embedded nuts. It showed that the behaviour of these bolts with a single embedded nut was very similar to the welded studs in terms of shear resistance and slip capacity.

Research without embedded nuts in solid concrete slab was conducted by Hawkins (1987) and investigations were carried out using shear and tensile forces to test the anchor bolt with a diameter of 19 and 25 mm. But the installation of bolts was not very clearly explained. It was reported that the anchor bolts can achieve 80% shear resistance without an embedded nut compared to welded studs. But shear stiffness was just 15%.

A post installation method was adopted by Kwon et al (2010) to strengthen old non-composite bridges as shown in Figure 2-11. This work was a continuation of Schaap's (2004) research work. ASTM A325 friction grip bolts with an embedded nut were examined under static and fatigue loading. But the demountability of the composite beam was not considered in this research. Research showed that post installation of bolted shear connectors using A325 and A449 bolts is possible and is a viable method to convert the non-composite structure into a composite structure.

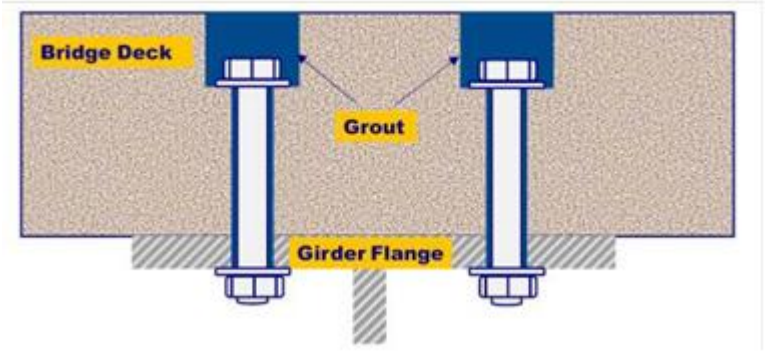

Figure 2-11 High tension friction grip bolt in composite beam test [Kwon, 2010]

Mirza et al. (2010) and Pathirana et al. (2012) carried out research on demountability using blind bolts. It was found that blind bolts behaved in a very similar way to welded headed connectors in terms of stiffness and strength but the blind bolt had a relatively brittle behaviour. Whereas, Henderson et al. (2012) discussed different types of shear connection under dynamic loading and reported that the removable shear connectors had very similar stiffness and strength as welded headed studs in composite beams.

Post installation method was also adopted by Atei et al (2016) and Liu et al (2015 and 2016) to investigate the behaviour of high strength friction grip bolts in geo-polymer concrete slab and normal concrete slabs respectively through push tests and full scale composite beam test techniques. Lee and Bradford (2013) conducted two push-out tests according to EC4, using M20, G-8.8, bolted shear connectors with a single embedded nut while Ataei and Bradford (2014) tested pretension bolts with precast solid concrete slabs for demountable connection system.

Pavlovic et al. (2013) studied the M16 Gr8.8 bolted shear connector through push-off tests in solid slabs and compared the experimental results with welded headed shear studs in solid slabs. It was found that the Gr8.8 bolted

shear connectors with a single embedded nut achieved about 95% of the shear resistance under static loads, but the stiffness reduced by 50% compared to the welded headed stud. However, their research was only focussed on solid slabs with high strength bolts.

A full scale composite beam test with profile metal decking was reported by Moyniah and Allowed (2014) using Gr 8.8 M20 bolts as shear connector in composite beam. In this research an embedded nut was used to attach the profiled metal decking with the steel beam. In their beam test, the number of shear connectors were not equally distributed throughout the composite beam. In half of the specimen single connector was used in each trough of the profiled metal decking and pair of connectors were used in other half of the specimen. This is not a common practice in construction industry. It was concluded that demountable connectors can be used as they behave in a similar way to welded connectors and the slabs can be taken off easily. The oversized hole of 24mm diameter was drilled through the top flange of a steel beam. The authors have not carried out any push tests to evaluate the ductility, shear capacity and stiffness of the Gr 8.8 M20 bolts under maximum shear capacity.

There is very little research on demountable shear connectors in a profiled metal decking composite concrete slab. Researchers have used high strength bolts and an embedded nut to hold the profiled metal decking with steel beam. However, it appears that no research has reported the behaviour of demountable shear connectors in composite structures with profiled metal decking and utilised demountable connectors without embedded nuts.

2.7 New demountable shear connector

The new demountable shear connector as shown in Figure 2-12 considered in this research study to investigate the load slip behaviour of demountable shear connector in composite structures with a profiled metal decking composite concrete slab. This research is focused on using the new demountable shear connector without an embedded nut as the connector is shaped to hold the profiled metal deck to the steel beam.

This new demountable shear connector is the traditional Nelson headed stud transformed into the shape of a shear connector. It is different from the high strength A449 bolt, A325 bolt, blind bolt and Gr 8.8 M20 bolts in terms of tensile and yield strength. It is also a cost-effective shear connector compared to other connectors.

The behaviour of his type of demountable shear connector was also investigated by Lam and Saveri (2012) and Dai et al (2015) to observe the load slip behaviour of demountable shear connectors without embedded nuts in RC solid slabs through push tests and finite element analysis techniques to assess its potential and suitability in terms of replacing the welded headed shear connectors in solid concrete slabs.

Figure 2-12. Traditional Nelson stud (left) and transform shape as a demountable shear connector (right)

2.8 Concluding remarks

An overview of past and ongoing research on shear connectors in composite beams is presented in this chapter. The main attention is given to demountable shear connectors due to main subject of this thesis. From the literature review, it was found that previous research on demountable connectors was carried out using high strength bolts with solid concrete slabs utilising embedded nuts.

There is a little research carried out with profiled metal decking composite concrete slabs as few composite beam tests were reported with demountable shear connectors using the Gr 8.8 M20 bolts and embedded nuts but no push tests have been conducted using demountable shear connectors with profiled metal deck composite concrete slabs. Therefore, this thesis will

mainly focus on the behaviour of demountable shear connectors without embedded nuts in a profiled metal decking composite structure.

Chapter 3
Push off tests

3.1 Introduction

This chapter describes the main experimental work carried out to investigate the feasibility of demountable shear connectors in composite structures as an alternative to welded shear connectors using the push off test technique. This chapter includes the push off test arrangements, test parameters, instrumentation, material testing and test results. The main parameters investigated in this experimental study were the number of shear connectors per trough of profiled metal decking, different types of reinforcement cages, concrete compressive strength and the diameter of shear connectors.

3.2 Description of test specimens

The push-off test arrangements adopted in this experimental study were very similar to that described in Eurocode 4 (2004). The detailed layouts of specimens are shown in Figures 3-1 to 3-4, which clearly show a single layer of the steel reinforcement cage (S), double layers of the steel reinforcement cage (D), and the modified steel reinforcement cage (M). Two demountable shear connectors per trough and a single demountable shear connector per trough were adopted for the tested specimens.

Each push off test specimen consists of two identical composite concrete slabs with profiled metal decking, a steel beam and demountable shear connectors. Richard Lees Rib E60 type profiled metal decking with the steel grade of S350 was used for the composite concrete slab as shown in Figure

3-5. The depth (h_p) of the profiled metal decking is 60 mm, the average width (b_o) is 145 mm and the sheeting thickness (t) is 0.9 mm.

The type and details of demountable shear connectors is presented in Figures 3-6 and 3-7. The nominal height of the demountable shear connectors in concrete for all specimens was 120 mm. Shear connectors with a shank diameter of 19mm embedded in the concrete slab were adopted in specimens S1, S2, D1, D2 and M1 to M6. The remaining connector's length includes a collar (diameter 17mm) passing through the flange of the steel beam and a threaded portion with a diameter of 16mm. Specimens M7 and M9 have a demountable connector with a shank diameter of 22mm and a collar with a threaded portion that has a diameter of 20mm. In specimen M8 and M10 a pair of M20 Gr 8.8 bolts were used in each slab.

The dimension of the composite concrete slab is 610 x 510 x 150 mm. Two slabs in each push off test are connected through demountable shear connectors, as shown in Figure 3-7 through a predrilled hole in a steel section of UB 203 x 203 x 52. The tested specimens were divided into 7 groups as presented in Table 3-1. In each group, two replicate specimens were tested. These specimens cover different reinforcement arrangements, concrete compressive strengths, connector diameters and types.

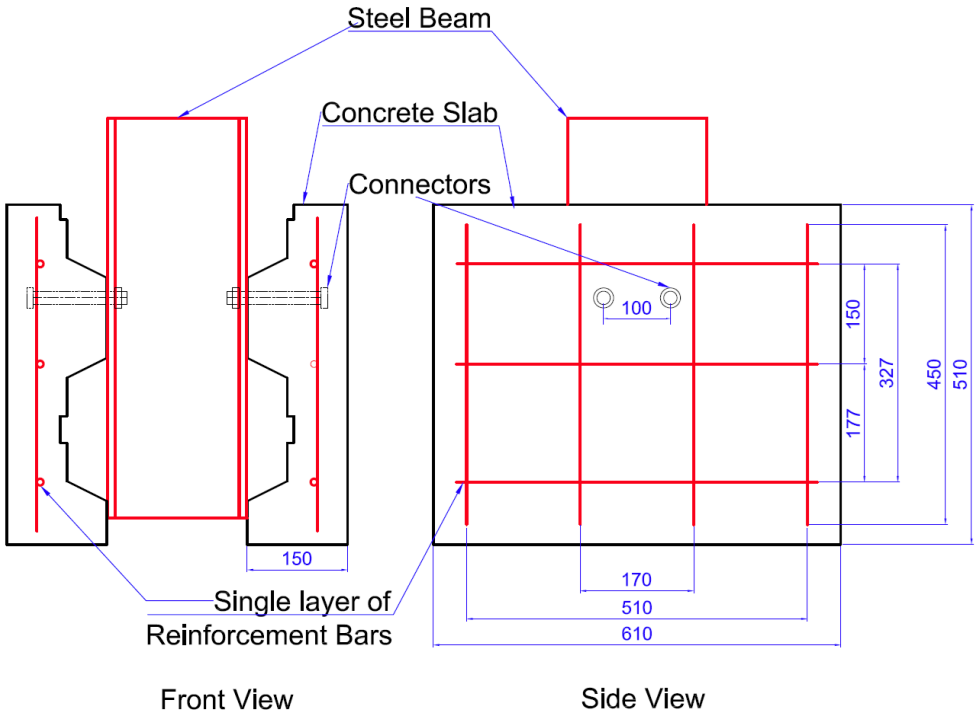

Figure 3-1 Push-off test specimen with single layer reinforcement cage (S) and two connectors per trough

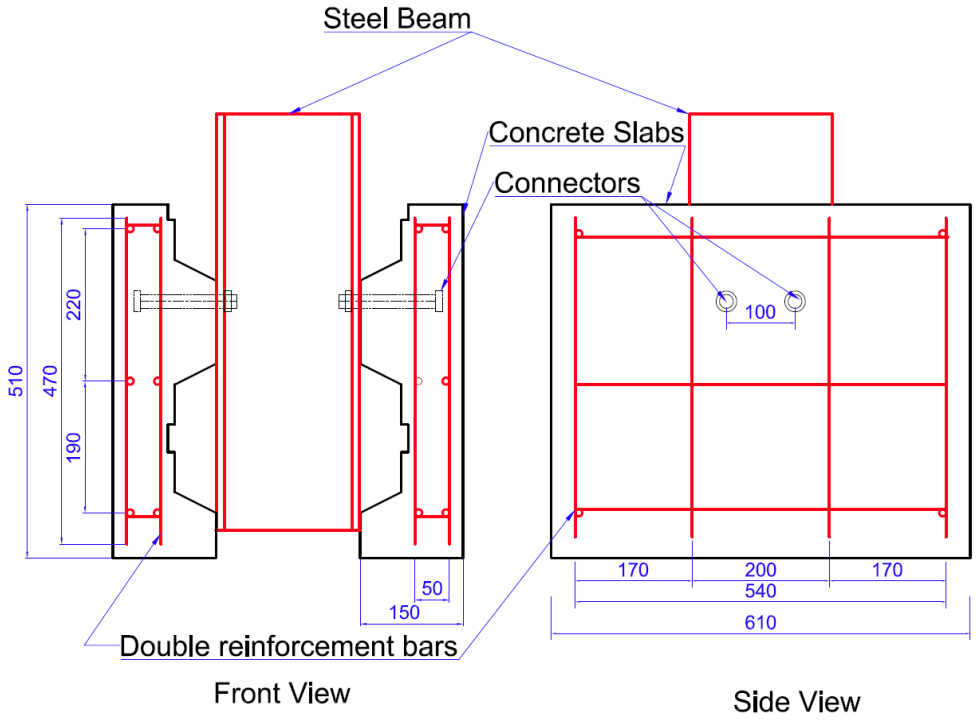

Figure 3-2 Push-off test specimen with double layer reinforcement cage (D) and two connectors per trough

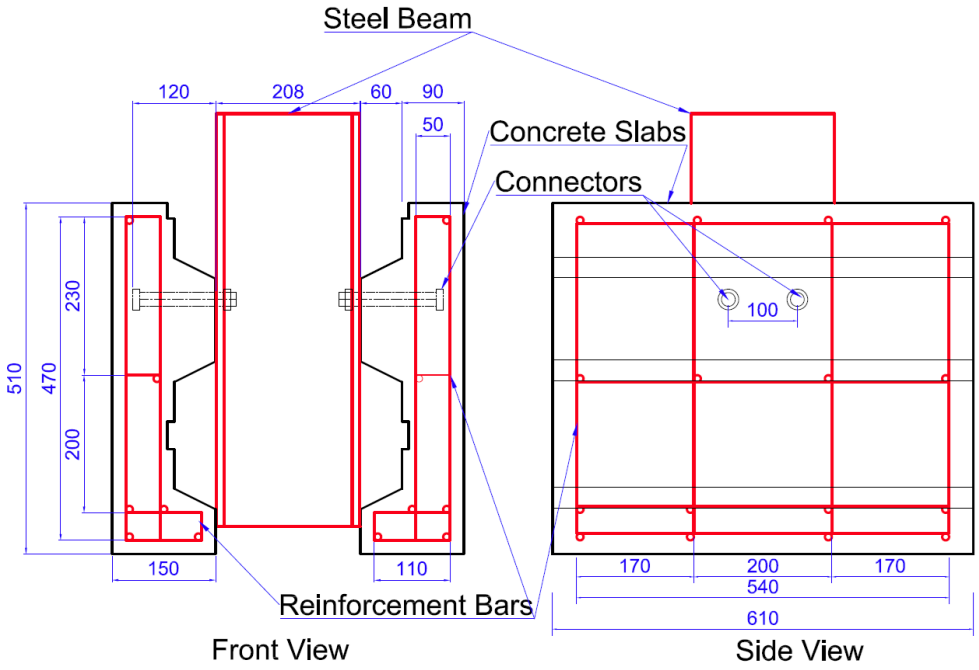

Figure 3-3 Push-off test specimen with modified reinforcement cage (M) and two connectors per trough

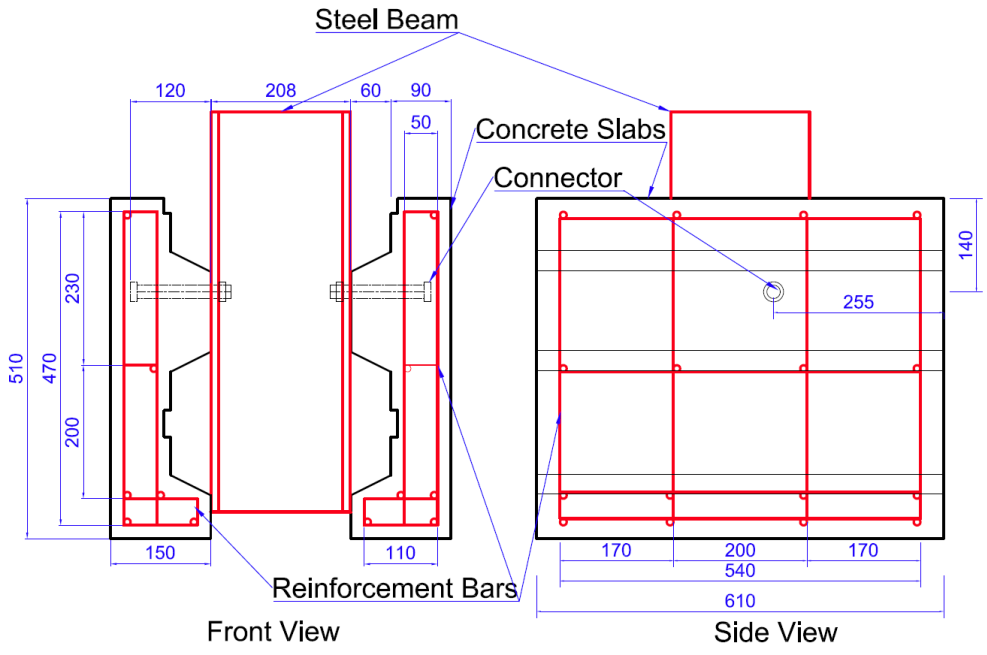

Figure 3-4 Push-off test specimen with modified reinforcement cage (M) and one connector per trough

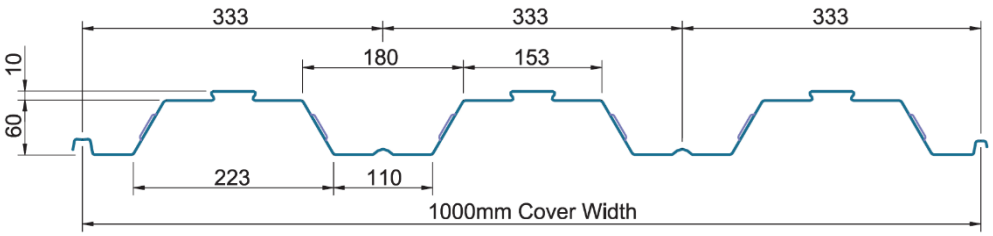

Figure 3-5 Richard Lees Rib E60 type profiled metal decking

Figure 3-6. Different type of demountable shear connectors

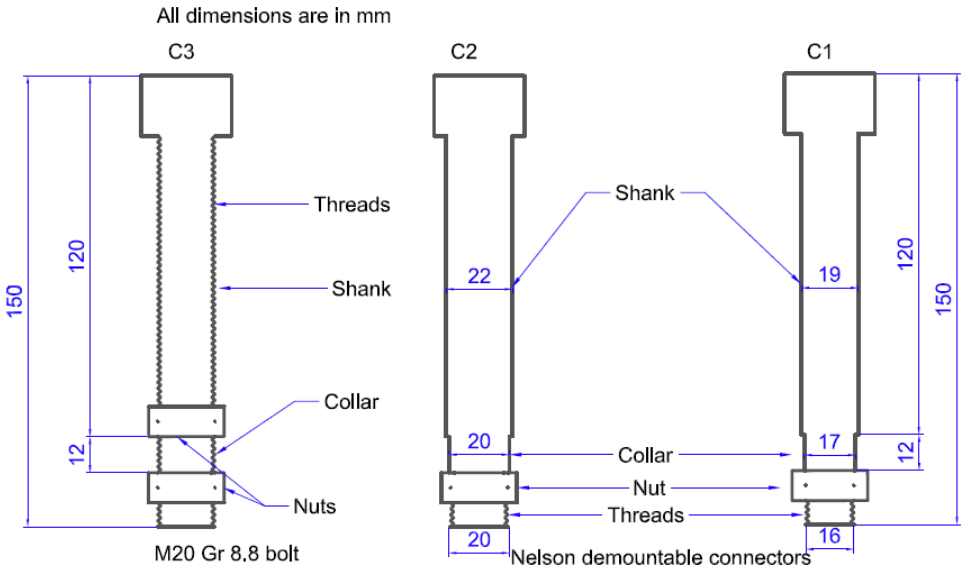

Figure 3-7 Detail of demountable shear connectors

3.3 Specimen preparation

The holes for the demountable shear connectors were drilled in the steel beam flanges and profiled metal decking before the specimens were assembled. The clearance between the hole in the steel flange and collar (shank) of the shear connector bolt was 1 mm and 1mm clearance was provided for the hole in the profiled metal decking. The profiled metal decking was put into the wooden module and fixed using demountable shear connectors as shown in Figures 3-8 to 3-10.

The steel reinforcement cage was laid down on top of the metal profiled decking and concrete was poured on it at the University of Bradford laboratory. The concrete was compacted using a vibrating poker and then, finished with level surfacing. Test specimens were covered using polythene sheeting to prevent moisture loss. All composite concrete slabs for each group specimen were casted horizontally with designated concrete mixes.

Figure 3-8 Arrangement of pair connector per trough before casting

Figure 3-9 Arrangement of single connector per trough before casting

Figure 3-10 Arrangement of Gr 8.8 M20 bolts before casting

Ribbed steel bars with a diameter of 10mm were used for the reinforcement cage. The transverse spacing between two connectors was 100mm in the specimens with two demountable shear connectors per trough. The minimum distance between the shear connectors and the vertical reinforcement cage bar was 50mm. After curing the concrete, the composite concrete slabs were attached to the steel flange using the demountable shear connectors and nut. The nuts were tightened to 100 N-m using a torque. This value is used by Moyen and Allwood (2014) to tighten the nuts for demountable shear connectors in composite structure.

3.4 Summary of tested specimens

A number of parameters including reinforcement cage type, concrete compressive strength, type of shear connectors and number of shear connectors per trough of profiled metal decking were used to study the behaviour of demountable shear connectors in composite structures. Table 3-1, describes all the investigated parameters utilised in this study.

Table 3-1 Test parameters of push off test specimens

	Test Specimen ID	Connector type	Reinforcement arrangement ID	Average concrete cube strength (MPa)	Shear connectors per slab
Group1	S1	C1	S	57.5	2
	S2	C1	S	54.5	2
Group2	D1	C1	D	29.4	2
	D2	C1	D	28.5	2
Group3	M1	C1	M	43.4	2
	M2	C1	M	40.9	2
Group4	M3	C1	M	36.2	1
	M4	C1	M	30.5	1
Group5	M5	C1	M	55.7	2
	M6	C1	M	58.1	2
Group6	M7	C2	M	22.7	2
	M8	C3	M	19.2	2
Group7	M9	C2	M	50.8	2
	M10	C3	M	51.3	2

3.5 Material Testing

The material properties of reinforcement bar, profiled metal decking and shear connectors were obtained from the tensile coupon test. The concrete compressive strength was obtained from cube tests.

3.5.1 Concrete testing

Four different concrete mixes were adopted in the push off test specimens to compare the effect of concrete strength to the shear connector behaviour. All concrete mixes were designed according to British Standards (BS 8500). The concrete mixes for different specimens are presented in table 3-2.

Table 3-2 Proportions of different contents in concrete mix design

Group	Cement (kg)	Water (kg)	Fine aggregate (kg)	Coarse aggregate 10mm (kg)	Coarse aggregate 20mm (kg)
Group1	527	195	597	354	707
Group2	286	195	724	395	780
Group3	405	195	640	380	760
Group4	286	195	724	395	780
Group5	527	195	597	354	707
Group6	271	195	690	408	816
Group7	527	195	597	354	707

The compressive strength of the concrete slab was determined through cube tests and by taking the average value (see table 3-1) of six cube (100x100x100 mm) specimens casted at the same time as the concrete slabs. After concrete casting, all specimens (concrete slabs and cubes) were covered with polyethylene sheets for curing and tested on the test day.

3.5.2 Reinforcement steel bar testing

The mechanical properties of the steel reinforcement bars were established through tensile tests on three specimens of steel bar. These tests were conducted using the Instron universal testing machine as shown in Figure 3-11. The test procedure adopted for coupon test is listed below:

Step-1: Preparation of specimen

1.1 Specimens are prepared according to BS EN ISO 6892-1 (2009) for shear connectors and profile decking as shown in figures 3-11, 3-12 and 3-13. The reinforcement bar specimens of diameter of 10 mm are cut into the length of 250mm.

1.2 Clean the surface and measure the original cross-sectional area (three cross sections, using mean values to minimize error measuring as recommended in BS EN ISO 6892-1), based on cross-sectional shape, thickness, width.

1.3 Mark the original gauge length, parallel length and strain gauge positions

(strain gauges locate at mid-length, on both sides of the specimens) by using fine lines or scribed lines; measure the gauge length and parallel length.

1.4 Clean the surface again and then attach strain gauges in the longitudinal direction of the specimens.

Step-2: Set-up

2.1 Clamp the upper grip end of a specimen, ensure the specimen is vertical or in line with the load applying direction.

2.2 Set loading and strains to zero and then clamp the other end of the specimen, ensure the grip lengths at both ends are equal, then set the extension to zero.

Step-3: Pre-load

3.1 Apply tensile load to the specimen, which is lower than a value corresponding to 5% of the expected yield strength.

3.2 Observe the loading, extension and strains, ensure the loading versus extension curves are correct, and that the strain gauges work well.

3.3 Unload the specimen, set the loading, extension and strains to zero.

Step-4: Loading procedure

4.1 The loading rate of the tensile tests is controlled by crosshead separation rate at a velocity equal to the desired strain rate multiplied by the parallel length; in the initial range from the beginning up to the end of yielding, the separation rate is 0.005mm/s (estimated strain rate is 0.00007/s); after the yielding stage, this rate increases to a constant value of 0.2mm/s (estimated strain rate is 0.00286/s) according to the specified strain rates given in BS EN ISO 6892-1.

4.2 Stress relaxation is applied twice during the tensile tests achieved by pausing the loading for 100s each time to obtain the static material properties; the first holding point is during the yielding stage and the second holding point is near the ultimate strength.

4.3 Stop the test after entire fracturing of the specimen; extract test data of load and strains; remove the two pieces from the testing machine, measure the gauge length and parallel length again as well as the fractured cross-sectional area.

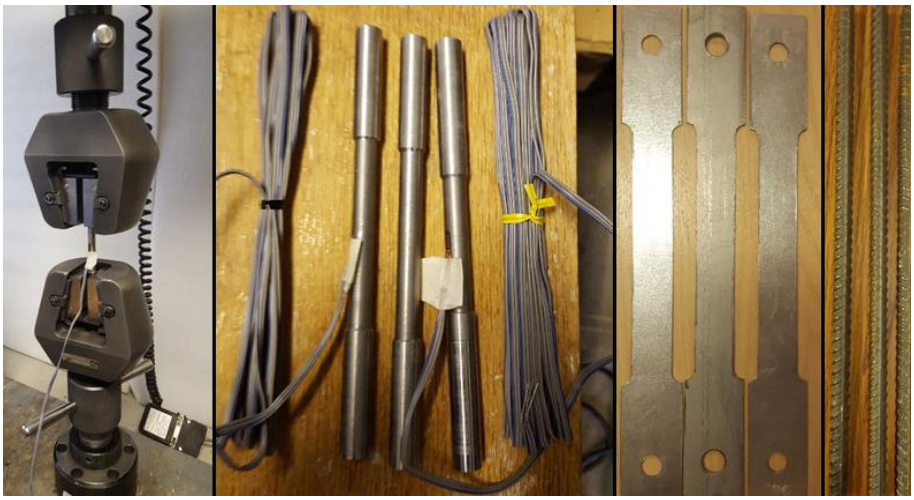

Figure 3-11 Coupon test set up and material (Instron machine, shear connectors, profiled metal decking and steel bars), (left to right)

Table 3-3 illustrates the value obtained from coupon test. The young modulus was found 210 GPa. The average ultimate yield stress was found to be about 610N/mm2 as shown in Table 3-3.

Table 3-3 Mechanical properties of steel reinforcement bars

Test Ref	Yield strength (N/mm2)	Ultimate strength (N/mm2)	Cross Sectional area (mm2)
SB1	525.5	610.5	78.5
SB2	525.8	612.3	78.5
SB3	523.1	608.1	78.5
Mean	524.8	610.0	78.5

3.5.3 Shear connector testing

Three coupon tests were conducted to determine the mechanical properties of the demountable shear connector of type C1 and C3. Shear connectors were machined into dog-bone shape (as shown in Figure 3-11 and 3-12) according to Annex D in BS EN ISO 6892-1 (2009) to carry out coupon tensile test using Instron machine. Figure 3-11 depict the sample dimensions designed for the shear connectors. In the parallel segment, connector diameter was machined to be 10mm while in the gripped portion it was 12mm.

The results of the coupon tests are presented in Tables 3-4 and 3-5. The young modulus was found 210 GPa.

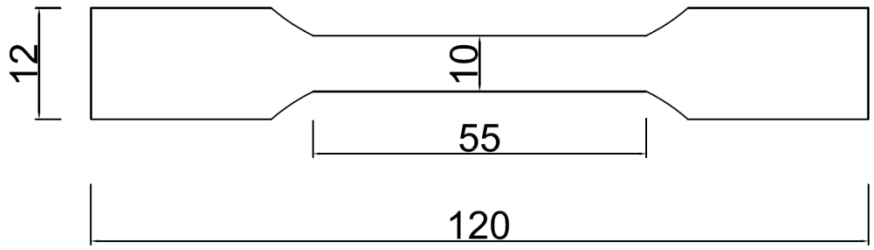

Figure 3-12 Dimensions of connector's tensile coupon specimen (mm)

Table 3-4 Mechanical properties of type C1 connectors

Test Ref	Yield strength (N/mm2)	Ultimate strength (N/mm2)	Cross Sectional area (mm2)
C1_1	425.5	509.2	78.5
C1_2	430.8	509.5	78.5
C1_3	433.1	511.0	78.5
Mean	429.8	510.0	78.5

Table 3-5 Mechanical properties of type C3 Gr 8.8 M20 bolt

Test Ref	Yield strength (N/mm2)	Ultimate strength (N/mm2)	Cross Sectional area (mm2)
C3_1	675.5	762.8	78.5
C3_2	680.8	769.9	78.5
C3_3	683.1	773.6	78.5
Mean	679.8	768.8	78.5

3.5.4 Profiled metal decking testing

Three coupon tests were conducted with three flat pieces taken from metal profiled decking to determine the mechanical properties. The coupon specimens were designed and tested in accordance with BS EN ISO 6892-1 (2009) as shown in Figures 3-11 and 3-13. Table 3-6 illustrate the yield strength and ultimate strength obtained from coupon test of the profiled metal decking. The young modulus was found 195 GPa.

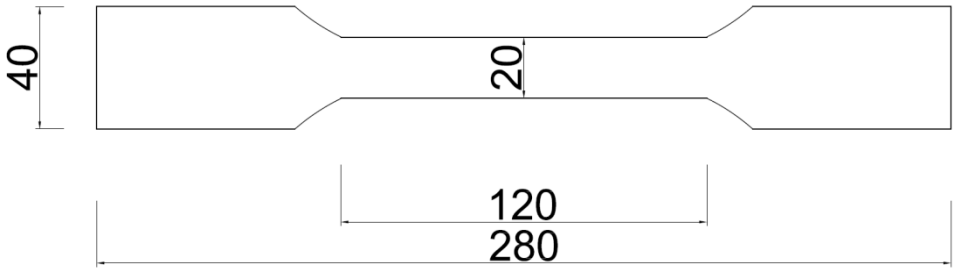

Figure 3-13 Coupon dimension for profile metal decking (mm) in accordance ISO 6892-1

Table 3-6 Mechanical properties of metal profile decking

Test Ref	Yield strength (N/mm2)	Ultimate strength (N/mm2)
PD1	388.8	466.7
PD2	385.8	465.9
PD3	385.1	463.6
Mean	386.6	465.4

3.6 Test setup and instrumentation

3.6.1 Test setup

Figure 3-12 shows the complete test setup of the push off test including the positions of the linear variable displacement transducer and the hydraulic jack. The specimen was placed on the testing rig under the centre of a 100 tonne hydraulic jack. A spreader steel plate was used between the hydraulic jack and the steel section to distribute the load evenly on the specimen.

3.6.2 Displacement recording

In each test, eight linear variable displacement transducers (LVDTs) were installed at the top of the steel beam and concrete slabs, as shown in Figures 3-14 and 3-15 to measure the vertical displacements, which subsequently used to calculate the relative slip between the steel beam and the concrete slab. The readings of load and displacement were recorded by the data logging system. The stored data was transformed into spreadsheet and used for further analysis of the tests.

3.6.3 Loading procedure

During the test, the push-off load was applied through a hydraulic jack with a constant amplitude increment rate of 5 KN with a time interval of 5 minutes until the push-off load reached 40% of the predicted failure load. The predicted failure load was determined using Eurocode 4 equations available for welded shear studs in a composite beam. After this stage the load-control method was changed to the displacement-control method to avoid any sudden failure, in which a constant increment rate of 0.2 mm/min was adopted until the failure of the specimens was observed, i.e. rapid reduction of the load capacity.

Figure 3-14 Push off test set up

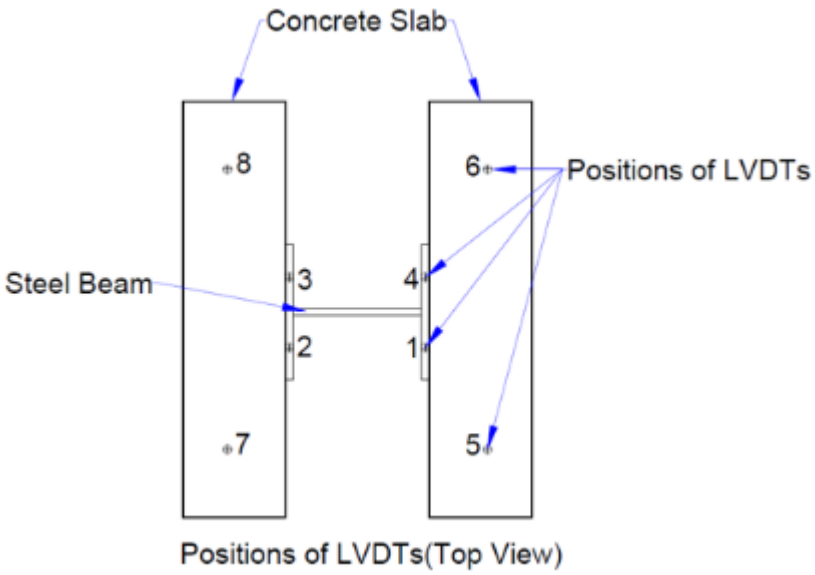

Figure 3-15 Positions of LVDTs on concrete and steel beam

3.7 Experimental results

The behaviour of the demountable shear connectors in composite structures was investigated through push off tests and the results are presented in Table 3-7. The main purpose of the experiments was to examine load slip behaviour, maximum shear capacity and observe modes of failure.

Table 3-7 Summary of maximum shear resistance and failure modes

Test Specimen ID	Concrete cube strength (MPa)	Max Shear capacity (kN/stud)	Slip value at Maximum load (mm)	Slip value at failure (mm)	Mode of Failure
S1	57.5	61.5	5.6	10	Concrete
S2	54.5	44.5	6.9	9.2	Concrete
D1	29.4	63.5	3.9	7.8	Concrete
D2	28.5	53.6	5.6	6.5	Concrete
M1	43.4	69.9	9.2	21.2	Connector
M2	40.9	68.2	7.2	18.7	Connector
M3	36.2	80.0	16	17.9	Connector
M4	30.5	79.6	26	28.2	Connector
M5	55.7	76.1	6.8	10.6	Connector
M6	58.1	82.6	7	9.5	Connector
M7	22.7	66.3	4.1	6	Concrete
M8	19.2	63.5	5.8	6.6	Concrete
M9	50.8	80	4.5	6.1	Concrete
M10	51.3	87	6.0	7.9	Concrete

3.7.1 Test S1 and S2

Test specimens S1 and S2 were tested with a single layer of reinforcement and two shear connectors per trough in each composite slab. Both specimens failed with buckling and splitting of the concrete slab. The early cracks on the surface of the concrete slabs started around the middle of the slab at a load of about 25kN per connector. This is due to the single layer of reinforcement which could not provide enough strength in the concrete slab to stop the propagations of the cracks and the buckling. Therefore, these test

specimens did not reach their actual shear capacity due to the premature failure. The test was terminated when progressive splitting and bending of concrete slabs occurred as shown in Figure 3-16.

Figure 3-16 Bending and splitting of concrete slab of test S1

Figure 3-17 shows the load slip behaviour of specimens S1 and S2. Both specimens had good ductile behaviour and the slips at the failure were recorded as 5.6 mm and 6.9 mm respectively for specimen S1 and S2, but the shear connections did not reach their real shear capacity due to premature failure of the concrete slabs. The test specimens S1 and S2 failed at the maximum loads of 61.5 kN and 45.5 kN per shear connector respectively.

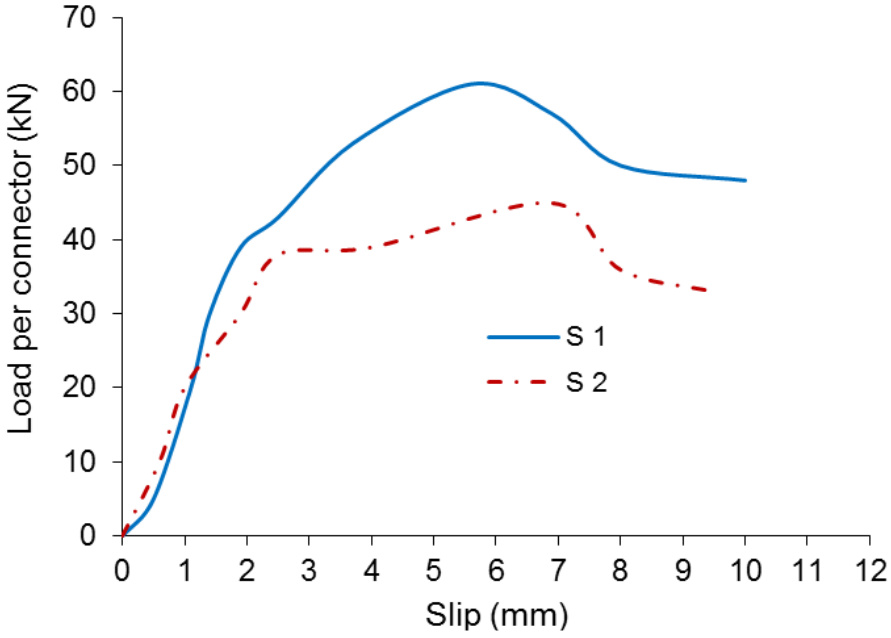

Figure 3-17 Load-slip curves of push-off test specimens S1 and S2

3.7.2 Test D1 and D2

To overcome the premature buckling and splitting failure as observed in test S1 and S2, a double layer reinforcement cage (D), as shown in Figure 3-2, was developed and utilised for specimens D1 and D2. In these tests small cracks were observed on the outer surface of the concrete slabs at a load of about 35 kN per shear connector but they did not propagate inside the concrete slab due to the double layer of reinforcement. Both specimens behaved better compared to specimens S1 and S2. However, these specimens developed a local premature failure at the toe of concrete slab as shown in Figure 3-18. This premature failure prevented the shear connections to achieve their true shear capacity.

Figure 3-18 Premature failure at concrete toe in specimen D2

The load slip behaviour curves of specimens D1 and D2 are presented in Figure 3-19. The maximum failure load was recorded for specimens D1 and D2 as 63.5 kN and 53.6 kN per shear connector with a slip of 3.9 mm and 5.6 mm respectively.

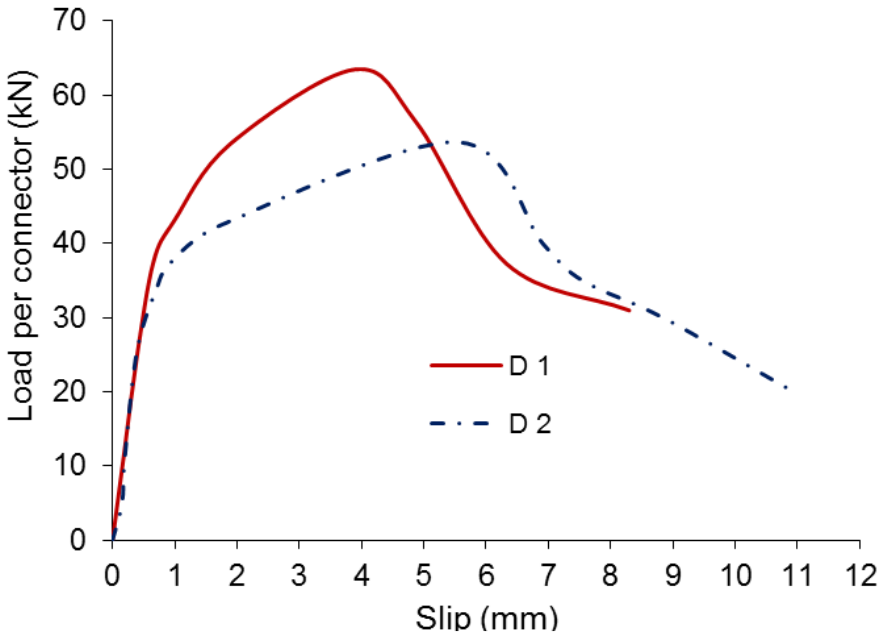

Figure 3-19 Load-slip curves of push-off test specimens D1 and D2

3.7.3 Test M1 and M2

To prevent this local premature toe failure as observed in tests D1 and D2, the double layer reinforcement cage (D) was modified with toe reinforcement as shown in Figure 3-3. The modified reinforcement cage was used in specimens M1 and M2 with two shear connectors per trough in each composite concrete slab. The modified reinforcement cage enabled the demountable shear connector to achieve its maximum shear capacity.

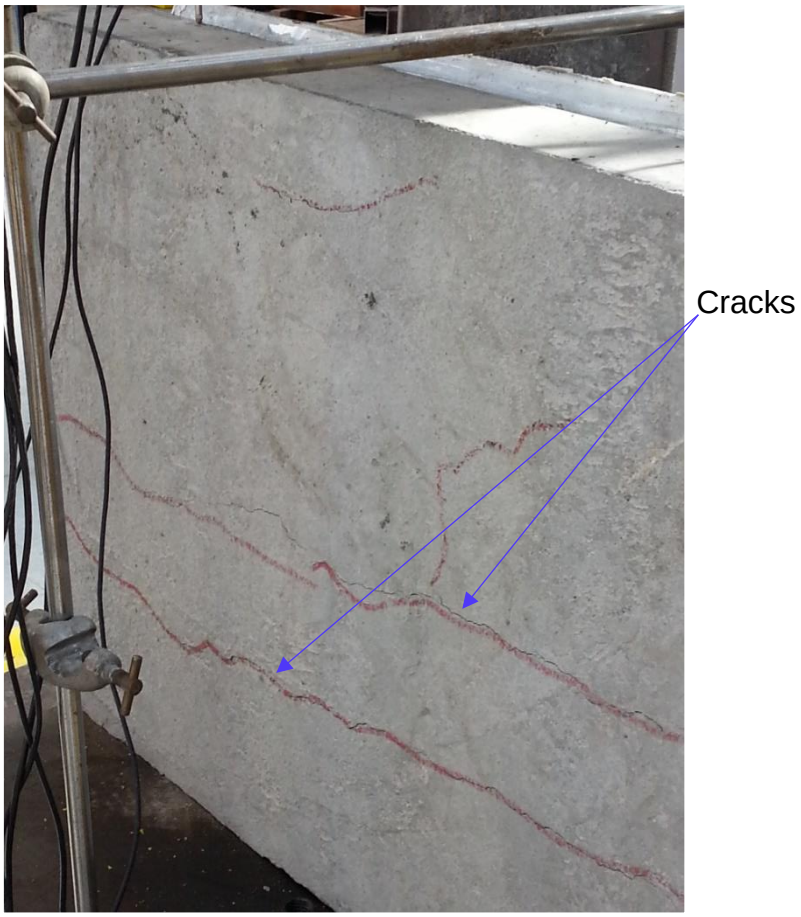

Figure 3-20 Small cracks on the outer surface of concrete slab in specimen M1

Initial cracks were observed on the outer surfaces of the concrete slabs at a load of 40 kN per shear connector as shown in Figure 3-20. Due to using the specific designed reinforcement cages, the initial cracks did not propagate deeply inside the concrete slabs. The de-bonding was observed, as

expected, between the profiled metal decking and the concrete slab in both specimens M1 and M2 as can be seen in Figure 3-21.

It was observed in test specimens M1 and M2 that the modified reinforcement cage effectively prevented the local premature failure due to the progressive splitting and buckling of the concrete slabs and toe failure in the concrete slab.

Figure 3-21 De-bonding of metal decking observed in specimen M1

The specimens failed with the shearing of the connectors as presented in Figure 3-22. The load slip behaviour curves of specimens M1 and M2 are shown in Figure 3-23. Both specimens behaved in a very similar way up to the load of 60 kN per connector. The ultimate shear capacity of both

specimens was recorded as 69.9 kN per connector and 68.2 kN per connector at a slip of 9.2mm and 7.2 mm.

Figure 3-22 Shearing of shear connectors in specimen M1

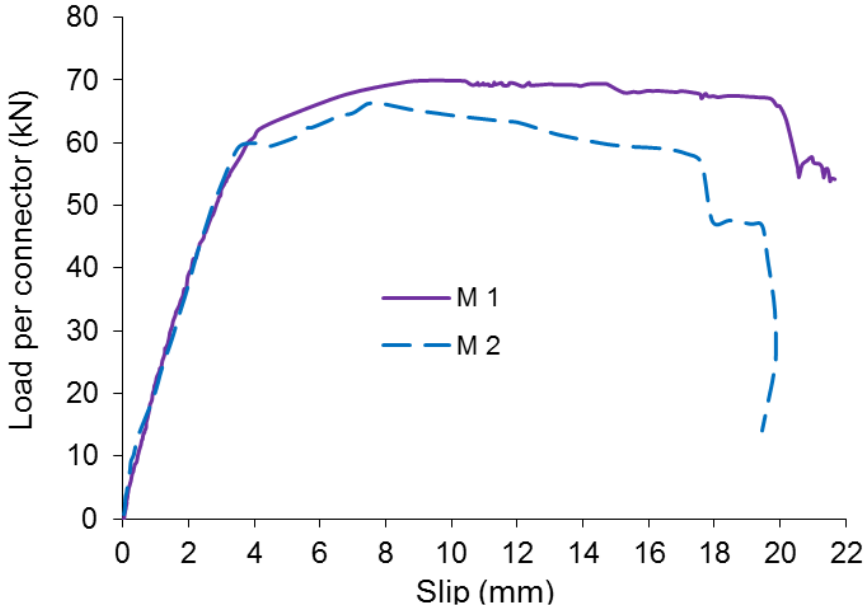

Figure 3-23 Load-slip curves of specimens M1 and M2

3.7.4 Test M3 and M4

A single shear connector per trough in each composite concrete slab was adopted for the test specimens M3 and M4. The load was applied slowly and

initial cracks were noticed at a load of about 43 kN per shear connector at the outer surface of the concrete slab. These initial small cracks did not propagate deep inside the slab with an increase of applied load due to the reinforcement cage. Both specimens failed with shearing of the shear connectors as shown in Figure 3-24.

Figure 3-24 Shearing of shear connector in specimen M3

Figure 3-25 presents the load slip behaviour curves of specimens M3 and M4. Both specimens showed consistent behaviour up to the load of 50 kN per connector. The behaviour in plastic is slightly different. This could be the effect of concrete strength as the concrete cube strength of the M3 specimen was about 20% higher than specimen M4.

Both specimens showed very ductile behaviour and they fulfilled the ductile limit of 6 mm slip. The maximum shear capacities of M3 and M4 were 80.0

kN per connector and 79.6 kN per connector at the slip of 16 mm and 26 mm respectively.

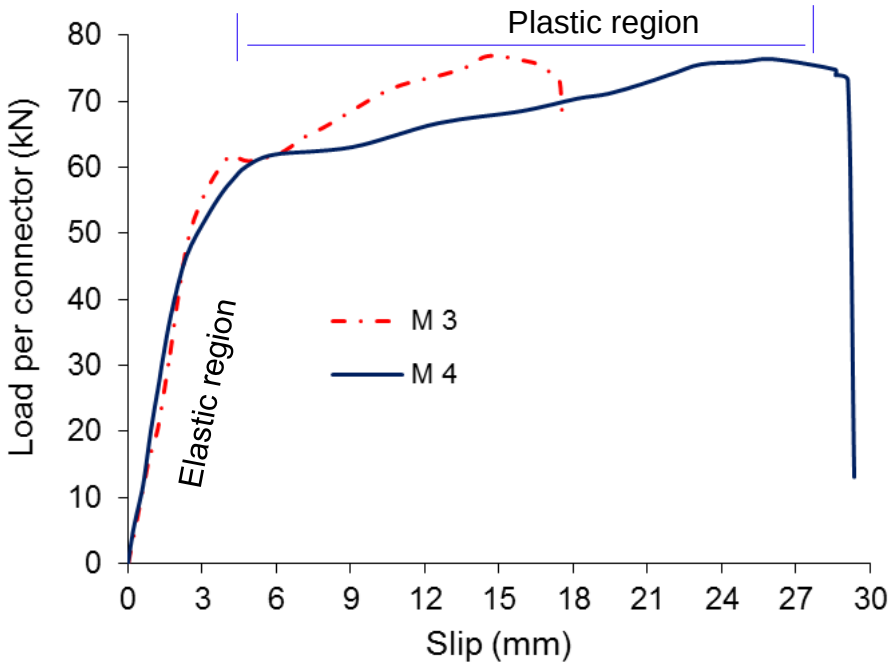

Figure 3-25 Load-slip curves of push-off test specimens M3 and M4

3.7.5 Test M5 and M6

To compare the concrete strength effect on the shear connection performance, a higher concrete strength was utilised for specimens M5 and M6 to observe the failure mode and shear capacity. These specimens had two connectors in each trough of the composite concrete slab. Both specimens M5 and M6 failed with connector shearing as shown in Figures 3-26 and 3-27. Higher concrete compressive strength did not affect the mode of failure compared to specimens M1 and M2 although the concrete cube strength of M1 and M2 was about 30% lower than that of specimens M5 and M6. A similar crack pattern (see Figure 3-28) was observed to specimens M1 and M2.

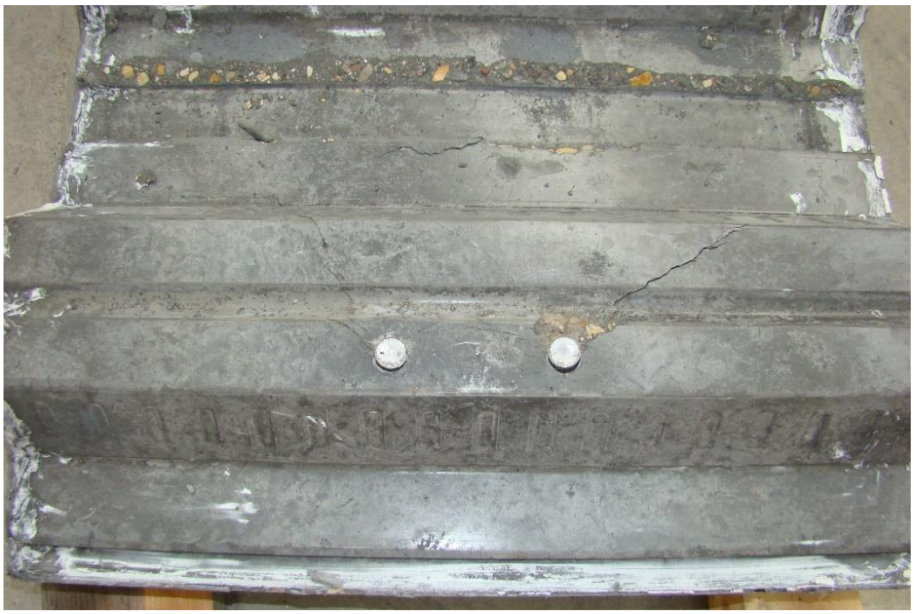

Figure 3-26 Shearing of shear connector observed in specimen M5

Figure 3-27 Stud shearing failure observed from specimen M6

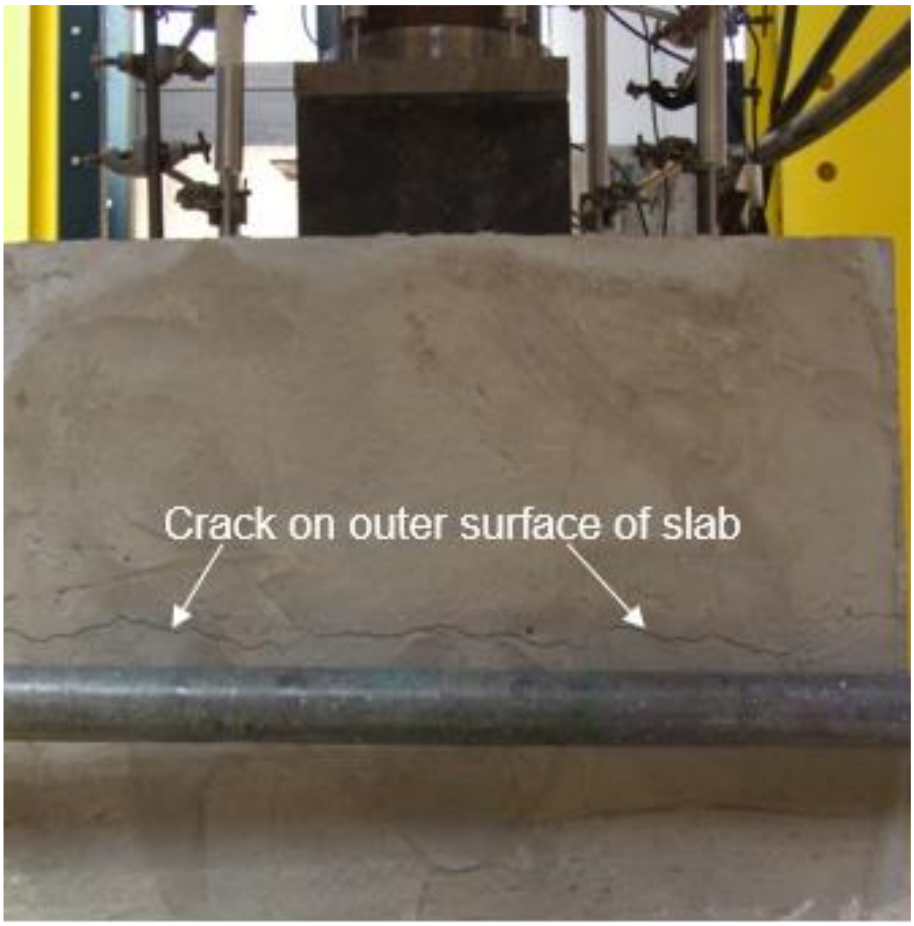

Figure 3-28 Transverse cracks on outer surface of a slab observed from test specimen M6

The initial load slip behaviour curves and ultimate shear capacities as illustrated in Figure 3-29 for push off test specimens M5 and M6 are different. The difference in initial slip could be due to the clearance provided between the connector and the steel flange hole or the effect of tightening the nuts. The difference in ultimate shear capacity could be due to the effect of the compressive strength of the concrete as the concrete strength of M6 was about 5% higher than M5 by cube tests.

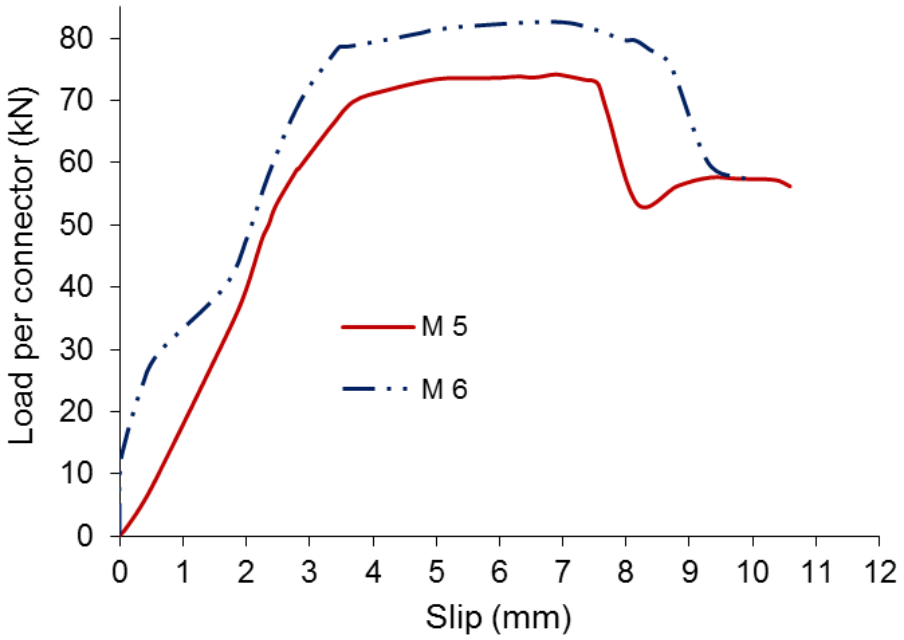

Figure 3-29 Load-slip curves of push-off test specimens M5 and M6

3.7.6 Test M7 and M8

Connectors (type C2 as shown in Figures 3-6 and 3-7) with a larger shank diameter of 22mm and collar diameter of 20mm were adopted in specimen M 7 and the Gr 8.8 M20 bolt connectors (type C3 as shown in Figures 3-6 and 3-7) were used for specimen M8 to investigate the effect of different shear connectors on the shear connections. The behaviours of both types of connectors were similar and both failed due to concrete cone failure. Most of the concrete failure was observed around the connector inside the concrete slab as in Figures 3-30 and 3-31.

The load slip behaviour as shown in Figure 3-32 was also very similar in terms of initial stiffness and ultimate shear capacity. The ultimate shear capacities recorded were 66.3 kN and 63.5 kN per connector for M7 and M8 at a slip of 4.1 mm and 5.8 mm respectively. Both specimens showed reasonably good ductile behaviour in the lower concrete strength.

Figure 3-30 Formation of concrete cone observed in specimen M7

Figure 3-31 Formation of concrete cone observed in specimen M8

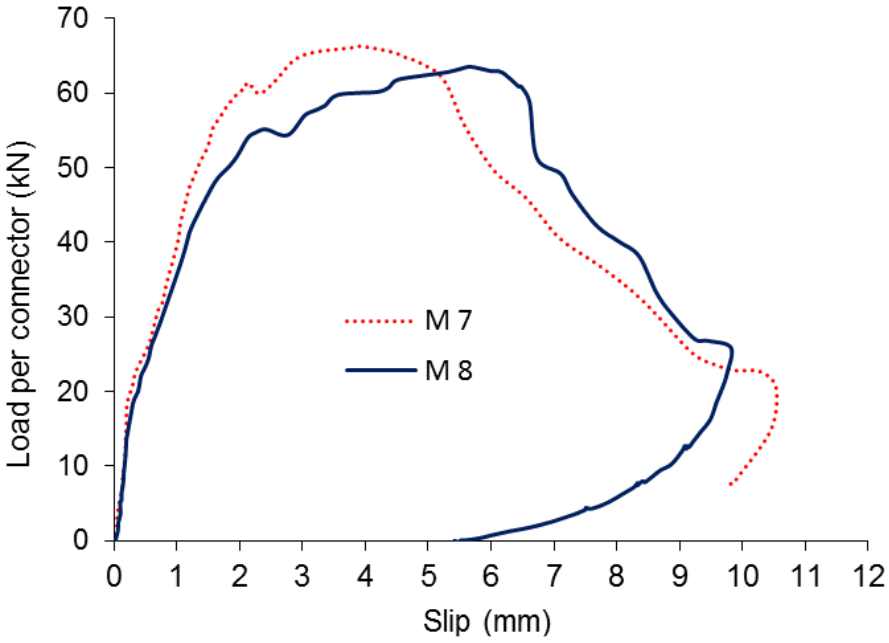

Figure 3-32 Load-slip curves of specimens M7 and M8

3.7.7 Test M9 and M10

Same type of shear connectors were used in specimen M9 and M10 as those utilised in specimen M7 and M8 respectively, but concrete strength use was higher to investigate the effect of higher concrete on shear capacity, modes of failure and load slip behaviour. Both specimens again failed due to concrete cone failure as shown in Figures 3-33 and 3-34. The shape (Pattern) of the cone in specimen M9 and M10 was very similar to specimen M7 and M8 respectively. This indicates that the increase in concrete strength did not affect the mode of failure in specimens with higher strength connectors. But the ultimate shear capacity was increased about 31% as can be seen in Table 3-7. This shows a clear effect of concrete strength on shear capacity of the test specimens with higher strength connectors.

Figure 3-35 presents the load slip behaviour of specimens M9 and M10. Both specimens (M9 and M10) showed very ductile behaviour and the maximum

shear capacities of 80 kN per connector and 87 kN per connector were achieved at a slip of 4.6 and 6.5 mm respectively.

Figure 3-33 Mode of failure in test M9

Figure 3-34 Mode of failure in specimen M10

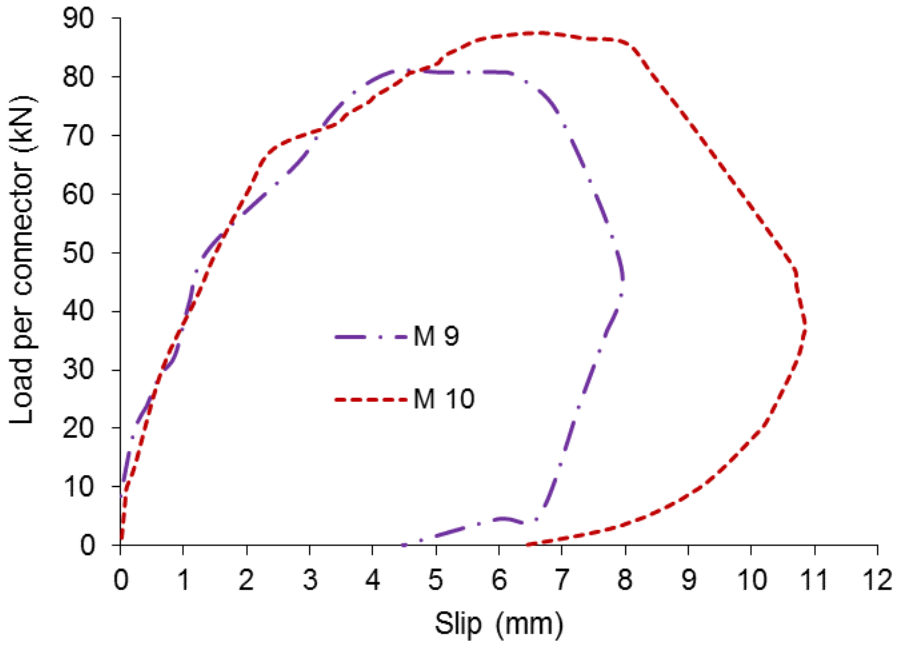

Figure 3-35 Load-slip curves of push-off test specimens M9 and M10

3.8 Summary

Fourteen push-off tests have been conducted using demountable shear connectors in profiled metal deck composite slabs. Their detailed setup, testing procedure and test results have been explained in this chapter. Three different types of steel reinforcement cages and demountable shear connectors with different compressive strengths of concrete and a number of shear connectors in each composite concrete slab were tested under static shear loading to assess the shear capacity, stiffness and ductility.

The demountable shear connectors could be demounted easily after and before tests. This made it possible to separate the steel beam from the composite concrete slab. Table 3-7 summarizes the maximum shear capacity per shear connectors, amount of slip at maximum load and at failure and the mode of failure observed in the push-off tests. Two main modes of failure

were observed during push off tests: concrete failure and shearing of shear connectors.

Coupon tests were also conducted to determine the mechanical properties of demountable shear connectors, the steel bar and the profiled metal decking. Concrete properties were determined using cube tests of the concrete samples. The discussion on push off test results will be presented in chapter 4.

Chapter 4
Discussion of push off tests

4.1 Introduction

A comprehensive discussion on the results of the push off tests described in chapter 3 is presented in this chapter. It includes the load slip behaviour, shear connection capacity, ductility, stiffness and modes of failure of composite structures with demountable shear connectors. In addition, the effect of various parameters such as number of shear connectors per trough, different types of reinforcement cages, concrete strengths and types of connectors are also discussed in this chapter. Furthermore, the push off test results are compared with other researcher work.

4.2 Behaviour of demountable shear connector

4.2.1 Load slip behaviour

In all specimens in the push off tests the load-slip relationship was recorded at both sides. The shear connectors on both sides behaved in a very similar manner as shown in Figures 4-1 to 4-4 for typical specimens M1, M2, M4 and M5. This confirms a reasonable even distribution of shear forces within all shear connectors in the push off test specimen.

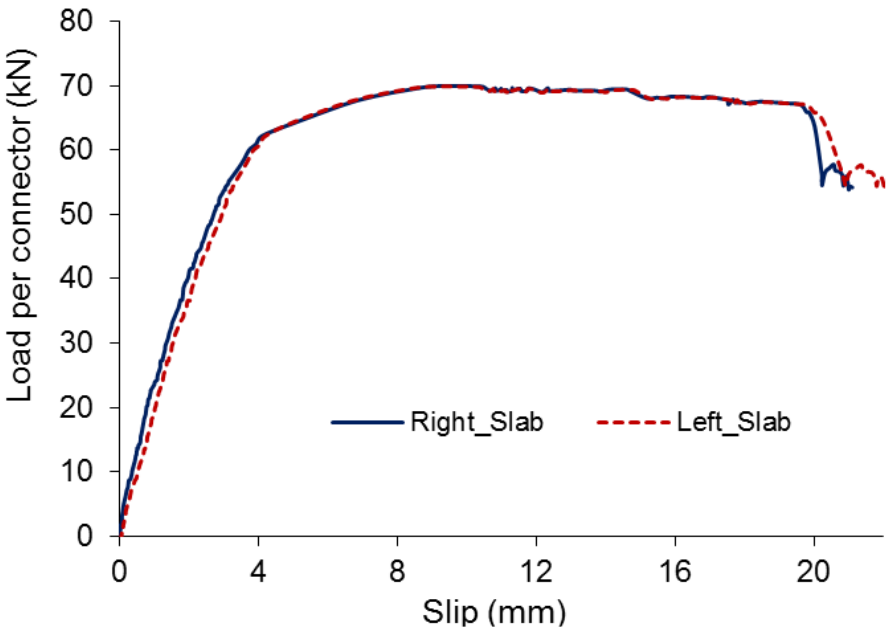

Figure 4-1 Load-slip curves recorded on both sides of specimen M1

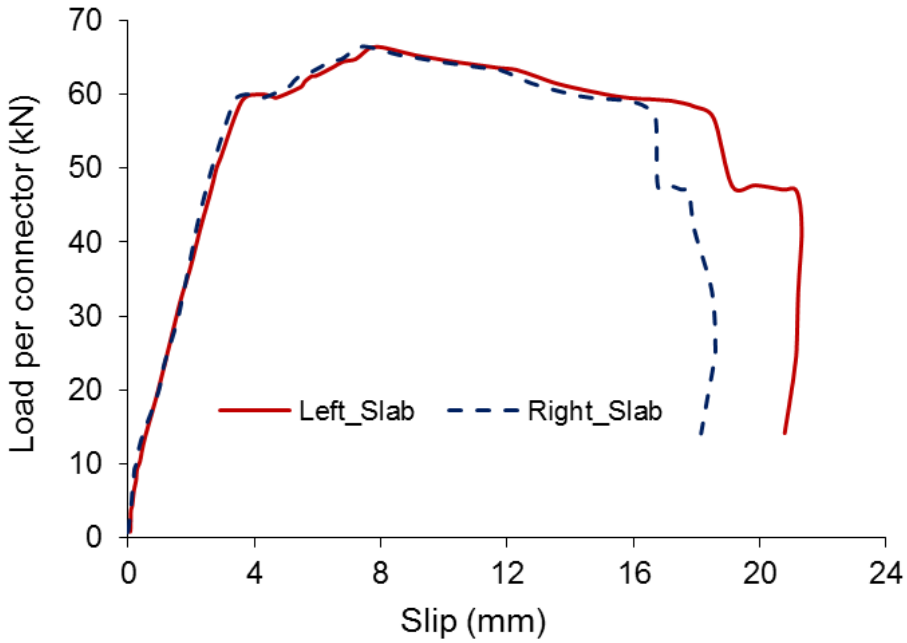

Figure 4-2 Load-slip curves recorded on both sides of specimen M2

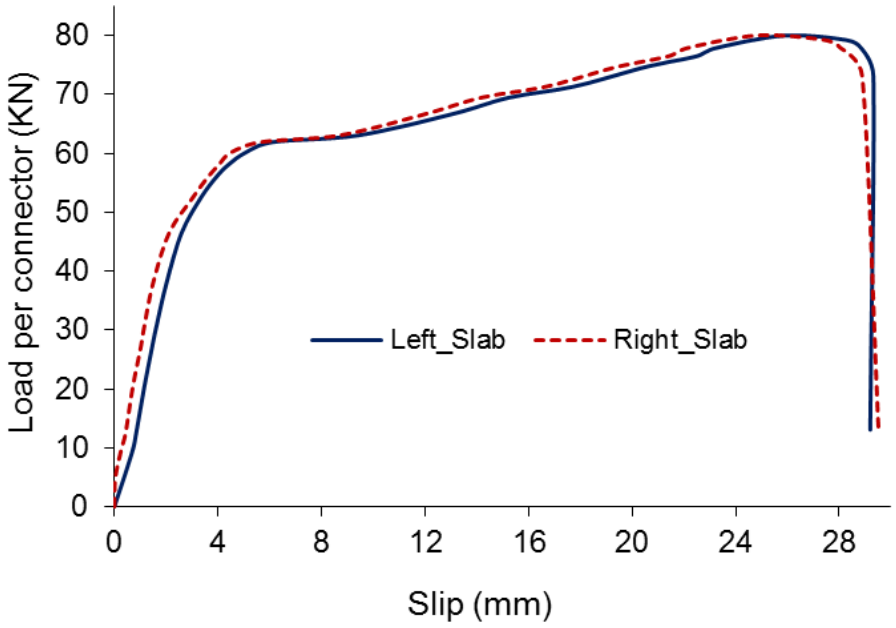

Figure 4-3 Load-slip curves recorded on both sides of specimen M4

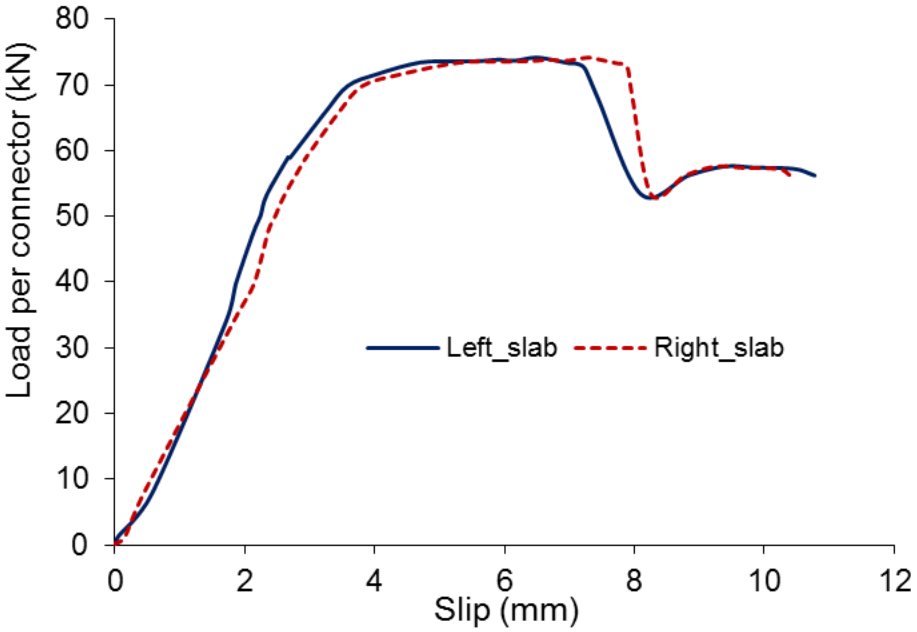

Figure 4-4 Load-slip curves recorded on both sides in specimen M5

All load-slip curves have clear elastic and plastic portions. In the elastic region, the load slip curves show an almost linear relationship for all

specimens but in the plastic region the slip increases and stiffness decreases rapidly.

4.2.2 Shear capacity

In all push off tests with connector type C1, the highest shear capacity, observed in the specimen M6 with paired connectors per trough, was 82.6 kN per connector owing to the highest concrete strength (58.1 MPa) of the specimen. Similar shear capacity (80.0 kN per stud) of specimen M3 with only one shear connector per trough connecting a slab to the steel beam was also observed. There was no significant difference between the shear capacities (load per connector) of specimens M6 and M3, although the slab concrete strength of the latter was much lower. This could be due to the overlap of stresses in the pair connector's specimen.

Regardless of slab concrete strength, an average shear resistance of 73.5 kN per connector was obtained from the specimens with pair connectors of 19 mm diameter per trough. This is about 5 % lower than the average shear strength of the specimens with a single shear connector of the same diameter. The overall average shear resistance per connector was 75.45kN for all six specimens M1–M6 with a modified reinforcement cage, using the same connector diameter and height.

4.2.3 Ductility

Demountable shear connectors with a shank diameter of 19mm showed very ductile behaviour in this study. The average slip of the paired connector specimens, with the modified reinforcement cage and connector shank diameter of 19 mm, achieved more than 6 mm slip at the maximum load as

shown in Figure 4-5. This fulfils the ductile limit of 6 mm according to Eurocode 1994-1-1:2004. The slip of specimen M6 with the higher concrete strength is less than half that of specimen M1 with lower concrete strength. This is due to the effect of the concrete strength. The slip of specimen M3 with a single shear connector per trough is similar to the specimen M1 with pair connectors per trough and both specimens have almost similar concrete strength. This indicates that the number of connectors does not have too much effect on ductility.

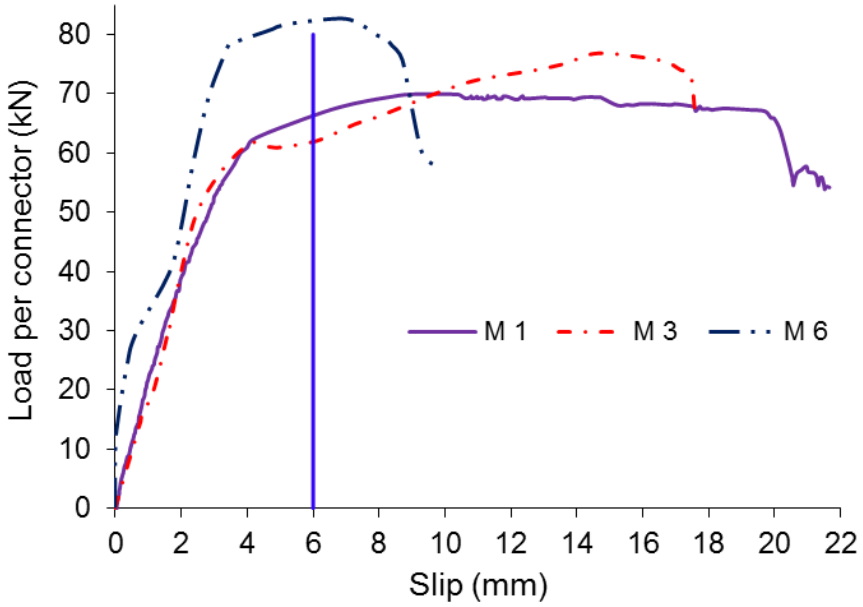

Figure 4-5 Load per connectors at the slip of 6 mm

The specimens (M3 and M4) with single shear connectors per trough showed a very ductile behaviour. The slip at maximum load was up to about 16 mm in specimen M3 and about 26 mm in specimen M4. The load bearing capacity increased with the increase of slip. After achieving the maximum shear resistance, the slip did not increase significantly before the connector sheared off as the connectors were fully yielded at this point.

4.2.4 Stiffness

The initial stiffness of this demountable shear connection was observed to be low when compared to the welded shear connector as shown in Figure 4-6. This is the possible effect of the oversized holes provided in the steel flange for the shear connector to connect the steel beam and composite concrete slabs. Even with lower initial stiffness the ultimate load bearing capacity was similar. However, the stiffness of the demountable shear connector might be increased by reducing the clearance in the hole or pre-tensioned the connector.

The stiffness is worked out according to Eurocode 1994-1-1:2004 (section B.2.5 (4)). The initial stiffness of the demountable shear connectors of Gr 8.8 bolt with embedded nut in specimen M10 was observed to be slightly higher, as presented in Figure 4-7, compared to specimen M6 without an embedded nut although both specimens have similar concrete strength. This is the possible effect of the embedded nut which made the shear connection stiffer in specimen M10. The other factors could be the oversized hole in the steel flange and profiled metal decking of specimen M6 which reduces the stiffness at low load levels.

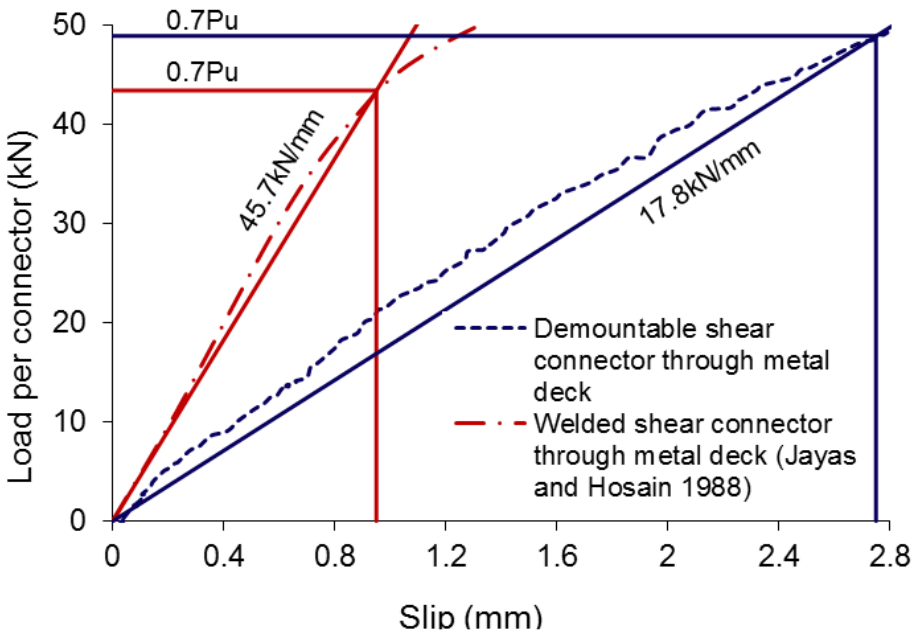

Figure 4-6 Comparison of stiffness of welded shear connector and demountable shear connector

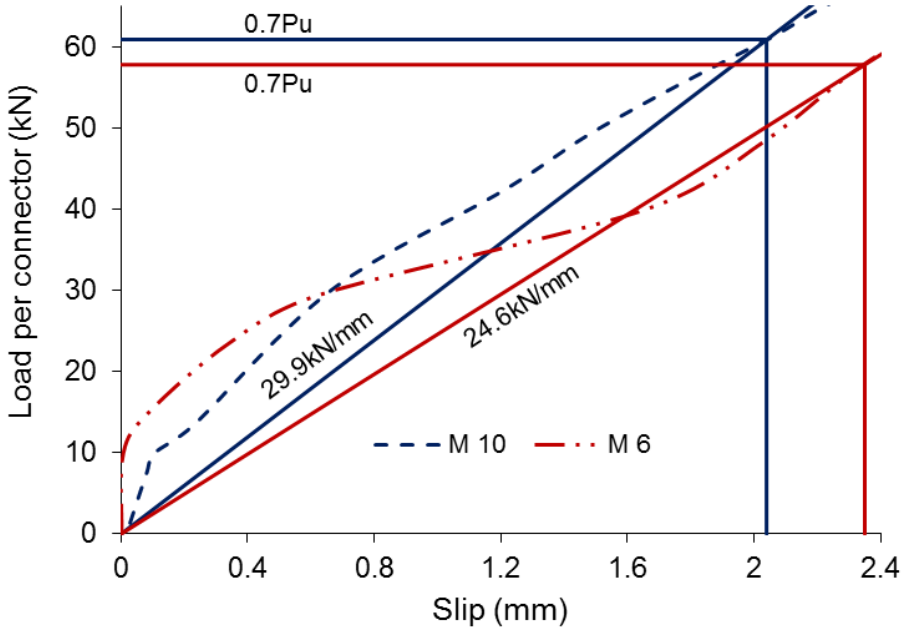

Figure 4-7 Stiffness of demountable shear connectors

4.3 Effect of parameters

4.3.1 Effect of concrete strength

Concrete strength has a significant effect on the shear resistance of demountable shear connections. The shear capacity increased with the increase of concrete strength as shown in Figures 4-8 and 4-9. The maximum shear resistance of specimen M6 was about 17% higher than that of specimen M1 due to the concrete strength of M6. The concrete strength of M6 was about 35% higher than M1.

The strength of concrete also affected the load slip behaviour. Specimens M5 and M6 with higher concrete strength failed with a brittle behaviour. The slip was about 7 mm at maximum load and this fulfilled the ductility limit of 6 mm by the EC4 requirement. The shear connector fractured without significant concrete crushing (see Figure 3-20) compared to specimen M1 and M2 where significant concrete crushing was observed (see Figure 3-24). In addition, the deformation of connectors in specimens with higher strength concrete was not as big as that of connectors embedded in specimens M1 with lower concrete strength.

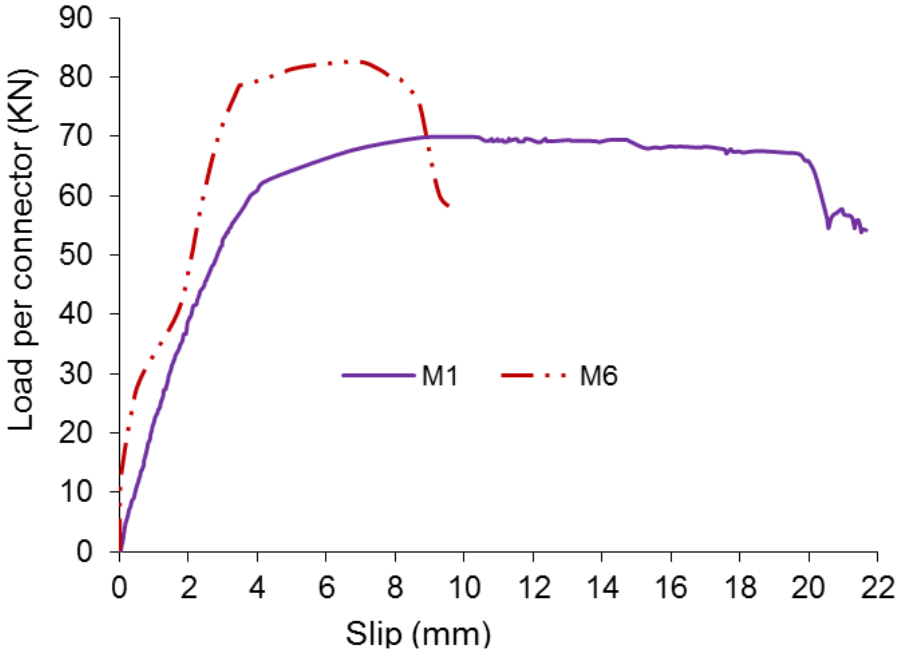

Figure 4-8 Effect of compressive concrete strength in specimen M1 and M6

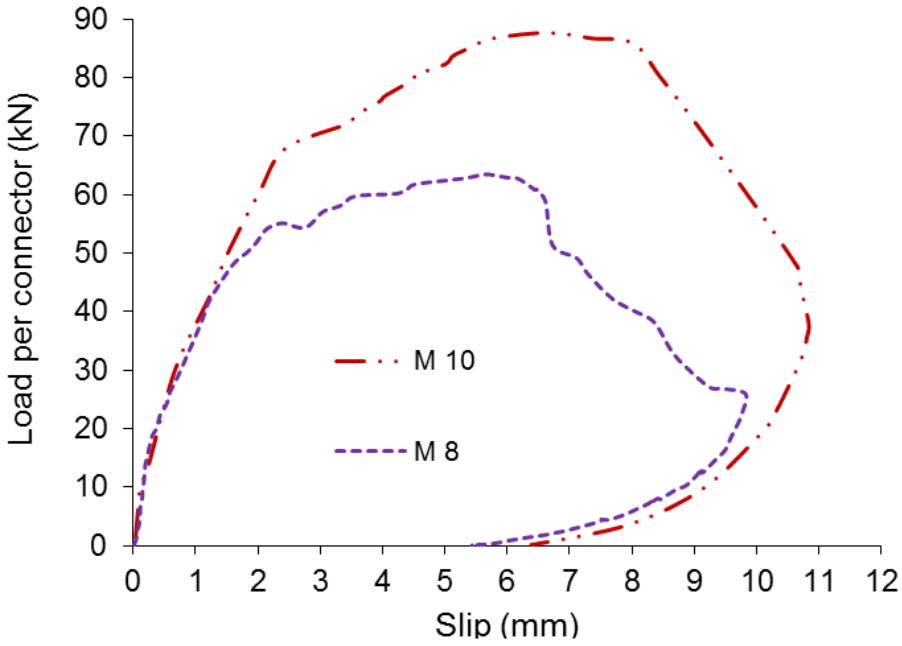

Figure 4-9 Effect of concrete strength in specimen M8 and M10

4.3.2 Effect of number of connectors

Figure 4-10 compares the effect of number of connectors per trough on the load slip behaviour of demountable shear connectors in composite structures. The initial stiffness of specimen (M1) with paired shear connectors

per trough was similar to that of specimen (M3) with a single shear connector per trough. The shear capacity of both specimens is very similar at the yielding point and at a slip of 9mm. However, it was observed that the reduction in shear strength of the specimens with paired connectors per trough was about 13% although the concrete strength was lower in specimens with a single shear connector. This is a possible effect of overlapped stresses in specimens with two connectors per trough.

Figure 4-10 also shows that shear resistance increased with an increase in slip in specimens with single shear connectors and failed in brittle behaviour compared to paired connector specimens where the connection showed more ductile behaviour.

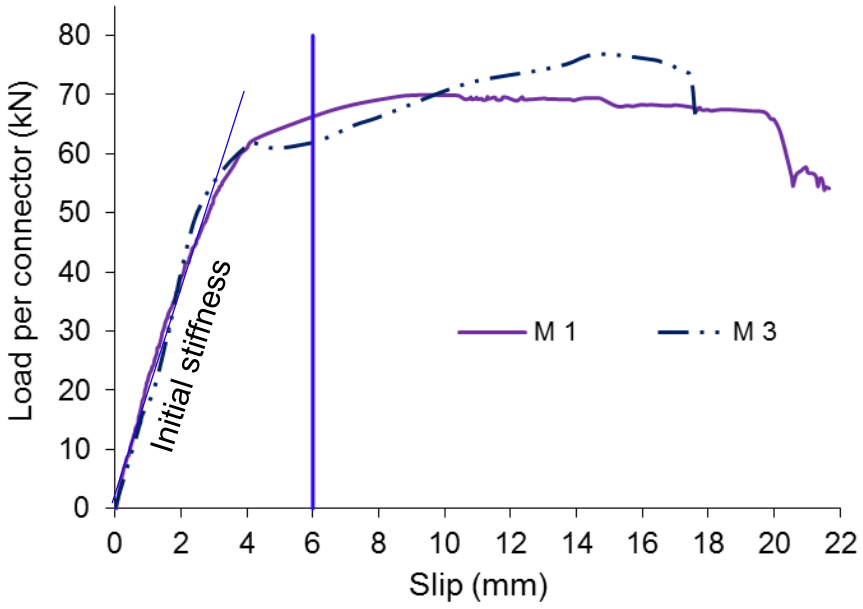

Figure 4-10 Comparison of specimens with pair connectors per trough and single connector per trough

4.3.3 Effect of Reinforcement

The experimental results showed that specimens (M1 to M10) with a modified reinforcement cage had higher shear capacity than those specimens with single or double layer reinforcement cages. As presented in Table 3-7, the overall average load capacity of specimens with modified reinforcement cages was about 75% higher than specimens S1 and S2 with the single layer reinforcement cage and about 65% higher than specimens D1 and D2 with the double layer reinforcement cages. The modified reinforcement cage had a significant effect on the ultimate shear capacity and prevented the premature failure of the concrete slabs as observed in the specimens with single and double layer reinforcement cage.

4.3.4 Effect of connector types

Figure 4-11 compares the load - slip behaviour of specimens with the M20 Gr 8.8 bolt shear connectors and demountable shear connectors with a shank diameter of 22 mm and 19 mm. It can be seen that all three specimens behaved in a very similar way. The specimens with the larger shank (22 and 20 mm) diameter connectors failed with concrete cone failure and specimens with smaller shank (19 mm) diameter failed in connector shearing.

The different types of connectors did not have a significant effect in terms of shear capacity although all specimens had very similar concrete compressive strength. But all the connectors had an effect on the mode of failure. As more concrete damage was observed with larger shank diameter as can be seen in Figures 3-20, 3-24, 3-28, 3-29, 3-33 and 3-34.

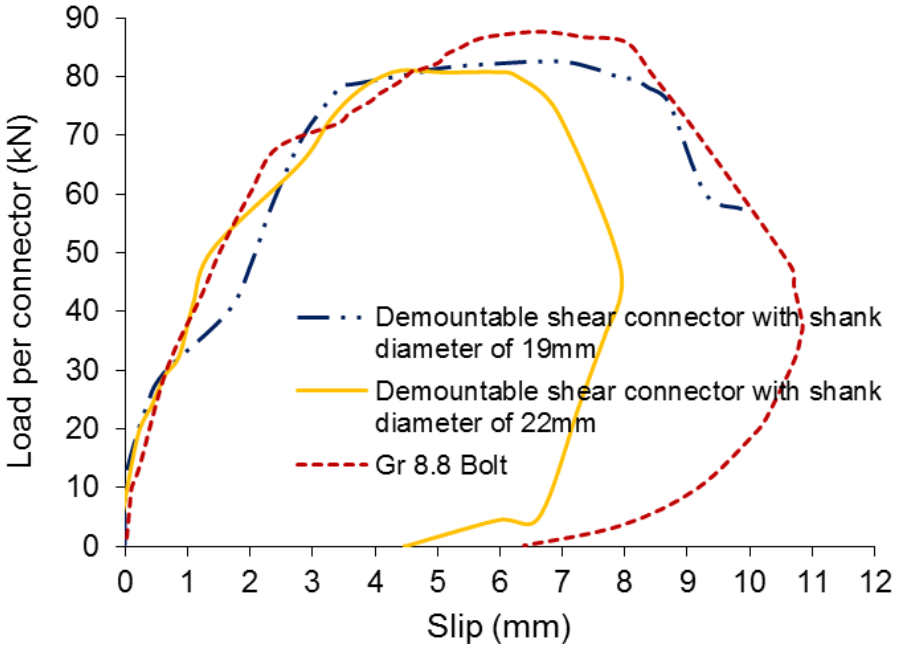

Figure 4-11 Comparison of Gr 8.8 bolt connector and demountable shear connector

4.4 Modes of failure

Two main failure modes were observed in these push off tests. The first mode of failure is concrete cone failure with concrete crushing and cracks where no connector fracture was observed. In this type of failure, the concrete around the connector failed in compression before the connector yielded. Crushing of the concrete started from the vicinity of the connector head and cracks developed through the depth of the concrete slab forming a cone shape around the shear connectors and these cracks were very visible when the profiled metal deck was dismantled from the concrete slab after the test.

Cracks on the outer surfaces of the concrete slab were observed in all tested specimens. These cracks were more evident in specimens with low strength concrete than those with higher strength concrete. The transverse concrete cracks first appeared on the outer surface of the slabs just near the middle of

the slabs as shown in Figures 3-20 and 3-26, but they did not propagate inside the slab when the modified reinforcement cage was used.

The concrete damage patterns observed in different specimens are very similar irrespective of the shear connector arrangement and the concrete strength. Figures 3-20 and 3-22 illustrate typical failure modes which were characterised by the combination of connector fracture, concrete cone and the cracks around the root of the connector due to compressive forces.

However, the average width of concrete cone in the specimens with a single shear connector per trough was less than those specimens with paired shear connectors per trough. The average width of the cone was about 260 mm in the specimens with the paired connectors of 19 mm shank diameter connections. This is approximately double the bottom width of the profiled trough (110 mm) and about 25% wider than the width of the steel beam flange.

The average width of the cone was about 130 mm with a single shear connector connection which is half that of the specimens with paired connectors per trough. It was observed that the average cone width was up to 360mm for the specimen with paired connectors of 22 mm shank diameter which is 100 mm larger than that of specimens with connectors of 19 mm shank diameter. This is possibly due to the larger diameter, the stresses become higher in the concrete around the demountable shear connectors. This results in more damage to the concrete.

The deformation of the hole in the profiled metal deck was also observed during the test. This behaviour was an indication that part of the load was

being resisted by the profiled metal deck. This tearing of the profiled metal deck at the connector hole was more prominent in specimens with a single shear connector compared to the paired connector specimen as shown in Figure 4-12.

Figure 4-12 Elongation of hole in metal deck in test specimen of Single shear connector per trough(Left) and Pair of shear connectors per trough (Right)

The second mode of failure is that the shear connector fractured at the collar. For this mode of failure, the connector fully yielded and fractured at the collar of the shear connector. The connector reached its maximum yield stress while the concrete slab did not reach its maximum stress. In the paired connector specimens M1, M2, M5 and M6 the connectors sheared off as expected due to high concrete strength. A similar connector failure was also observed in single shear connector specimens M3 and M4. Typical fractures occurred at the collar position close to the slab as shown in Figure 4-13.

Figure 4-13 Fractured connector in test specimen M 5

4.5 Comparison with results from other researchers

The load slip behaviour of demountable shear connectors was compared with a similar welded shear connector experiment conducted by Jayas and Hosain (1988). The shear capacity of a demountable shear connector is slightly higher than the shear capacity of a similar welded shear connector as shown in Figure 4-14. The ductility of the demountable shear connector is found to be better than the welded shear connector, but the initial stiffness is much lower. The difference was possibly caused by the clearance hole in the steel flange for the demountable shear connector.

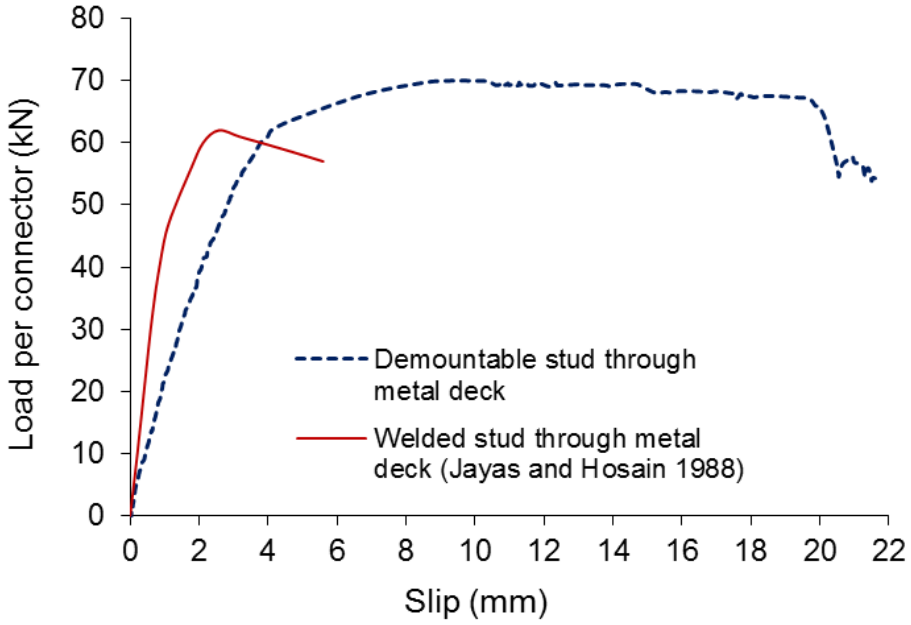

Figure 4-14 Comparison of demountable shear connector with welded shear connector

The other reason for low initial stiffness in the demountable connectors could be the torque applied to the demountable shear connectors. This may not have been enough to develop the friction forces between the interface of the steel beam and the composite concrete slab. Therefore, the shear connection was not able to transfer the initial shear forces at the interface

through friction and the demountable shear connectors started resisting the applied load by bearing.

Figure 4-15 compares the load-slip relationship of a demountable shear connector in profiled metal decking composite concrete slab (current research) with a similar shear connector in a solid concrete slab, the research was conducted by Lam and Saveri (2012) and Dai et al (2013). It is found that the shear resistance capacity, ductility and stiffness behaviour of a demountable shear connector embedded in a solid concrete slab and embedded in a composite concrete slab are very similar except that the ultimate strength of demountable connectors in a solid slab is about 28% higher compared to the composite concrete slab. This is due to the higher concrete confinement around the shear connectors in solid slabs which do not have troughs like a profiled metal decking composite concrete slab.

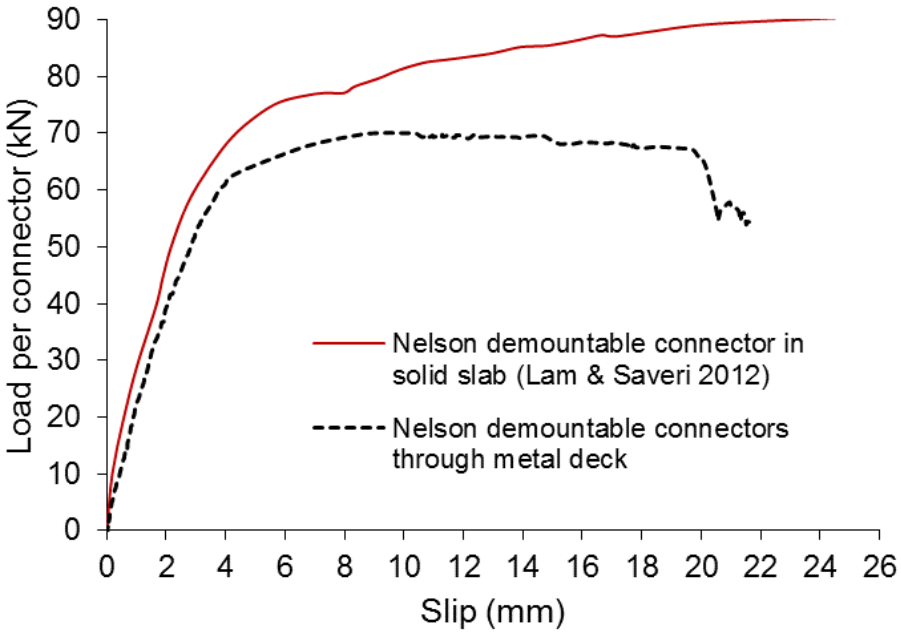

Figure 4-15 Comparison of demountable shear connector in solid slab and metal decking slab

A comparison is carried out using test results from demountable shear connector (type C1) in a composite concrete slab and the Gr 8.8 M16 bolt with an embedded nut in a solid concrete slab, experiments performed by Pavlovic et al. (2014) in Figure 4-16. It is found that the Gr8.8 bolt with embedded nuts in a solid slab has very stiff behaviour and the maximum resistance is approximately 25% higher than the demountable shear connector in a composite concrete slab. This may be due to the embedded nuts in a solid slab and more concrete confinement as compared to the profiled metal decking concrete slab.

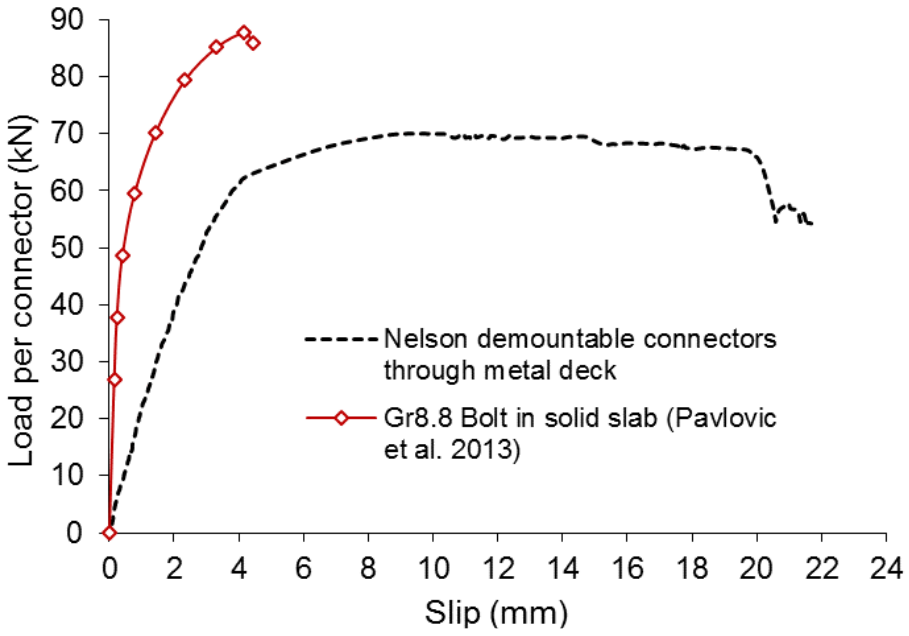

Figure 4-16 Comparison of demountable shear connector in metal deck slab and Gr 8.8 bolt connector in solid slab

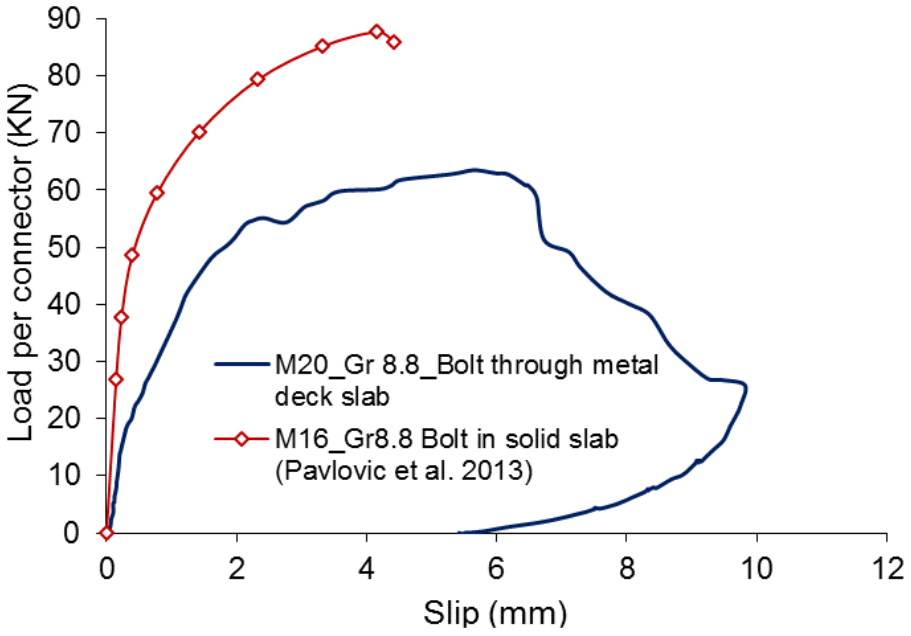

Figure 4-17 Comparison of M20 Gr 8.8 bolt connector in metal deck slab and M16 Gr 8.8 bolt connector in solid slab

Although the stiffness with the embedded nut in a solid slab is higher but the ductility of demountable shear connectors in composite concrete slabs is much better. The slip of the M16 bolt in a solid slab corresponding to the maximum load is about 4.5 mm and which is less than the slip of a demountable shear connector in a composite concrete slab.

Figure 4-17 presents a comparison of load-slip of the Gr 8.8 bolts in a profiled metal decking slab (current study) and the M16 Gr8.8 bolt in a solid slab. It can be seen that solid slabs with Gr 8.8 M16 bolts behaved in a stiffer manner than the Gr 8.8 M20 in a profiled metal decking concrete slab and had a higher shear capacity although the bolt diameter was smaller. This is because specimens with a profiled metal deck had lower concrete strength and the composite slab provided less confinement to the shear connectors compared with the solid slab.

4.6 Conclusions

Fourteen push-off tests have been conducted to investigate the shear strength, ductility and stiffness of the demountable shear connections in profiled metal deck composite slabs. The following conclusions may be drawn:

- The demountable shear connections have high ductility and similar shear capacity and behaviour compared with their equivalent welded shear connectors although the initial stiffness is slightly lower.
- The shear connector arrangement affects the shear connection's behaviour. Connection with a single connector per trough allows the development of full shear resistance of the connector, but the specimen with two connectors per trough provides better ductility.
- Concrete strength affects the behaviour of the demountable shear connectors. It appears that the ultimate shear resistance increases with the increase of concrete strength, however the connector's ductility decreases.
- Similar to the welded shear connectors, demountable shear connectors have two main failure modes: connector fracture and concrete crushing.
- The use of the modified reinforcement has improved the splitting resistance of a concrete slab and overcomes the possibility of premature failure of the concrete slabs. Therefore, it is recommended for use in all push-off tests.
- The demountable headed shear connectors have a good potential to be used as an environmentally friendly alternative to welded headed studs in

a profiled metal deck composite slab, which will allow the steel beam to be reused after dismantling.

Chapter 5
Composite beam test

5.1 Introduction

The structural behaviour of the composite beam with demountable shear connectors in a profiled metal decking composite concrete slab is reported in this chapter. This chapter also includes the testing of an identical composite beam with welded shear connectors to compare the structural behaviour of both composite beams. In addition, two companion push off tests were carried out to study the load slip behaviour and shear capacity of demountable shear connectors under maximum shear forces. The shear capacity was later used to work out the degree of shear connection in a demountable composite beam.

5.2 Test specimens

5.2.1 Demountable composite beam specimen (DCB)

A full-scale composite beam was tested with demountable shear connectors in a profiled metal decking composite concrete slab. The details of the demountable shear connectors are presented in Figure 5-1. The overall dimensions of the tested specimen are shown in Figures 5-2, 5-3 and Table 5-1. The length, width and thickness of the composite slab was 5200 mm, 1340 mm and 130 mm respectively. The steel beam IPE 300 with a length of

5600 mm and a Cofraplus 60 profiled metal deck was used in tested specimen.

The standard A142 mesh was adopted as steel reinforcement in the concrete slab. Holes with a diameter of 18 mm were drilled in the flange of the steel beam as shown in Figure 5-4. The 17 mm diameter was adopted for the profiled metal decking to hold the demountable shear connectors.

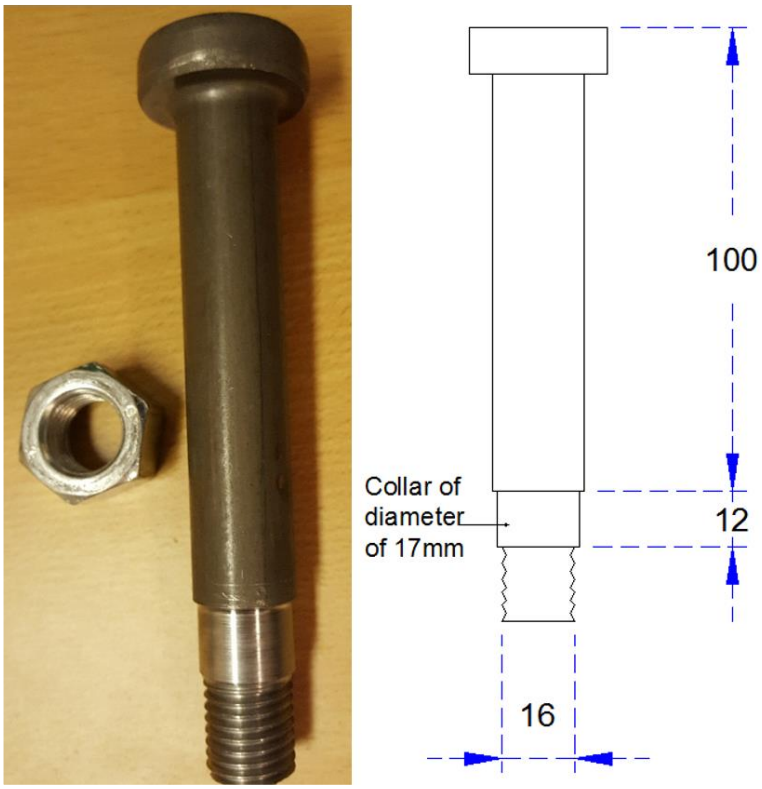

Figure 5-1 Demountable shear connector's detail

The steel beam was set as a simply supported beam with a span of 5.2 m. The profiled metal decking was laid down on the steel beam. The demountable shear connectors were installed through pre-drilled holes provided in the profiled metal decking and steel beam flange to assemble the specimen as shown Figures 5-5 and 5-6. The nuts were tightened manually

and then a torque wrench was used to ensure all demountable shear connecters were tightened equally up to the torque of 60Nm.

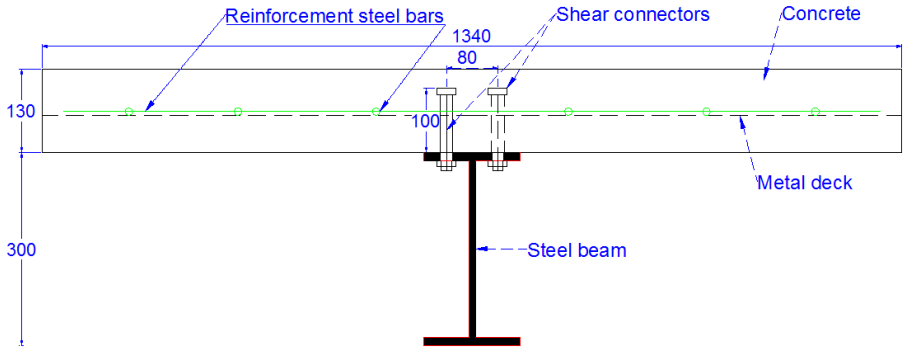

Figure 5-2 Cross sectional view of the test specimen with demountable shear connectors (DCB) (all dimensions are in mm)

The composite floor beam system was designed with a partial shear connection and a single shear connector was adopted in each trough of the profiled metal decking. The connectors were placed in a staggered position along the longitudinal direction of the steel beam as shown in Figure 5-5.

The height of the shear connectors was 100 mm and the diameter was 19mm inside the concrete. The collar diameter of the shear connector was 17mm passing through the metal deck and steel flange and the threaded portion was 16mm to match the M16 nut.

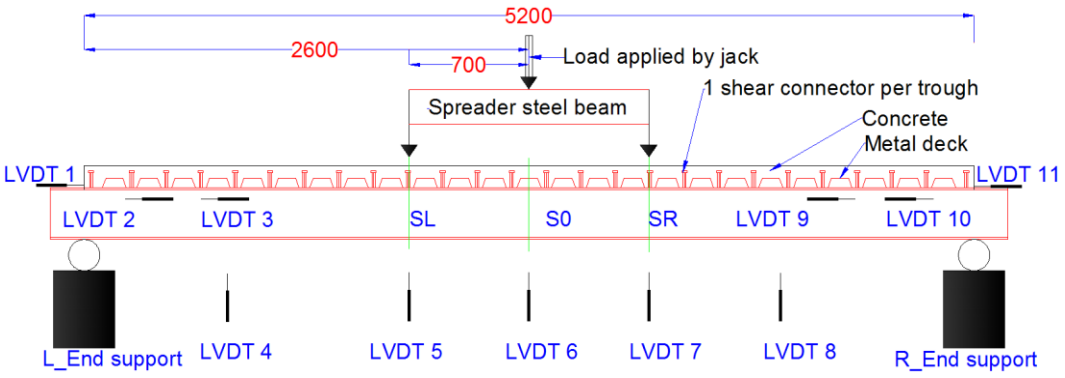

Figure 5-3 Details of test layout and instrumentation

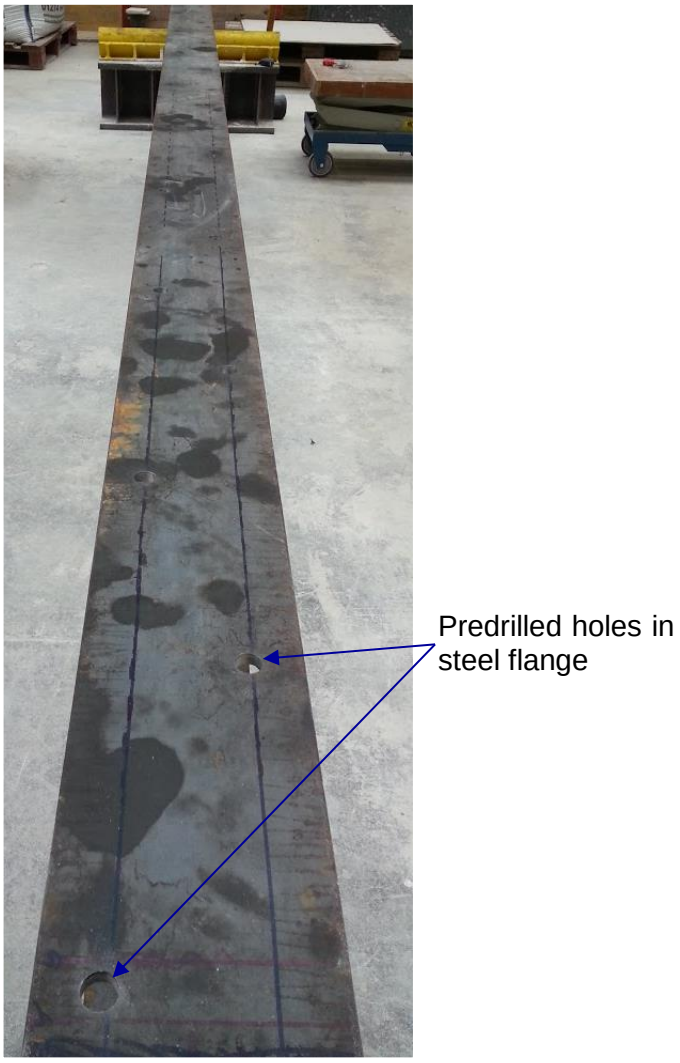

Figure 5-4 Predrilled hole in steel flange

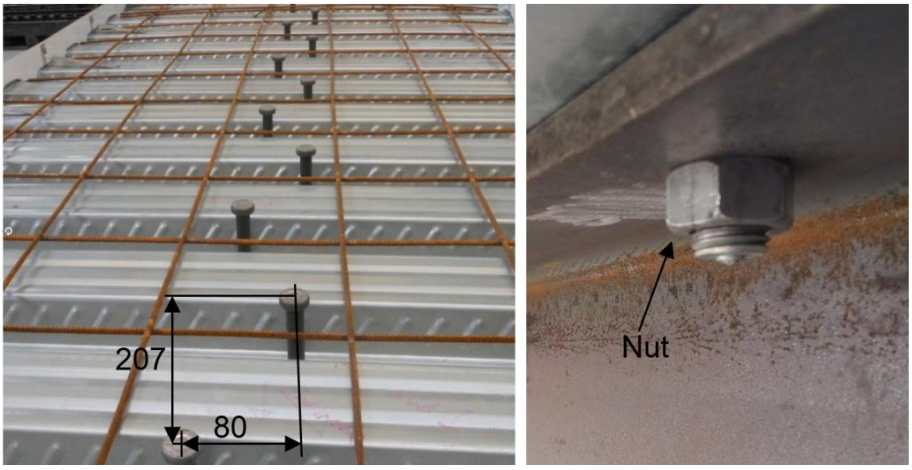

Figure 5-5. Staggered position of predrilled hole in steel flange and Installed demountable shear connectors

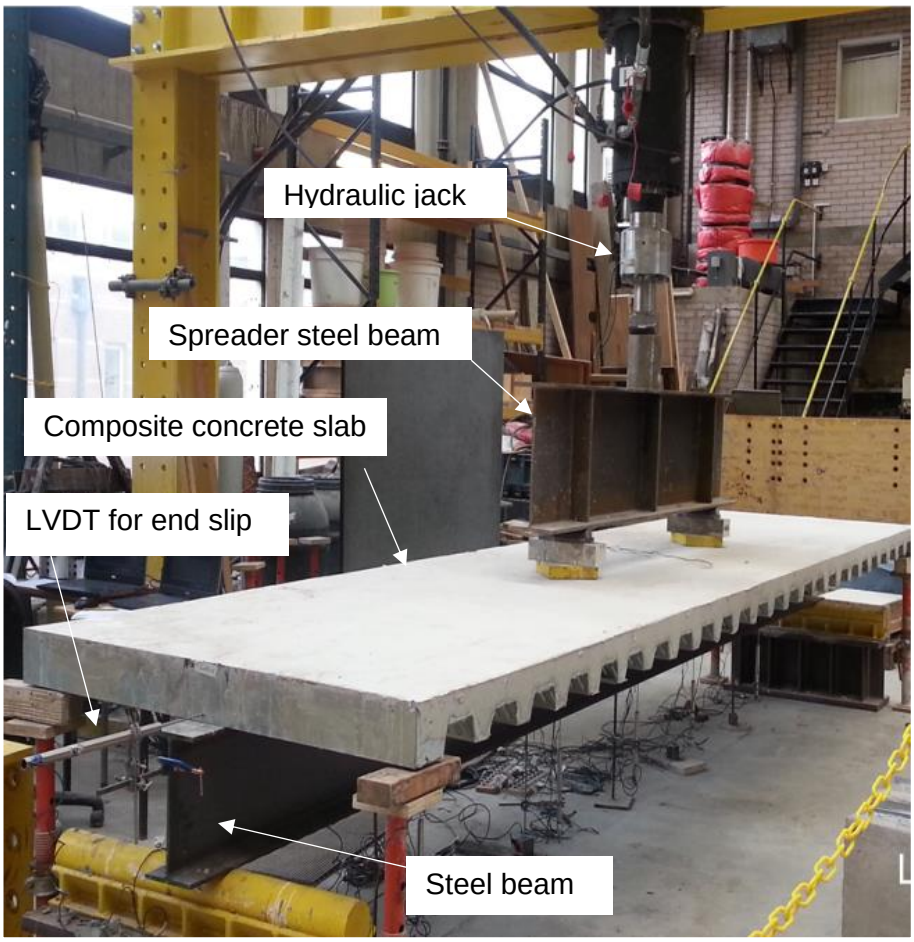

Figure 5-6 Test set up of DCB specimen

The specimen was propped during the casting (wet concrete) stage so that the full self-weight load was applied to the shear connectors once the props were removed. This method of propping (construction) ensures the same thickness of the concrete slab throughout the specimen and minimise the pond effect due to wet concrete. The concrete was cured for 28 days and the concrete strength was determined by taking the average of four cubes casted on the same day with same concrete mix and tested on the test day. The mean compressive cube strength of the concrete was 37MPa. The ultimate tensile strength of a shear connector was found to be 510MPa using the coupon test as explained in section 3.5.2.

Table 5-1 details of test specimen

Total length of steel beam	5600 mm
Span length between supports (l)	5200 mm
Steel section	IPE 300
Thickness of steel flange (tf)	10.7 mm
Thickness of steel web (tw)	7.10 mm
W_{Ply} of steel beam	602 cm^3
A_a cross sectional area	53.80 cm^2
f_y of steel beam	410 MPa
Concrete compressive cube strength	37 MPa
Distance between a point load and support (a)	1900 mm
Width of composite concrete floor (B_e)	1340 mm
Overall depth of composite concrete slab (h_s)	130 mm
Metal profiled decking	Cofraplus 60
Position of reinforcement mesh	Top of the metal decking
Height of metal decking	58 mm
Number of connectors	26
Trough spacing	207mm
Reinforcement mesh type	A142 (Standard)

5.2.2 Welded composite beam specimen (WCB)

An identical composite beam was tested with conventional welded shear connectors. All the dimensions were kept the same as used for the demountable composite beam test and presented in Figures 5-2, 5-3, 5-5 and Table 5-1. An identical steel beam section IPE 300, profiled metal deck Cofraplus 60, shear connector (same dimensions, such as diameter and

length inside concrete slab) as shown in Figure 5-7, reinforcement mesh and concrete mix design were used. The only difference between the two specimens was the types of shear connection (welded and demountable).

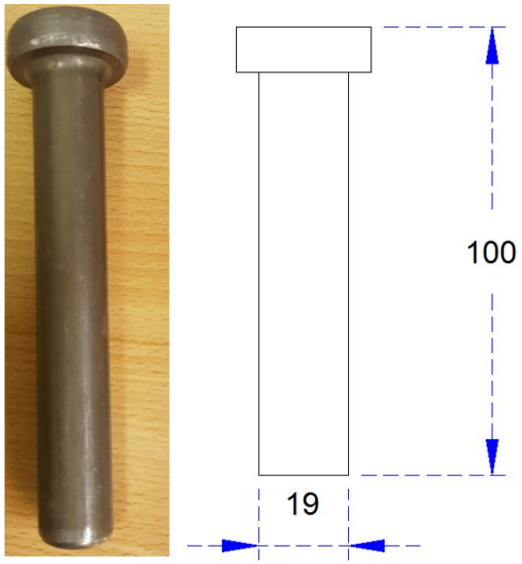

Figure 5-7 Detail of shear connector used for WCFS specimen

5.3 Instrumentation

The specimens were heavily instrumented to get as much information as possible. Eleven linear variable displacement transducers (LVDTs) were installed to measure the end slip, vertical deflection and relative slippage between the steel beam and the composite concrete slab as shown in Figure 5-3. Thirteen strain gauges were installed on the steel beam and three on the top surface of the composite concrete slab as shown in Figure 5-8, to measure the strains in the concrete and steel beam. A central computer-controlled logging system was adopted to record all data.

Three sets of strain gauges were placed on the steel beam at three different locations, one in the middle section (S0) and other two just under the loading section (SL and SR). In each set one strain gauge was placed on the top

flange and one on bottom flange. Two strain gauges were used on the web of each steel section at a distance of 75mm above and below the centre of web. One strain gauge was placed on the centre of web in the middle steel section (S0).

The gauges had 120±0.5Ω resistance with gauge factor of 2.13. The strain gauges were used to measure the strain distribution in the steel beam during bending and to monitor the yielding of the steel beam. Later the strain values were used to calculate the neutral axis.

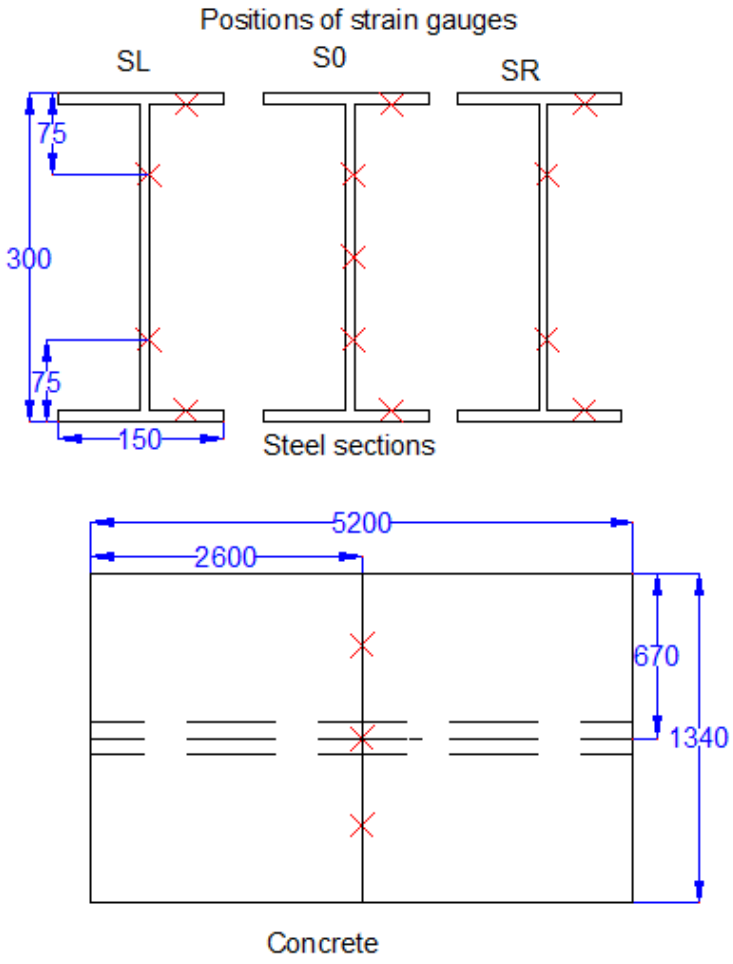

Figure 5-8. Positions of strain gauges at steel beam and concrete slab

5.4 Loading

Both composite beam specimens were tested under a two-point loading system as shown in Figures 5-3 and 5-6. The vertical downward load was applied by a 1000kN hydraulic jack and the load was distributed through a spreader steel beam into two points. Both specimens were tested using a similar loading procedure and conditions. The hydraulic jack, LVDTs and strain gauges were calibrated before the start of the test.

Four different static loading regimes were used to test the specimen under loading and unloading cycles. The specimen was loaded to observe the behaviour of the specimen under a normal working load of 5kN/m^2 (BS EN 1991-1-1:2002) and unloaded once the targeted load was reached. This loading was repeated for four cycles (C1-C4) for the demountable specimen to examine any initial slip and deflection due to the clearance holes between the shear connectors and the holes in the steel flange.

The second loading (C5) and third loading (C6) were 1.5 times (7.5 kN/m^2) and 3 times (15 kN/m^2) of the normal working load respectively. Finally, the specimen was loaded to its ultimate capacity (C7), which was 48.9 kN/m^2, about 9 times of the working load.

5.5 Companion Push-off test

5.5.1 Test specimens

Two identical companion push off specimens were tested to assess the shear capacity of a demountable shear connector under maximum shear loading. Two identical composite concrete slabs, demountable shear connectors and a steel section was used in the push off test as illustrated in

Figure 5-9. The width, height and thickness of the concrete slab was 610 mm, 510 mm and 150 mm respectively. The steel reinforcement of 10 mm diameter was adopted and a single demountable shear connector as shown in Figure 5-9 was used in the centre of each trough of the profiled metal decking with staggered positions as utilised in the composite beam test specimen.

The push off test specimens were prepared using the same profiled metal decking cofraplus 60 and demountable shear connectors as adopted in the composite beam test and casted on the same day with the same concrete mix as used for the composite beam specimen. The compressive strength of the concrete was determined on the day of the push off test using an average of four cube tests.

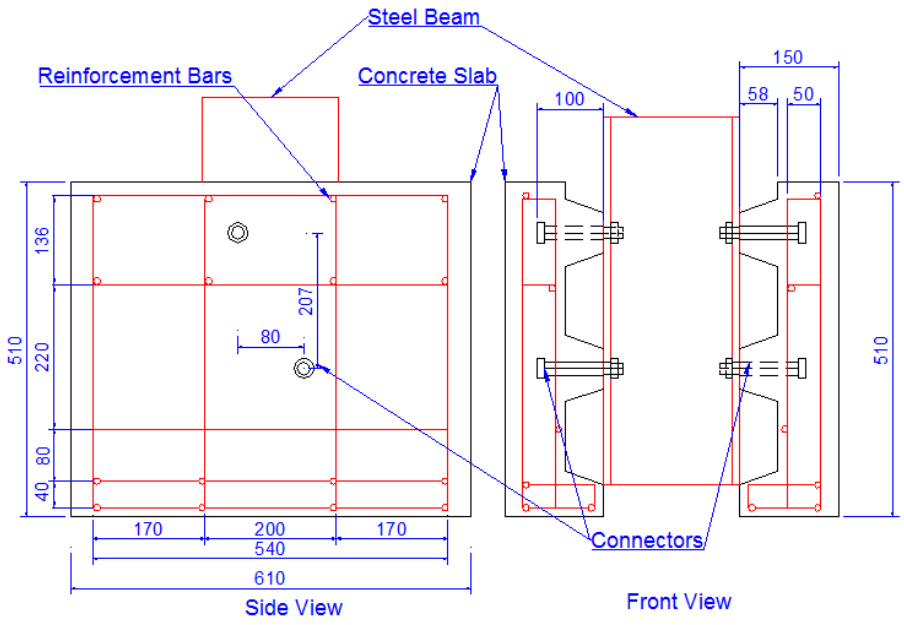

Figure 5-9 Push off test detail

5.5.2 Instrumentation

Eight linear variable displacement transducers (LVDTs) were installed at the top of the steel beam and on the composite concrete slabs to measure the vertical displacements as shown in Figures 5-10 and 5-11, which were subsequently used to calculate the relative slip between the steel beam and the composite concrete slab.

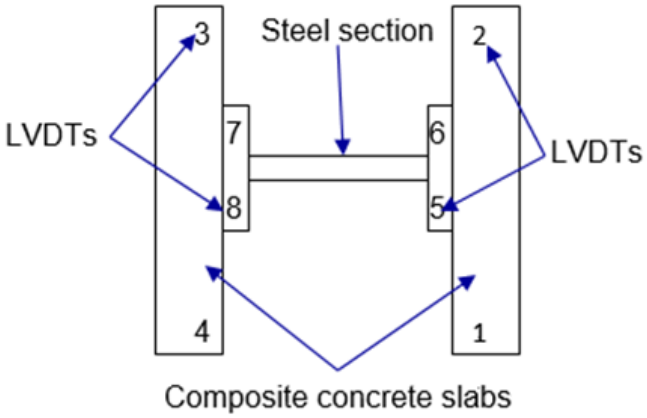

Figure 5-10. Position of LVDTs

5.5.3 Testing procedure

A Hydraulic jack was used to apply the load vertically downward on the top of the steel section as illustrated in Figure 5-11 until failure was reached. During the test, the applied load was increased by 5 kN/min until it reached 40% of the predicted failure load based on the Eurocode 4 (2004) equations ($P_{rd} = min\left(0.29\alpha K_t\, d^2\sqrt{f_{ck}E_{cm}}\,,\ 0.8K_t f_u \frac{\pi d^2}{4}\right)$). Then the loading was changed to displacement control method to see the plateau of the load slip curve until the failure of the specimen and to avoid any sudden failure. All the data was recorded automatically using a data logging system.

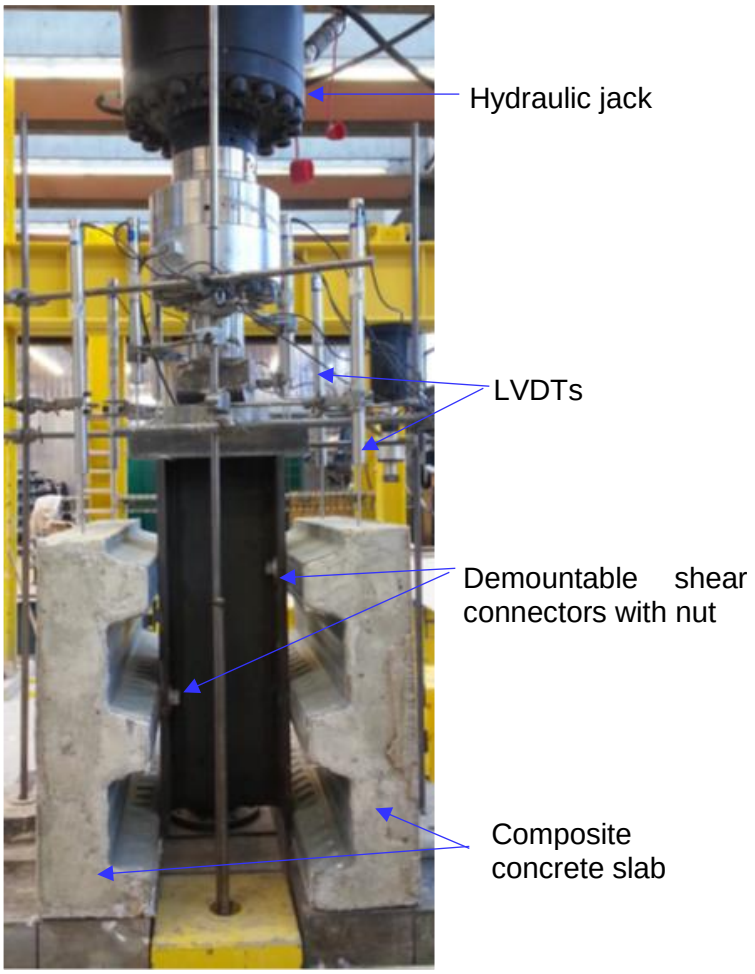

Figure 5-11. Push off test setup

5.6 Experimental results and discussion

5.6.1 Composite beam test results

Table 5.2 presents the ultimate load capacity and moment capacity of the demountable composite beam (DCB) and the welded composite beam (WCB). The ultimate loads do not include the self-weight of the composite beam and the spreader beam. Initially the specimens were loaded to 5 KN/m^2 and unloaded. Then specimens were further loaded up to 7.0 KN/m^2 and 15 KN/m^2 and unloaded respectively. This loading was undertaken to ensure that the specimen was in the elastic region in these initial loading regimes. Afterward, loading was increased statically with the increment of

1kN/m^2 to avoid any sudden failure until the ultimate load capacity was achieved.

The imposed failure load was recorded as 340.54 kN and 338.12 kN for the DCB and WCB specimens respectively. If the self-weight of the concrete composite slab, spreader steel beam and steel beam was taken into account in the DCB test specimen, the total failure load added up to 359.2kN. Considering the global safety factor of 2.5 for the un-factored load of 143.68kN. This load bearing capacity of 143.68 kN can be achieved well before the start of the plastic deformation of DCB specimen.

Table 5-2 Test results of composite floor systems

Test Specimen ID	Concrete cube strength (Mpa)	Total ultimate load (kN)	Ultimate deflection (mm)	Moment capacity (kNm)
DCB	37	340.54	81.19	323.5
WCB	36	338.12	59.11	321.2

5.6.2 Push off test results

Table 5-3 presents the results of the push off tests which are used to determine the shear capacity and degree of shear connection in the composite beam test. The average shear capacity of the demountable shear connectors was about 39 kN per connector in two push off tests. Figure 5-12, presents the load slip behaviour of two push off tests. The behaviour of demountable shear connections was very ductile as the limit of 6 mm for ductile behaviour according to Eurocode 4 is fulfilled.

Cone concrete failure mode was observed in these two push off tests as presented in Figures 5-13 and 5-14, which was possibly due to the smaller effective width of the profiled metal decking trough.

Table 5-3 Test results of push off specimens

Test specimen ID	Concrete cube strength (MPa)	Load per connector (kN)	Slip at maximum load (mm)	Slip at failure (mm)
POT1	37	39.2	11.60	12.80
POT2	36	38.5	11.20	12.40

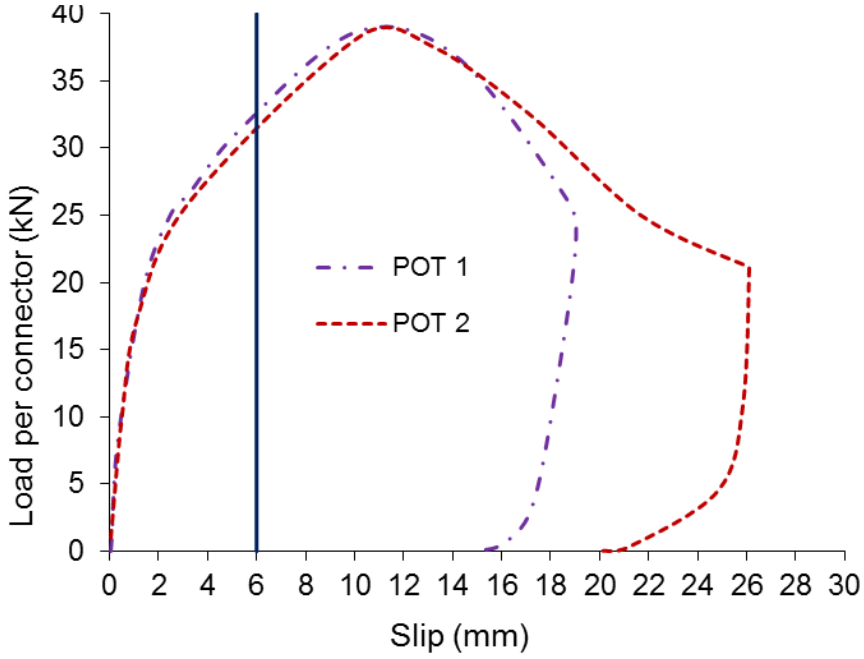

Figure 5-12 Load slip behaviour in push off tests and limit of 6 mm

Figure 5-13 Concrete cone failure in POT 1

Figure 5-14 Concrete cone failure of POT 2

5.6.3 Load deflection behaviour of composite beam test

Figure 5-15 presents the relationship between mid-span deflections at different loading cycles in the DCB specimen. The deflection at the 3 times working load was less than the span/500, which indicates the capacity of low residual deflection in demountable composite flooring systems. The deflection at ultimate load reached about span /65.

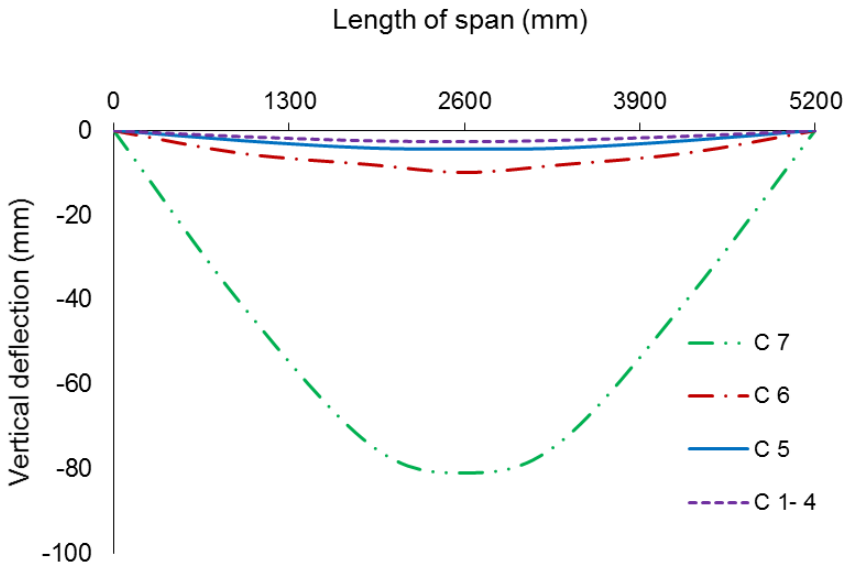

Figure 5-15 Deflection of DCB beam test at different loading cycles

Table 5-4 Deflection at mid span of DCB specimen

Load cycles	1.0 x working load (C1-4)	1.5 x working load (C5)	3.0 x working load (C6)	Ultimate loading (C7)
Load (kN/m^2)	5.0	7.5	15.0	48.87
Deflection at maximum load in each loading cycle (mm)	2.6	3.8	8.8	78.80
Residual deflection (mm)	0.6	0.8	1.0	43.26
Cumulative residual deflection (mm)	0.0	0.6	1.3	2.30
Cumulative deflection at maximum loading(mm)	2.6	4.4	10.1	81.19

The maximum mid-span deflection and residual deflection against a uniformly distributed load obtained from the test is given in Table 5-4. The residual deflection of 0.6 mm was observed under the first cycle of the working load. This was caused by the clearance holes in the steel flange and no further residual deflection was observed when the same working loading was repeated. The residual deflection was increased gradually with the increase in load.

5.6.4 Load slip behaviour of the composite beam

The load slip behaviour at both ends of the DCB specimen is presented in Figure 5-16. More than 6 mm of slip was recorded on both ends. This fulfils the EC4 requirement of ductility. Under the first cycle of normal working load,

an average end slip of 0.09 mm on the left end and 0.14 mm on the right end were observed.

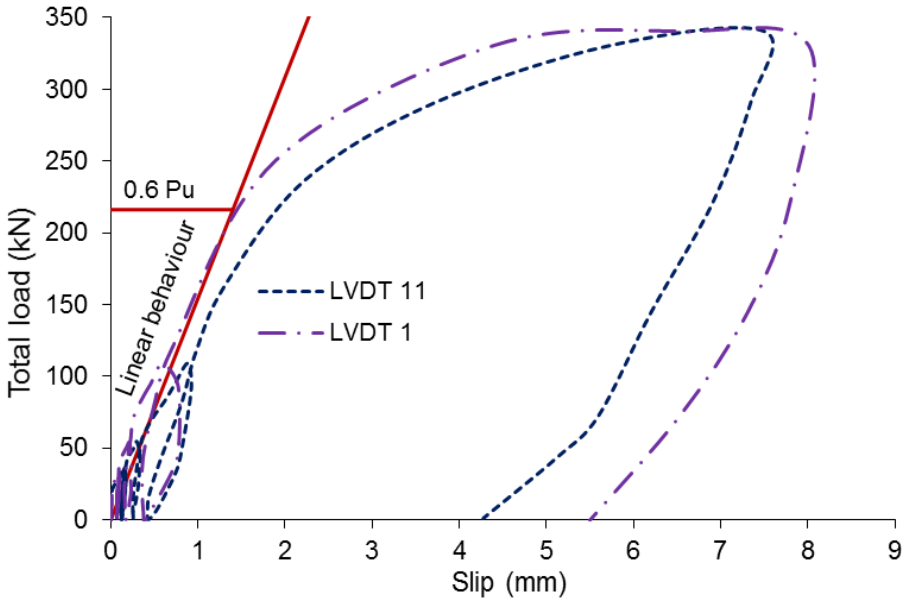

Figure 5-16 Load slip behaviour at LVDT 1 (Left end) LVDT 11 (Right end) of DCFS specimen

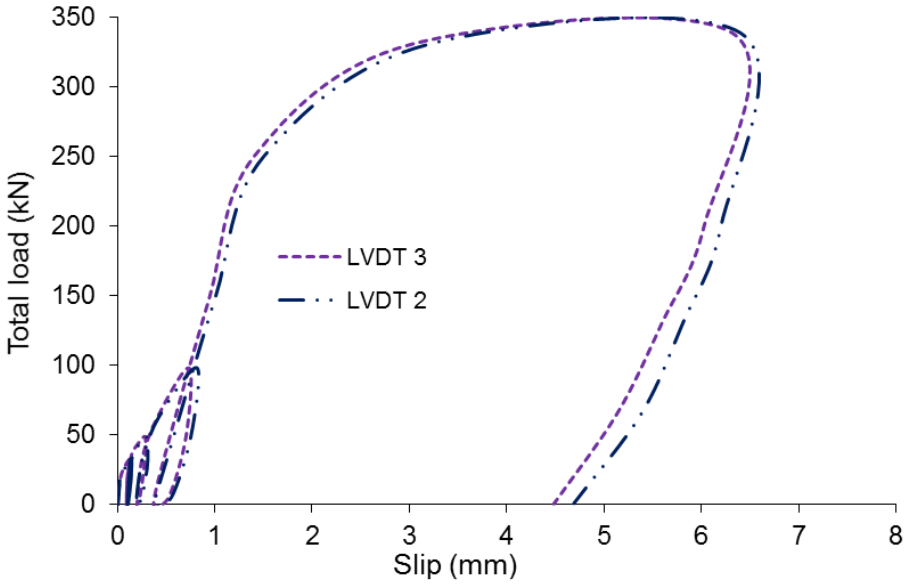

Figure 5-17 Load slip behaviour of 2nd (LVDT 2) and 4th (LVDT 3) connectors at left end of DCFS specimen

After four cycles of working load, the residual end slip was less than a quarter of a millimetre. This clearly indicates a low degree of end slip at the working

load. The load via end slip behaviour was almost linear up to 60% of the ultimate load as seen in Figure 5-16 at both ends of the DCB specimen.

The maximum end slip and residual slip for the specimen under various loading cycles is given in Table 5-5. It can be seen the end slip and the residual slip increased gradually with the increase in loading.

Table 5-5 Summary of end slips of DCB specimen

Load cycles	1.0 x working load (C1-4)	1.5 x working load (C5)	3.0 x working load (C6)	Ultimate loading (C7)
Load (kN/m^2)	5.0	7.5	15.0	48.87
Slip at each loading cycle LVDT1 (mm)	0.09	0.14	0.42	6.19
Residual slip LVDT1 (mm)	0.07	0.09	0.23	5.01
Cumulative residual slip LVDT1 (mm)	0.0	0.07	0.16	0.39
Cumulative slip by LVDT1 (mm)	0.09	0.21	0.58	6.58
End slip at each loading cycle LVDT11 (mm)	0.14	0.19	0.65	6.91
Residual slip LVDT11 (mm)	0.11	0.12	0.26	3.87
Cumulative residual slip LVDT11 (mm)	0.0	0.11	0.23	0.49
Cumulative slip by LVDT11 (mm)	0.14	0.30	0.88	7.40

The slip between the steel beam and the profiled metal deck composite concrete slab at the positions of the 2nd (LVDT 2) and 4th shear connectors (LVDT 3) was presented in Figure 5-17. It can be seen that both the 2nd and

4th connectors showed similar behaviour. The slip at the position of the 2nd connector was slightly higher compared to that of the 4th connector. An initial slip of about 0.1 mm was observed for both connectors under the first cycle of the normal working load.

Table 5-6 Slip behaviour at 2nd (LVDT2) and 4th (LVDT3) connector at Left End

Load cycles	1.0 x working load (C1-4)	1.5 x working load (C5)	3.0 x working load (C6)	Ultimate loading (C7)
Load (kN/m^2)	5.0	7.5	15.0	48.87
Slip at each loading cycle LVDT2 (mm)	0.1	0.13	0.69	6.03
Residual slip LVDT2(mm)	0.09	0.11	0.26	5.1
Cumulative residual slip LVDT2 (mm)	0.0	0.09	0.20	0.46
Cumulative slip by LVDT2 (mm)	0.1	0.22	0.79	6.47
End slip at each loading cycle LVDT3 (mm)	0.1	0.14	0.56	7.6
Residual slip LVDT3 (mm)	0.08	0.1	0.21	4.96
Cumulative residual slip LVDT3 (mm)	0.0	0.08	0.18	0.39
Cumulative slip by LVDT3 (mm)	0.1	0.22	0.74	7.09

Tables 5-6 and 5-7 present the maximum relative slip and residual behaviour between the profiled metal deck composite concrete slab and steel beam top flange at the positions of the 2nd and 4th shear connectors of the specimen from the end supports. The low residual slip, after loaded to 3 times the

working load indicates a good composite action between the steel beam and the composite concrete slab.

Table 5-7 Slip at 2nd (LVDT10) and 4th (LVDT9) connectors at Right End

Load cycles	1.0 x working load (C1-4)	1.5 x working load (C5)	3.0 x working load (C6)	Ultimate loading (C7)
Load (kN/m^2)	5.0	7.5	15.0	47
Slip at each loading cycle LVDT9 (mm)	0.13	0.15	0.31	5.95
Residual slip LVDT9 (mm)	0.10	0.10	0.75	5.13
Cumulative residual slip LVDT9 (mm)	0.0	0.10	0.20	0.95
Cumulative slip by LVDT9 (mm)	0.13	0.25	0.51	6.90
End slip at each loading cycle LVDT10 (mm)	0.13	0.17	0.39	6.10
Residual slip LVDT10 (mm)	0.11	0.10	0.15	6.10
Cumulative residual slip LVDT10 (mm)	0.0	0.11	0.21	0.36
Cumulative slip by LVDT10 (mm)	0.13	0.28	0.60	6.46

5.7 Comparison with welded specimen

The results of the full scale bending tests are given in Table 5-2 and load vs deflection curves are shown in Figure 5-18. The load deflection curve of the DCB tested specimen is compared with the WCB tested specimen. Similar load bearing capacity was observed in both specimens. However, the specimen with demountable shear connectors demonstrated better ductility,

which was about 30% higher than the specimen with conventional welded shear connectors. The mid-span deflection of the DCB specimen went up to 80mm (span/65) at ultimate loading. This showed that the DCB specimen exhibited excellent ductility. The load deflection curve was almost linear up to 70% of the ultimate load (P_u) as illustrated in Figure 5-18.

The overall stiffness was very similar in both specimens but the initial stiffness of the DCB specimen was lower compared to the welded (WCB) specimen. This was possibly caused by the tolerance of installation of the demountable shear connectors where the diameter of the shear connector collar is 1 mm smaller than the diameter of the hole in the steel beam flange.

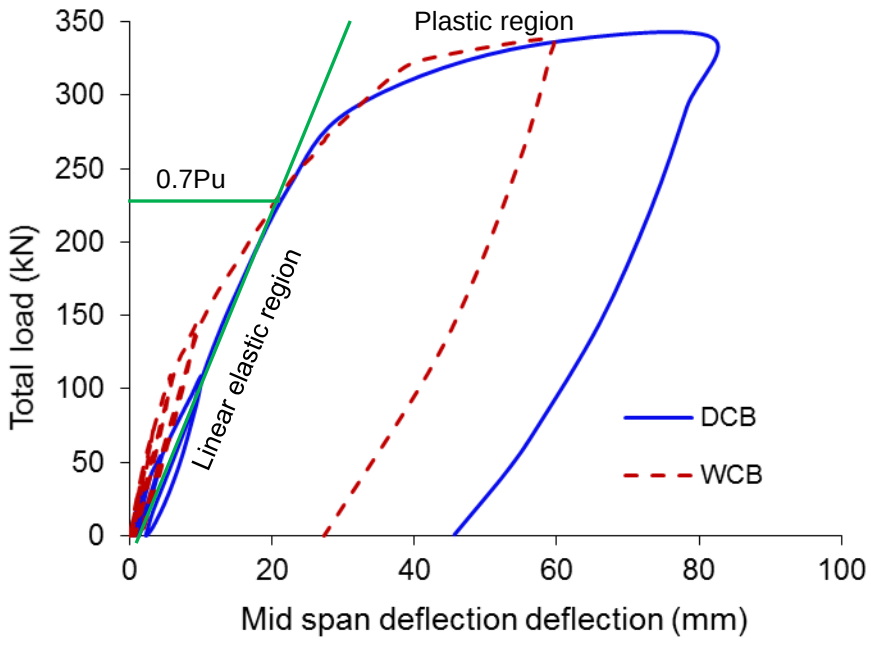

Figure 5-18 Load vs deflection of DCFS and WCFS beam test

There was an initial deflection of 0.6 mm due to the hole in the demountable (DCB) specimen but this initial deflection was not observed in the welded (WCB) specimen. The overall residual deflection was about 66% more

compared to the welded specimen as shown in Figures 5-19 and 5-20. The behaviour of both specimens is similar if the residual deflection was ignored in both cases as presented in Figure 5-21.

In both specimens, the initial slip was observed but the difference was 70% more in the demountable (DCB) specimen. The overall initial residual slip was 52% more in the demountable specimen compared to the welded specimen. The higher values for the difference could be the possible effect of an oversized hole or nut tightening forces.

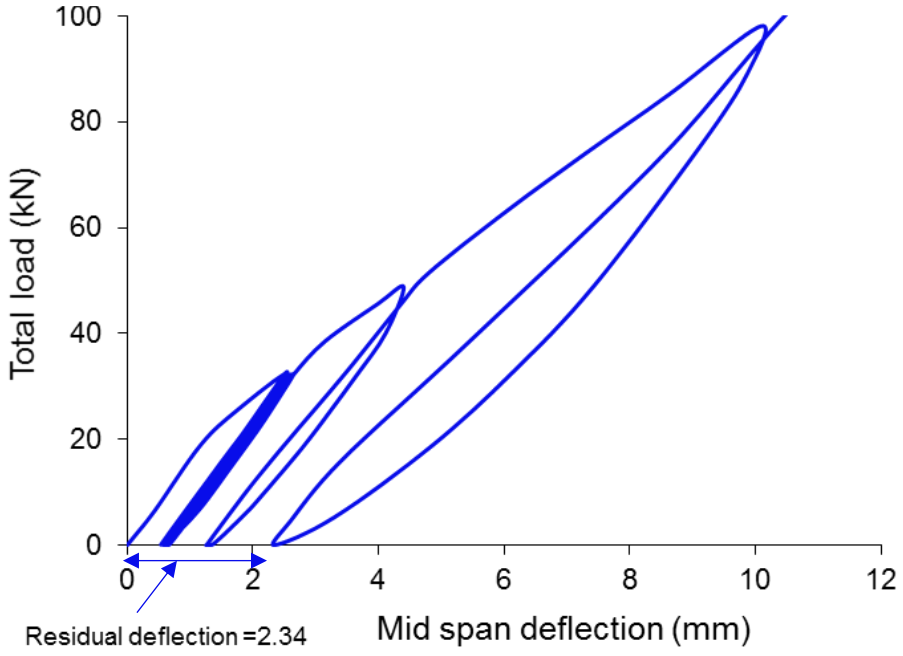

Figure 5-19 Residual deflection in DCB

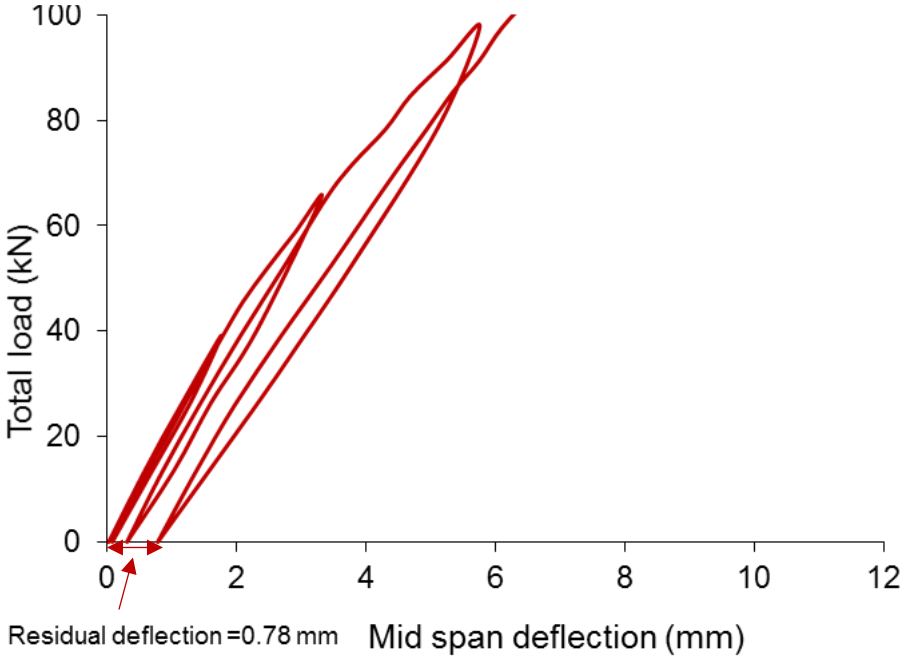

Figure 5-20 Residual deflection in WCB specimen

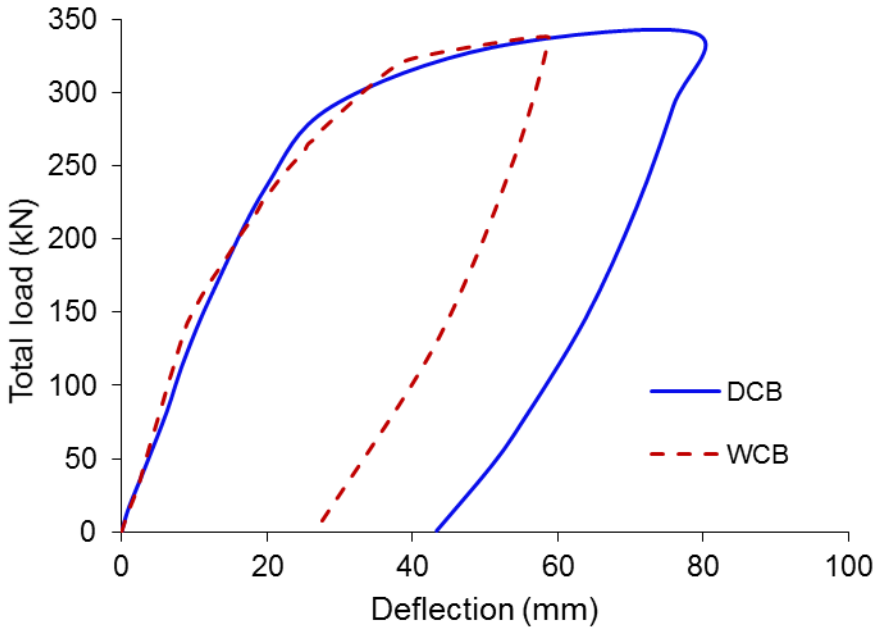

Figure 5-21 Load deflection behaviour with residual deflection

5.7.1 Stiffness

Figures 5-22 and 5-23 presents the stiffness of the WCB and DCB test specimens. The stiffness is worked using the end slip values and half of the total load. The stiffness in the demountable composite beam is very low

compared to the welded composite beam specimen. But the overall stiffness is similar and at 84% of the ultimate load, stiffness becomes almost equal.

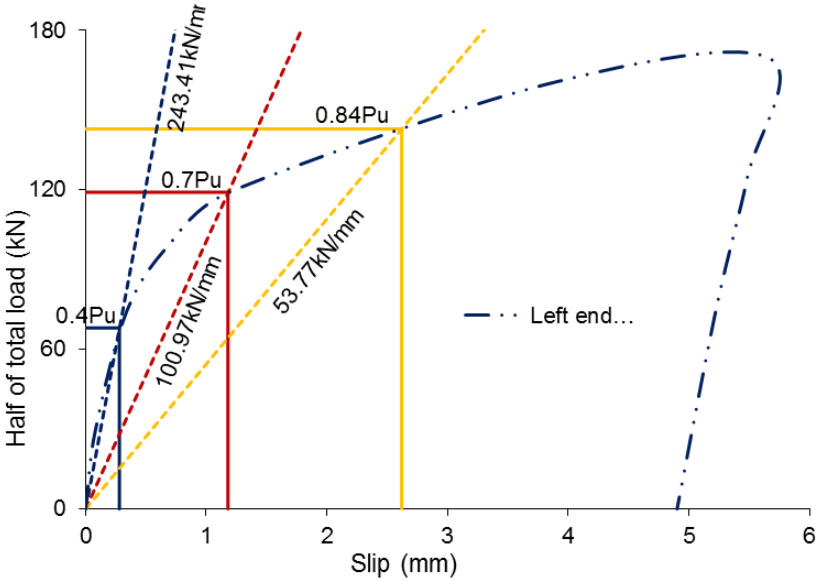

Figure 5-22 Stiffness in WCB specimen

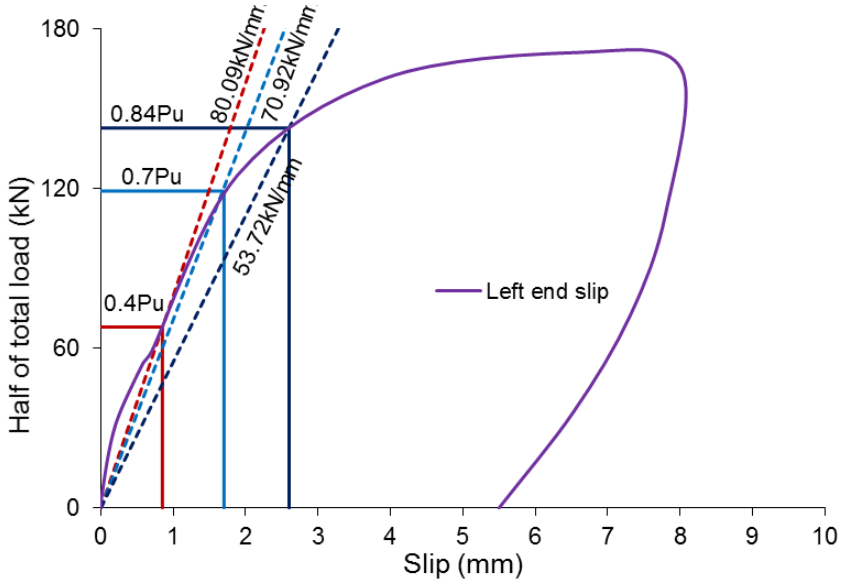

Figure 5-23 Stiffness in DCB specimen

5.8 Mode of failure

There was no major failure observed during the testing of the DCB specimen. The test was terminated when the steel beam was fully yielded as seen from

the strain values, the load carried remained approximately constant. There was no indication of a demountable shear connector or nut failure. Cracks were seen on the top surface of the slab in the longitudinal direction of the beam. No major cracks were detected on the side edges of the concrete slab. There was no evidence of deck separation or concrete pull out during the test. There was a little evidence of uplifting of a composite concrete slab at the middle section after unloading the specimen at the end of the test.

5.9 Demountability

The demountable composite beam (floor system) was also evaluated for demount- ability at the end of the test. To verify that the structural parts of the demountable composite floor system could be demounted and reused at the end of the design life. The demountable composite beam (DCB) was loaded up to its ultimate moment capacity and then unloaded. The nuts were checked at the end of the test and no failure was observed regarding the nuts as they were in their place. The nuts were easily demounted using an ordinary spanner.

After a careful examination of the tested specimen, a fork-lift truck and crane were used to lift the whole composite concrete slab off the steel beam. The composite concrete slab was completely lifted off the steel beam as shown in Figure 5-24 without any difficulty at the end of the test. There was no major damage to the collar or threaded parts of the shear connectors as can be seen in Figures 5-25 and 5-26.

Thus, the experiment demonstrated that the demountable shear connectors in a composite beam (floor system) allowed the demounting of a composite

concrete slab from a steel section, even when the specimen was loaded up to its ultimate capacity. This demonstrates that demountable shear connectors in composite floor systems have the potential to be used in sustainable composite construction. The demountable shear connectors will allow the steel beam and precast composite concrete slabs to be reused after the structural design life without going into the recycling process.

Figure 5-24. Demountability of specimen

Figure 5-25. Connectors after demounting

Figure 5-26 Demountable connectors after test

5.10 Conclusions

Full-scale composite beams with demountable shear connectors and conventional welded shear connectors were tested. The structural behaviour of a demountable composite beam is fully described in this chapter and a comparison with a welded composite beam was also carried out. According to the comparison and analysis, the following conclusions may be made.

- The structural behaviour of the demountable composite beam was very similar to the composite beam system using conventional welded shear connectors.
- The demountable composite beam (DCB) showed about 30% higher ductility compared to the specimen (WCB).

- The initial stiffness of DCB specimen was lower compared to that of WCB specimen, but it becomes almost equal at 84% of ultimate load.
- The deflection of the DCB specimen at three times the normal working load was just about span/500 and without any yielding of the steel beam section. This indicates the capacity of low residual deflection in demountable composite flooring systems.
- The deflection at ultimate loading was recorded about span /65.
- The low slip (less than 1mm) at both ends of DCB specimen after loaded to 3 times the working load indicates a good composite action between the steel beam and the composite concrete slab.
- Composite beams with demountable shear connectors can be demounted and reused successfully when loaded to within the service loading range.

Chapter 6
Finite element modelling and parametric study

6.1 Introduction

Although experimental tests provide more accurate and valuable results it is a very costly and time consuming practice. Also, it is not possible to cover the whole range of parameters in an experimental study, needed for a complete investigation. Therefore, a three dimensional finite element (FE) model was developed to simulate the structural behaviour of the composite structure with demountable shear connectors using finite element software ABAQUS (2012). The main purpose of the finite element model was to study the behaviour of demountable shear connectors in composite structures under the effect of different parameters.

The push off tests and composite beam test experiments explained in chapter 3 and 5 are used to develop the finite element (FE) model. The FE model was validated against the experimental results before a parametric investigation was considered. The main parameters, including concrete compressive strength, connector collar diameter, transverse spacing between connectors and the hole's clearance between the connector's collar and the steel flange hole, were used to investigate the behaviour of demountable shear connectors in a composite structure and the effect on the strength of a shear connection.

6.2 Finite element (FE) modelling of push off test

ABAQUS (2012) is a general purpose finite element programme and it may be used to simulate the push off test. The dynamic explicit analysis approach

is used in this study. The push off test experiments as described in section 3.2 and Figure 3-3 are used to develop a FE model. Only half of the geometry of the push off test was created due to the symmetrical conditions across the centre line of the web of the steel beam to save computational time.

The main components of the FE model included the profiled metal decking, concrete slab, steel beam, reinforcement steel cage and demountable shear connector as shown in Figure 6-1. All components were modelled separately and assembled together as shown in Figure 6-2 to form one half of the push off test specimen.

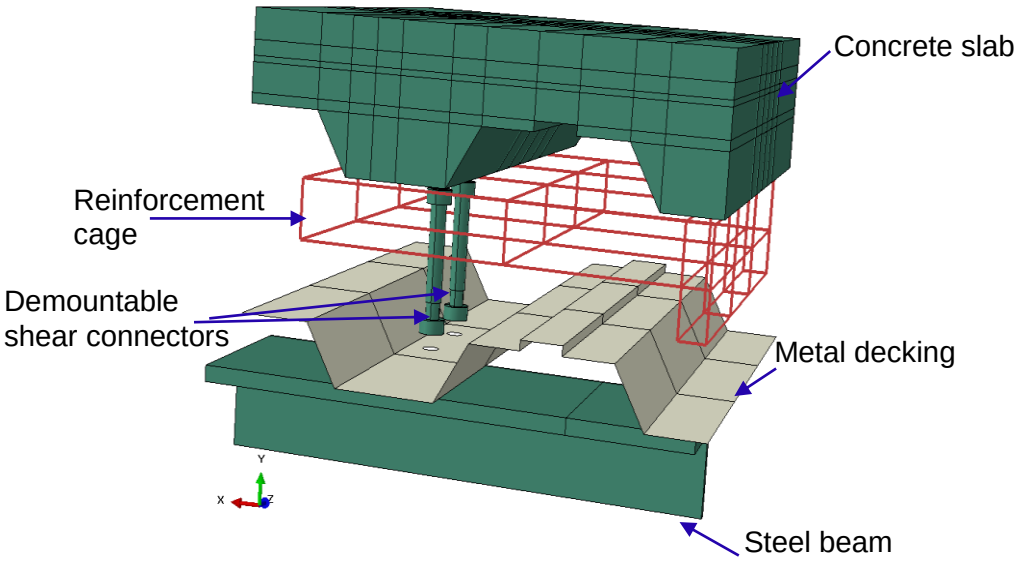

Figure 6-1 FE Model for push off test

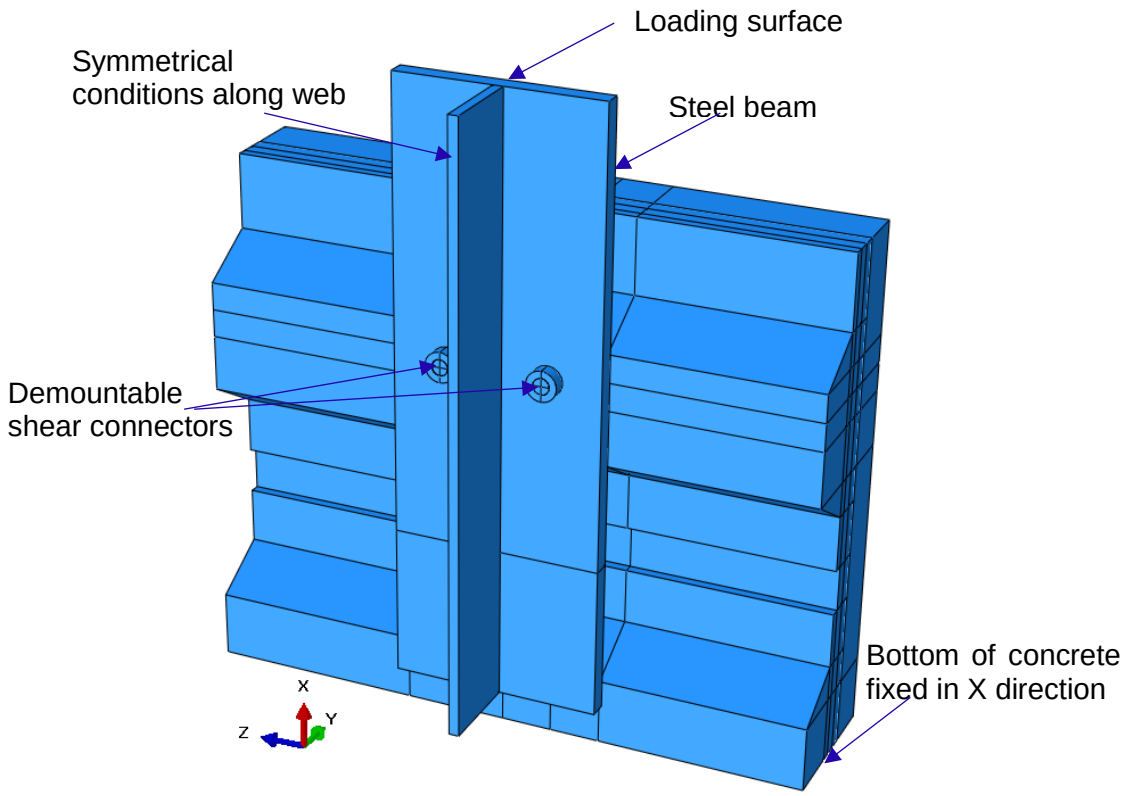

Figure 6-2 Assembled POT

6.2.1 Element type and mesh

The three dimensional eight nodes solid brick elements C3D8R with reduced integration is adopted to mesh the concrete slab, steel beam, shear connector and nut. In these elements, each node has 3 translational degrees of freedom (DOF) and prevents shear locking. The brick elements give a solution of comparable accuracy at a better rate of convergence and less computational time than the other elements.

A two node truss element T3D2 is used for the reinforcement bars. The truss element in ABAQUS can be used in two or three dimensions to present a slender structural element that resists and transfers only axial forces. It can also be used to model components where strain is calculated from the change in length (ABAQUS, 2012). The advantage of using a truss element

is that the perfect-bond can easily be defined by embedding the steel bars into a host region (concrete beam).

The metal profiled decking is a very thin material therefore shell element with reduced integration (S4R) is used for the metal profiled decking. Generally, this type of element is very useful for thin walled structures which observed large deformation.

6.2.2 Contact interaction and boundary conditions

Once all the parts of the push off test model are assembled together as shown in Figure 6-2 the appropriate contact interactions are defined between interacting surfaces of different components. The contact pair method is used to define the surface to surface contact between the concrete slab and the metal profiled decking. The normal behaviour is assumed to be hard as this type of normal behaviour allows minimum penetration of the salve surface into the master surface. The penalty method is used to define the tangential friction with a coefficient of 0.4 after using 0.3, 0.4 and 0.45 which give more reliable results as compared with the experimental results.

The contacts among the steel beam, shear connector and nut is also defined using the contact pair method. The normal behaviour is defined as hard contact and the tangential behaviour is defined as penalty frictional with a coefficient of 0.40 after calibration and similar value is adopted by Pathirana et al. (2016). The same contact pair method is used for the interaction of the steel beam with metal decking and interaction between concrete and shear connector.

All nodes of the concrete slab at the base are fixed only in X directions as shown in Figure 6-2 to simulate the actual experimental boundary conditions. The symmetry conditions were applied on the web of the steel beam. The reinforcement steel cage truss elements are embedded inside the solid elements of concrete using embedded constraint as it is assumed that no slip or deboning occurred between the concrete and steel bars.

6.2.3 Loading technique

The push off FE model is analysed using the dynamic explicit method, uniform velocity was used on the loading surface as shown in Figure 6-2 to push the steel beam downwards. A smooth amplitude function was adopted to achieve the quasi static conditions. Initially the steel beam was pushed downward vertically with the velocities of 0.15 mm/s 0.20 mm/s and 0.25 mm/s to examine the difference in results. The velocity rate of 0.20 mm/s was found to be the more appropriate velocity rate to simulate the push off model and also adopted by C. Xu et al. (2012). The total force applied to the specimen was calculated by summing up the vertical reaction forces for the loading surface.

6.3 Material Modelling

6.3.1 Material model of Concrete

The concrete model is a very important part of the simulation for the push off model, the concrete is mainly subjected to compression and tensile splitting as observed in the experimental study. It was observed that the failures were either due to concrete or connector shearing or a combination of sheared

connectors and concrete cone failure. Therefore, a suitable concrete material model is very important for the accuracy of the FE model.

In terms of the behaviour of concrete, the concrete damaged plasticity model was used to define the concrete in this study. This concrete model is capable to model the concrete under arbitrary loading, including cycling loading and assumes an isotropic damaged elasticity in tension and compression to present the inelastic behaviour of concrete.

The damaged plasticity model can be used for plain concrete as well as for RC structures subjected to monotonic, cycling and dynamic loading under low confining pressure (ABAQUS, 2012). Concrete damage plasticity model has been successfully used for the concrete slab by Qureshi and Lam (2012, 2013) in numerical modelling. The damage plasticity model may deal with two basic failure modes, compressive crushing and tensile cracking of concrete. In this study, the damage plasticity model was adopted and the maximum tensile strength of concrete was taken as 10% of its compressive strength.

Elastic behaviour

The elasticity modulus E_{cm} used in the modelling was calculated based on BS EN 1992-1-1 method, as shown in equation 6-1. The poison's ratio for concrete was taken as 0.2 and density was considered as 2400 kg/m^3.

$$E_{cm} = 22\left(\frac{f_{cm}}{10}\right)^{0.3} \quad (6\text{-}1)$$

Concrete Damaged Plasticity model

Compressive behaviour

BS EN 1992-1-1 provides an equation for determining the compressive stress σ_c of concrete as shown in equation 6-2 under uniaxial compression. The stress strain relationship of concrete for nonlinear analysis is shown in Figure 6-3.

$$\frac{\sigma_c}{f_{cm}} = \frac{k\eta - \eta^2}{1 + (k-2)\eta} \quad (6\text{-}2)$$

$$f_{cm} = f_{ck} + 8 \quad (6\text{-}3)$$

$\sigma_c =$ Compressive stress in the concrete

Where, f_{cm}, is the mean value of the concrete cylinder compressive strength and f_{ck}, is the characteristic compressive cylinder strength of the concrete

$$k = \frac{1.05 E_{cm} |\varepsilon_{c1}|}{f_{cm}} \quad (6\text{-}4)$$

$$E_{cm} = 22 \left[\frac{f_{cm}}{10}\right]^{0.3} \quad (6.5)$$

$$\eta = \frac{\varepsilon_c}{\varepsilon_{c1}} \quad (6.6)$$

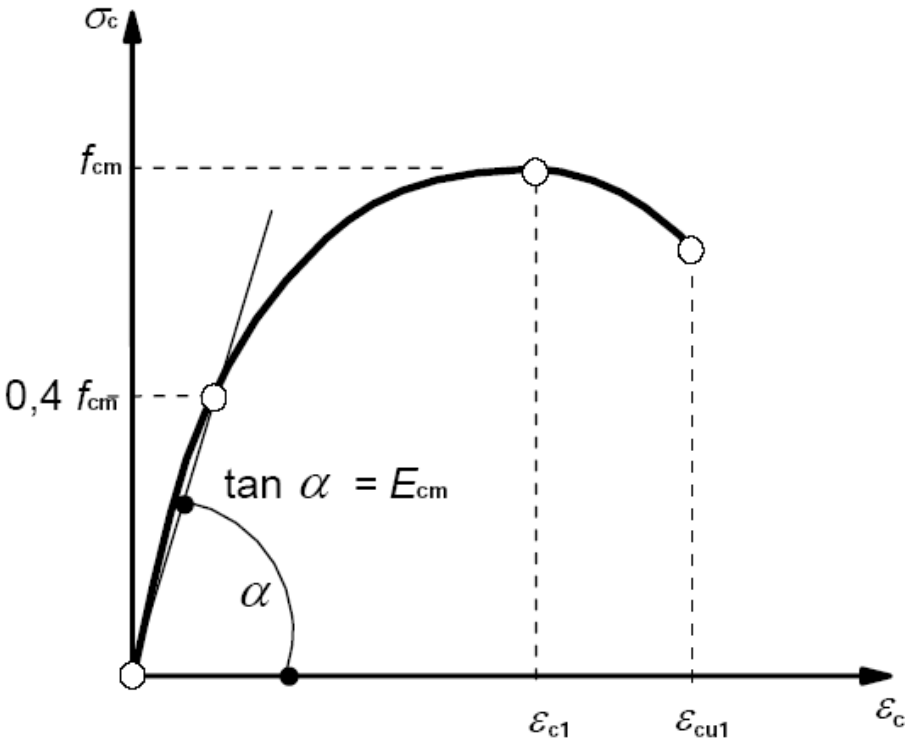

Figure 6-3 Schematic representation of stress strain relationship (BS EN 1992-1-1)

The value of the strain at peak ε_{c1} and nomial ultimate strain ε_{cu1} can be taken as 0.0022 and 0.0035 respectively, according to BS EN 1992-1-1, for the compressive cylinder strength of 12 to 50MPa. The nominal ultimate strain ε_{cu1} for concrete with a compressive strength greater than 50MPa can be calculated using the equation 6-7.

$$\varepsilon_{cu1} = 2.8 + 27\left[\frac{98 - f_{cm}}{100}\right]^4 \qquad (6\text{-}7)$$

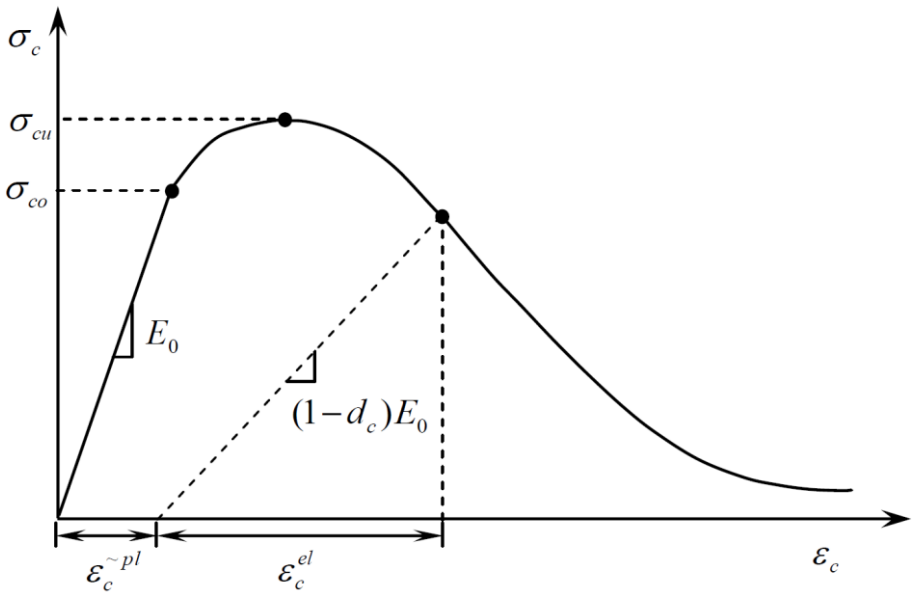

Figure 6-4 Response of concrete to uniaxial loading in compression (ABAQUS manual) (2012)

The response of concrete under uniaxial compressive loading is linear up to the initial yield stress σ_{co} as presented in Figure 6-4. After that concrete behaviour becomes plastic with stress hardening and followed by strain softening beyond the peak compressive stress σ_{cu} as shown in Figure 6-4. In the strain softening branch, the elastic stiffness of the material appears to be damaged if it is unloaded at any point and is known as the compressive damage variable, d_c. The value of zero for d_c is considered as undamaged and 1 is fully compressive damaged. The value of dc can be worked out using the equation 6-8 and 6-9 provided in the ABAQUS manual (2012). If E_0 is taken as elastic stiffness for undamaged concrete and ε_c is taken as total compressive strain.

$$\sigma_c = (1 - dc)E_0(\varepsilon_c - \varepsilon_c^{-pl}) \quad (6\text{-}8)$$

$$\varepsilon_c{}^{\sim in} = \varepsilon_c{}^{\sim pl} + \frac{d_c \sigma_c}{(1 - dc)E_0} \tag{6-9}$$

$\varepsilon_c{}^{\sim pl}$ is the compressive plastic strain and $\varepsilon_c{}^{\sim in}$ is the compressive inelastic strain

Tensile Behaviour

The softening behaviour of concrete can be expressed in a number of ways such as linear, bilinear and exponential. The ABAQUS manual provides a linear approach as shown in Figure 6-5 (a). Hillerborg (1985) developed a bilinear relationship as shown in Figure 6-5 (b). Cornelissen et al. (1986) presented an exponential relationship model for concrete softening behaviour as illustrated in Figure 6-5 (c).

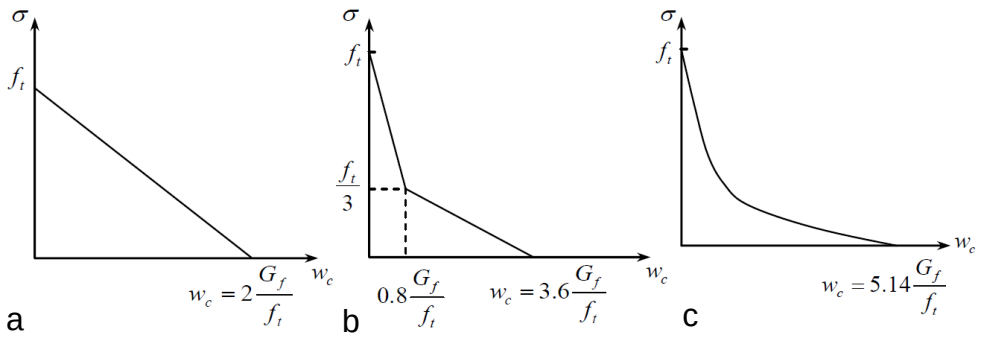

Figure 6-5 Tension softening model (a) linear (b) Bilinear (C) Exponential

As mentioned in previous sections, the axial tensile strength of concrete is worked out according to BS EN 1992-1-1 and the maximum tensile strength was taken as 10% of the compressive strength. The tensile damage variable d_t is worked out using the equation 6-10. The cracking displacement w is obtained from equation 6-11 using equation 6-12 to 6-14.

$$d_t = 1 - \frac{\sigma_t}{f_t} \quad (6\text{-}10)$$

$$\frac{\sigma_c}{f_t} = f(w) - \frac{w}{w_c} f(w_c) \quad (6\text{-}11)$$

$$f(w) = \left[1 + \left(\frac{c_1 w}{w_c}\right)^3\right] \exp(1 - \frac{c_2 w}{w_c}) \quad (6\text{-}12)$$

$$W_c = 5.14 \frac{G_f}{f_t} \quad (6\text{-}13)$$

$$G_f = 73[f_{cm}]^{0.18} \quad (6\text{-}14)$$

c_1, is taken as 3.0 and c_2 is 6.93 for concrete with normal density. w_c is crack displacement at fully damaged and no tensile stress can be transferred. The fracture energy G_f is determined from MC 2010 CEB_FIP design code as expressed in equation 6-14.

6.3.2 Plasticity parameters adopted

Five parameters need to be determined in order to use the concrete damage plasticity (CDP) model provided in the ABAQUS programme. The dilation angle (ψ) which is defined as a material parameter that controls the plastic strain of concrete. It is also defined as the internal friction angle of concrete or the angle of inclination of the failure surface which evaluates the inclination of the plastic potential under high confining pressure. The dilation angle was iteratively calibrated during analysis to get the best results and it was found 38^0 giving the best results.

The eccentricity defines the rate of hyperbolic flow potential and default value recommended by ABAQUS 2012 was used. The other parameter is the ratio

of concrete strength in the biaxial state to that in the uniaxial state (σ_{bo}/σ_{co}). The value chosen for the proposed model is 1.16 which is the default value in ABAQUS. The viscosity parameter used for visco-plastic regularization of concrete is ignored in this analysis. Table 6-1 summaries the five parameters.

Table 6-1 Plasticity parameters

Dilation Angle	Eccentricity	σ_{bo}/σ_{co}	K_c	Viscosity Parameters
38^0	0.1	1.16	2/3	0
where σ_{bo}/σ_{co} is the ratio of initial equibiaxial compressive yield stress to initial uniaxial compressive yield stress, K_c is the ratio of the second stress invariant in tension to that in compression.				

6.4 Material modelling of steel members

According to the Eurocode 2, the stress-strain relationship of steel starts with a linear elastic ascending branch up to the yield strength followed by a linear strain hardening up to the ultimate strength. In the current study, the mechanical properties of reinforcement steel bar, profiled metal decking and shear connectors are determined using coupon test and used to idealize the stress-strain relation shown in Figure 6-6. The modulus of elasticity (Es) is 210 GPa.

Three coupon tests were carried out to determine the mechanical properties of demountable shear connectors and Gr 8.8 bolt connectors, as described in section 3.5.3. The values of yield strength (f_y) and ultimate tensile strength (f_u) were used to model shear connectors for the FE modelling.

The mechanical properties of the reinforcement bars were determined using the coupon test using three reinforcement bars as described in section 3.5.2. These values were used for the modelling of reinforcement bars.

The steel beam was modelled using the yield strength of 410 MPa taken from the manufacture's specification. The effect of the steel beam was not very significant as observed during the push off tests. Therefore, the steel section was considered as linear elastic material with the young modulus of 210,000MPa and Poisson ratio of 0.3.

The mechanical properties of the profiled metal decking were determined through the coupon test which have been presented in section 3.5.4. The measured values were used in the FE models.

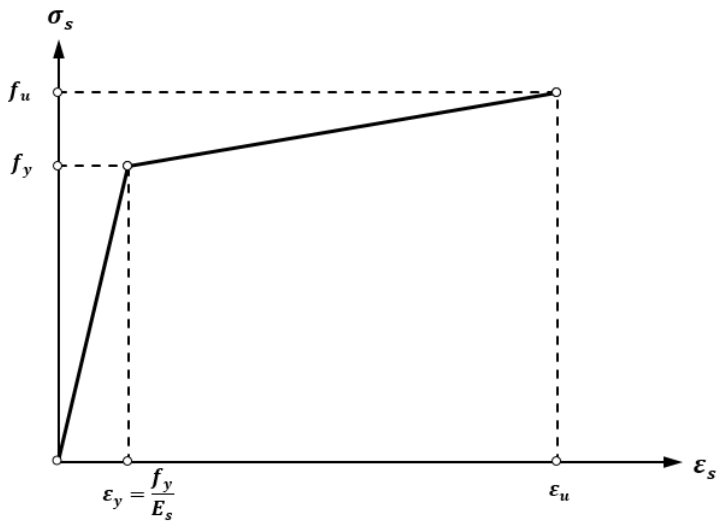

Figure 6-6 Stress strain relationship of steel reinforcement (BS EN 1992-1-1:2004)

6.5 Validation of FE model

6.5.1 Failure criteria

In order to identify the failure of the push off specimen in the FE model, the failure criteria were defined. There were two modes of failure observed in the

experiments, excessive concrete damage around the shear connectors and excessive yielding (fracture) of the shear connectors. Therefore, these were used to assess the failure of the members in the FE model.

6.5.2 Mesh sensitivity study

Sensitivity and computational efficiency analysis was carried out to determine a suitable mesh size for the concrete slab and shear connector as these parts play an important role in the finite element analysis of the push off test. Also, it was observed that the major failure occurred either due to concrete or shear connector failure during the experimental work.

Therefore, three different global mesh sizes 2, 4 and 6 (fine, medium and coarse) as shown in Figures 6-7, 6-8 and 6-9 were used for the shear connectors. The global mesh sizes of 10, 16 and 20 (fine, medium and Coarse) as shown in Figures 6-10, 6-11 and 6-12 were tried for the concrete slab to achieve the optimum results.

The shear connectors with fine, medium and coarse meshes are used with fine, medium and coarse meshes of concrete slabs respectively. The results obtained from different mesh sizes were compared with the experimental results as shown in Table 6-2. The percentage difference was worked as 11.5%, 6.9% and 11.7% for coarse, medium and fine respectively. The coarse and fine mesh provided a higher percentage difference compared to medium. The results obtained from the medium mesh were closer to the experimental results. Therefore the medium sized mesh was considered for the FE model for validation and parametric study due to the efficiency of results and similar approach was adopted by Mirza and Uy, (2010).

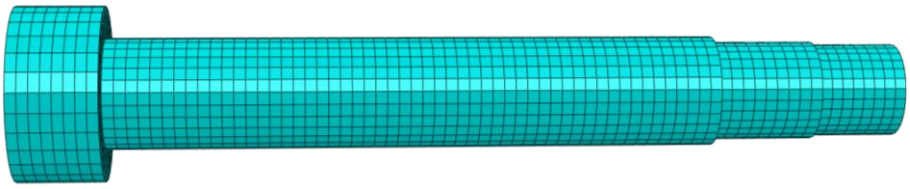

Figure 6-7 Global mesh size 2 for demountable shear connector

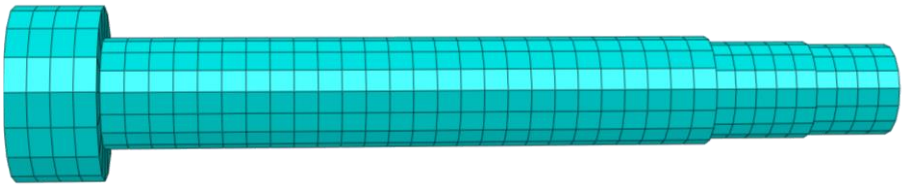

Figure 6-8 Global mesh size 4 for demountable shear connector

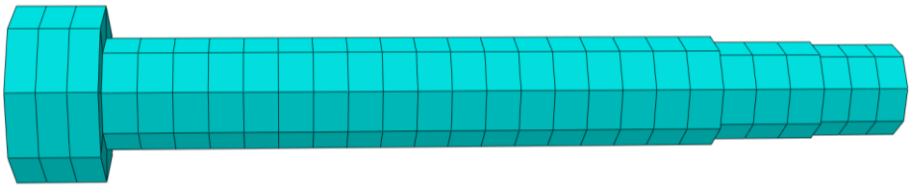

Figure 6-9 Global mesh size 6 for demountable shear connector

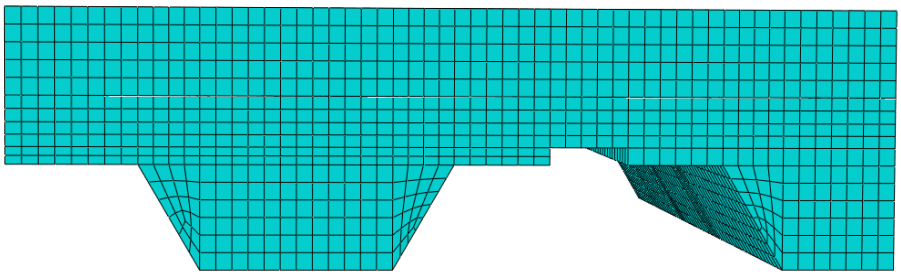

Figure 6-10 Mesh size 10 for concrete slab

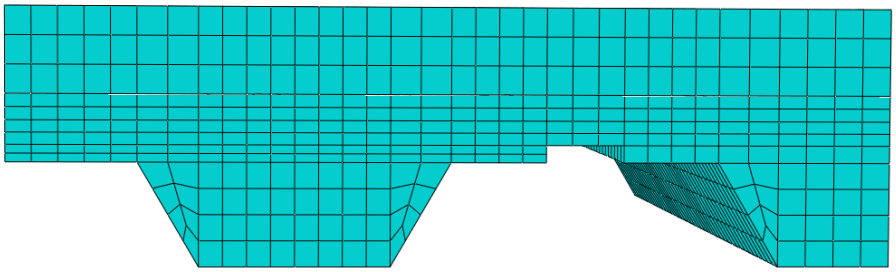

Figure 6-11 Mesh size 16 for concrete slab

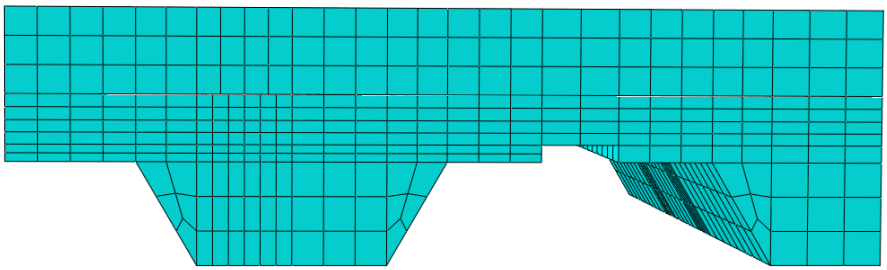

Figure 6-12 Mesh size 20 for concrete slab

Table 6-2 Mesh sensitivity study results

Test Specimen ID	P_{Test} (kN)	Coarse Mesh		Medium Mesh		Fine Mesh	
		P_{FE} (kN)	Difference (%)	P_{FE} (kN)	Difference (%)	P_{FE} (kN)	Difference (%)
M1	69.9	78.9	10.0	75.5	8.4	63.9	8.6
M3	80.0	88.6	10.7	84.1	5.1	69.9	15.4
M5	82.6	94.1	13.9	88.6	7.2	74.3	11.2
Average			11.5		6.9		11.7

6.5.3 Sensitivity study for loading rate

In dynamic explicit simulation, appropriate loading is very important to achieve the quasi static solution. The appropriate mesh determined in the previous section is adopted to determine the appropriate loading rate. Different loading rates of 0.15, 0.20 and 0.25 mm/sec are used to achieve an optimum loading rate. The results for sensitivity of loading rate are presented in Table 6-3. Based on the computational time and accuracy of the results, a loading rate of 0.2 mm/sec was considered as the optimum rate for the simulation of the push off tests.

Table 6-3 Sensitivity study for loading rate

Test Specimen ID	Loading rates	0.15 mm/sec		0.20 mm/sec		0.25 mm/sec	
	P_{Test} (kN)	P_{FE} (kN)	Difference (%)	P_{FE} (kN)	Differ-ence (%)	P_{FE} (kN)	Difference (%)
M1	69.9	66.9	3.5	71.5	2.2	75.5	8.4
M3	80.0	74.6	7.2	82.1	2.6	84.1	5.1
M6	82.6	79.1	4.4	80.1	3.1	88.6	7.2
Average			5.1		2.6		6.9

6.6 FE model results

After selecting the appropriate mesh size and loading rate through sensitivity studies, the developed FE model is adopted to conduct a numerical analysis of all the experimental push off tests with a modified reinforcement cage. The shear capacities, load slip behaviour and failure modes obtained by the FE models are compared with experimental observations.

The results of the finite element analysis model are shown in Table 6-4. It has been found that the results of FE modelling have very good agreement with the experimental results. The maximum shear capacity of the demountable shear connectors, predicted by the FE model was very close to the experimental values with an average ratio of 0.98 and coefficient of variance of just 0.016. The maximum difference of 4 and 6% between the experimental and the FE result was observed for test specimens M5 and M10. This showed that the FE model is capable of predicting similar behaviour of demountable connectors as observed in the experiments. Therefore, this model can be used for parametric studies to increase the data

for further understanding of the structural behaviour of composite structures with demountable shear connectors.

Table 6-4 Results of FE model

Test Specimen ID	Concrete cube strength (MPa)	P_{Test} (kN)	P_{FE} (kN)	P_{Test}/P_{FE}
M1	43.4	69.9	71.5	0.98
M2	40.9	68.2	67.9	1.01
M3	36.2	80.0	82.1	0.97
M4	30.5	79.6	81.6	0.97
M5	55.7	74.1	76.9	0.96
M6	58.1	82.6	80.1	1.03
M7	22.7	66.3	65.7	1.01
M8	19.2	64.7	64.1	1.01
M9	50.8	80.9	81.9	0.98
M10	51.3	87.6	82.4	1.06
Mean				0.98
COV				0.016

6.6.1 Test group1 (M1 and M2)

The load slip curves of test M1 and M2 obtained from the numerical analysis are compared with the experimental load slip curves. These load slip curves predicted similar behaviour compared to the experimental results as shown in Figures 6-13 and 6-14 in terms of stiffness and maximum shear capacity. The maximum load of 71.5 kN and 68.9 kN per connector was obtained from FE models of specimen M1 and M2 with a slip of about 11.8 mm 8.8 mm

respectively. While the maximum load of the experimental specimen M1 and M2 was 69.9 kN and 68.2 kN per connector with a slip of 9.2 mm and 7.3 mm respectively.

A combination of concrete conical failure and shearing of demountable connectors was observed in test specimen M1 and M2 as shown in Figure 6-15. The failure modes obtained from numerical analysis are compared with experimental failure modes of push off tests M1 and M2 as shown in Figures 6-16 to 6-18. The FE model for M1 and M2 have captured similar concrete damage failure and yielding in demountable shear connectors as observed in the experiments.

It can be observed that cracking in the finite element model and experiment occurred at the same location around the shear connectors. The compression and tensile damage variables (dc and dt) in the finite element model show that concrete failure happened during finite element analysis. The stress contour clearly shows the yielding of the demountable shear connector in Figure 6-18.

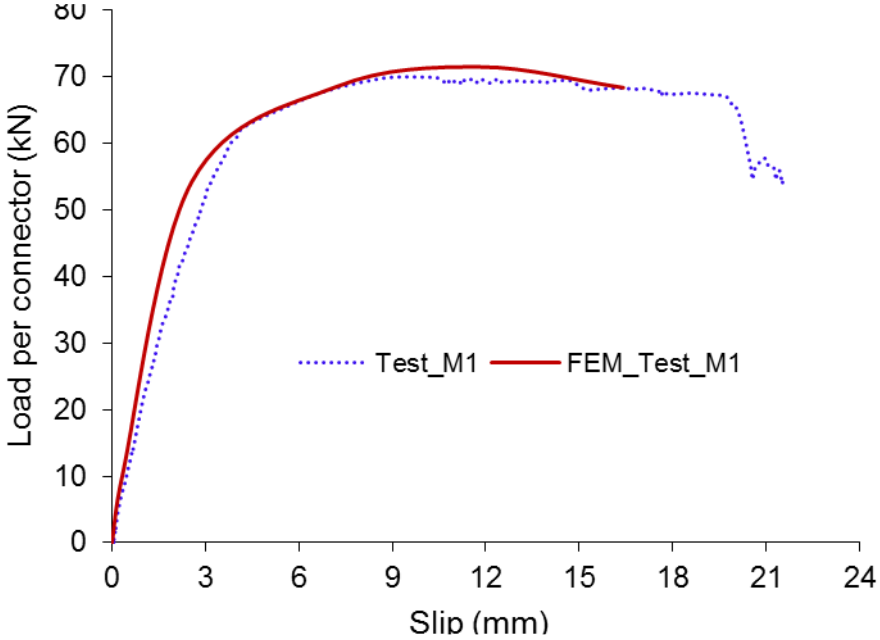

Figure 6-13 Comparison of load slip behaviour of FE and Experiment of test M1

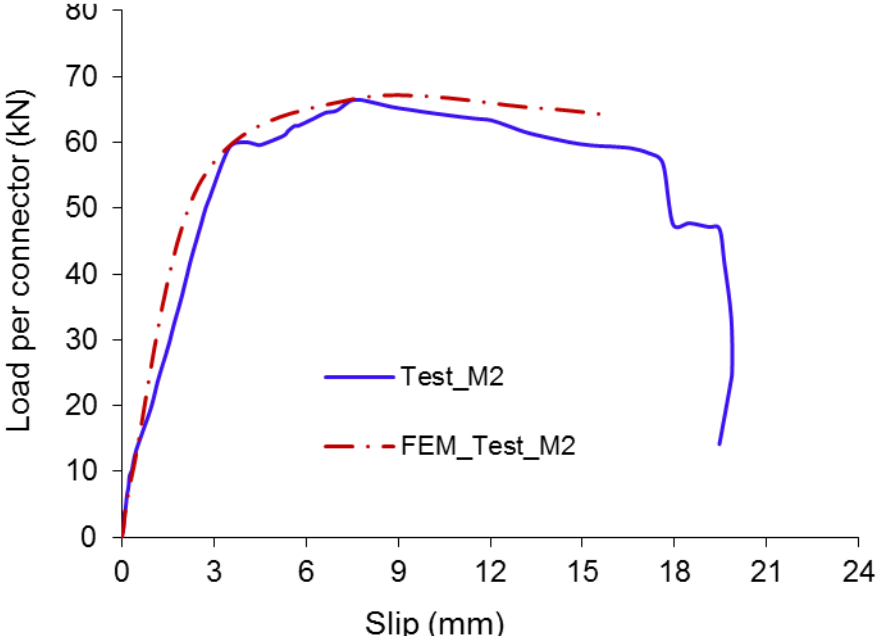

Figure 6-14 Comparison of load slip behaviour of FE and Experiment of test M2

Figure 6-15. Combination of connector shearing and concrete failure in specimen M1

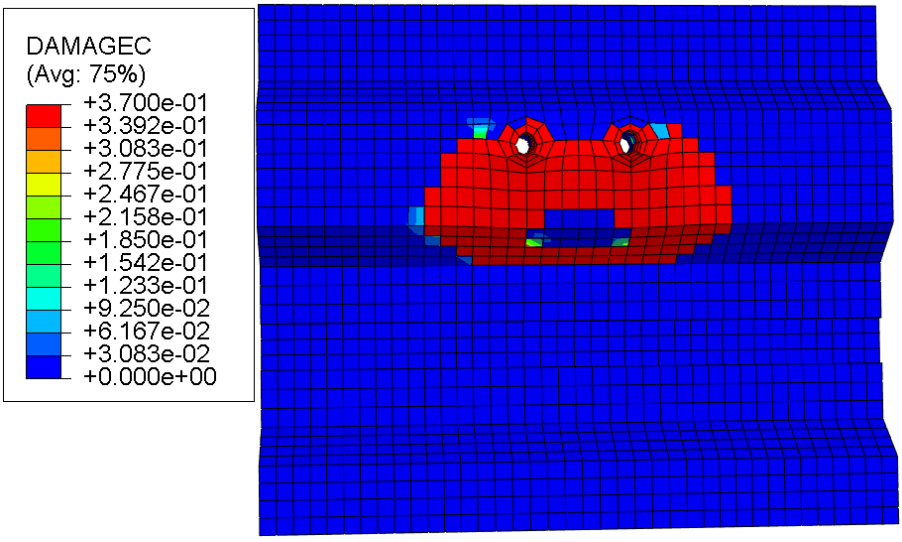

Figure 6-16 Concrete comparison damage in FE analysis model of test specimen M1

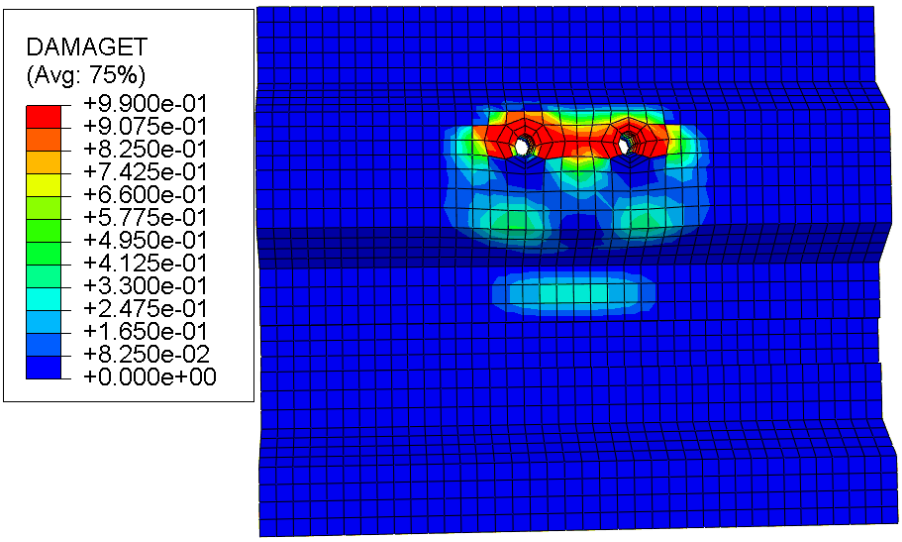

Figure 6-17 Concrete tensile damage in FE model of specimen M1

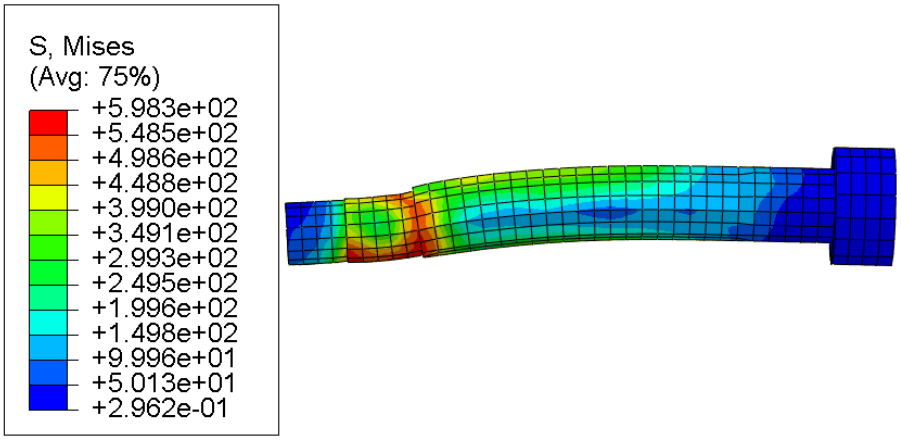

Figure 6-18 Deformed shape of demountable shear connector of test specimen M2 Experimental (top) and FEM (bottom)

6.6.2 Test group 2 (M3 and M4)

All material properties and model elements are kept the same as used in the first group except the concrete compressive strength and number of shear connectors per trough in the profiled metal decking. The finite element model was analysed with a single shear connector in each trough of metal profiled decking. Load slip behaviour of the FE analysis is compared with experimental results in Figures 6-19 and 6-20.

The behaviour of the FE model in terms of initial stiffness and maximum shear capacity was reasonably close to the experimental results. The maximum load was 82.1 kN and 81.6 kN per connector obtained from the FE model for test M3 and M4 at a slip of 12.8 mm and 14.2 mm respectively. While the experimental results showed a load of 80.0 kN and 79.6 kN per connector at the slip of 16.5 mm and 27.8 mm respectively. Experimental failure mode as shown in Figure 6-21 was successfully simulated through the finite element analysis model and presented in Figures 6-22 and 6-23. The concrete damage (dc) in concrete and stress contour in shear connectors clearly indicates a similar failure as observed in the experiments.

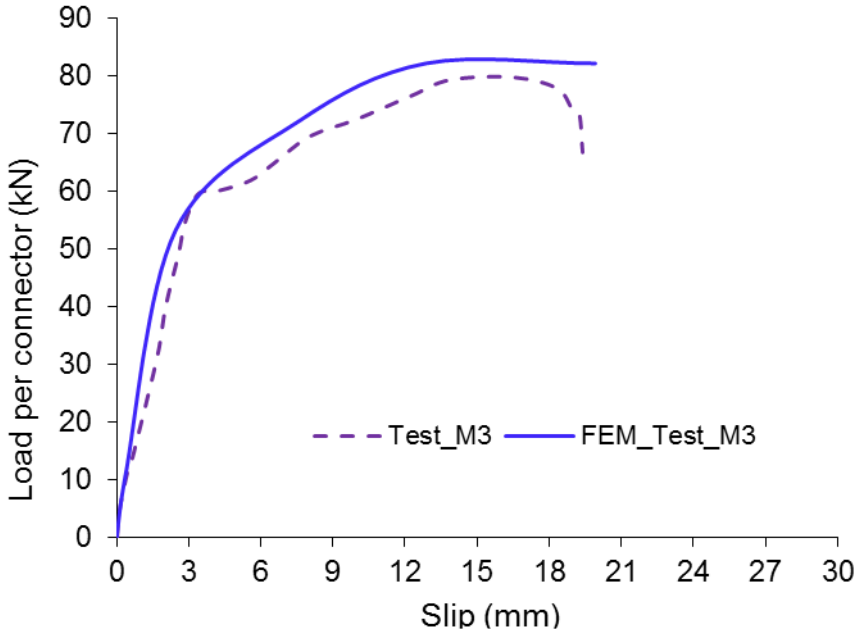

Figure 6-19 Comparison of FEM and experiment of M3

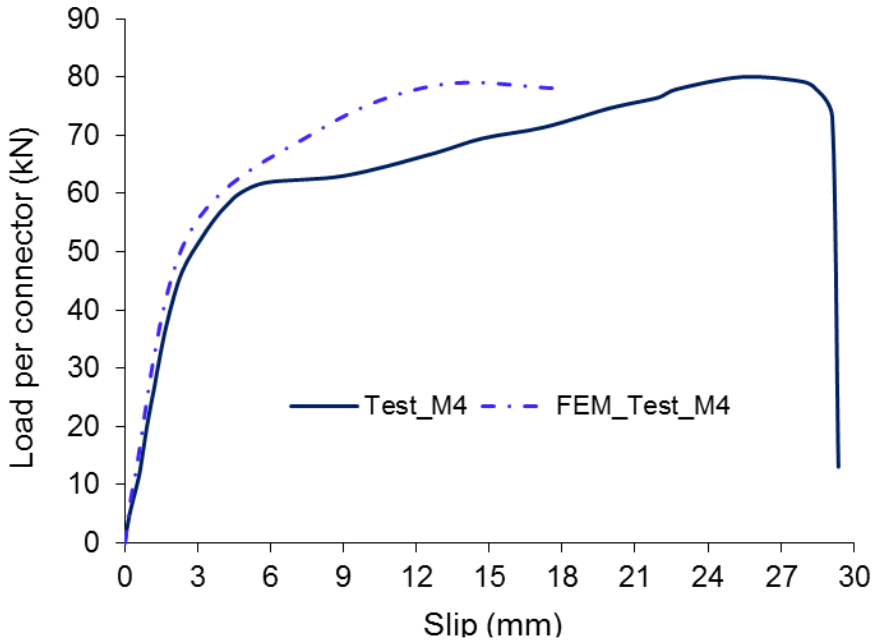

Figure 6-20 Comparison of FEM and experiment of M4

Figure 6-21 Mode of failures in specimen M3

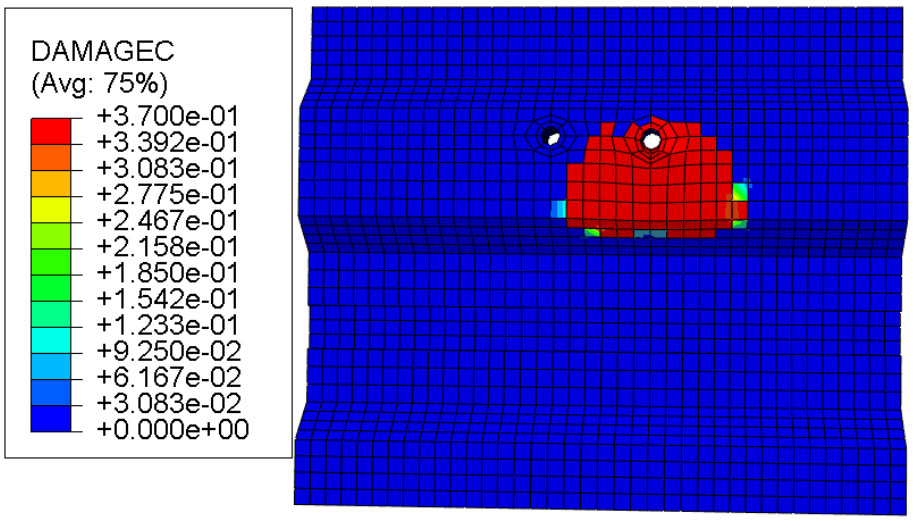

Figure 6-22 Concrete cone failure in FE model in specimen M3

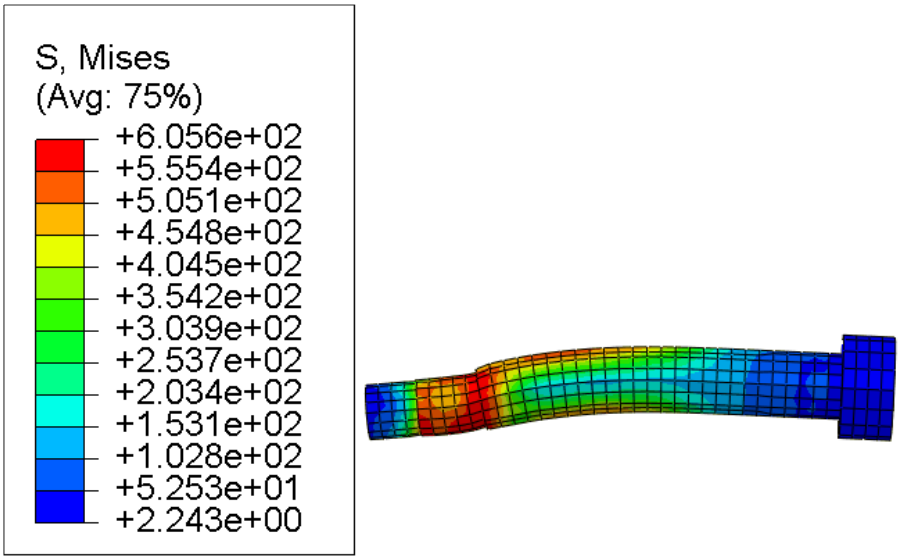

Figure 6-23 Stresses in demountable shear connector specimen M4

6.6.3 Test group 3 (M5 and M6)

The load slip curves obtained from finite element analysis are compared with the experimental results as illustrated in Figures 6-24 and 6-25. The load slip curves behaved in a very similar manner as observed through the experiments in terms of initial stiffness and ultimate load. The maximum load per connector in the case of test M5 and M6 was 74.1 kN and 82.6 kN with a

slip of 6.2 mm and 6.9 mm. While in the FE analysis the maximum load per connector for M5 and M6 were 76.1 and 80.1 kN per connector with a slip of about 4.8 mm and 5.0 mm respectively.

The failure modes were also investigated and compared with the experimental push off tests for specimen M5 and M6. In the experiment, both push off tests failed due to shearing of the demountable shear connectors this was correctly simulated through the finite element model. When the failure load was reached, deformation in the demountable shear connector became more prominent and the maximum stresses were experienced at the position of the collar as is evident from the stress contour plot of the shear connector in Figure 6-26.

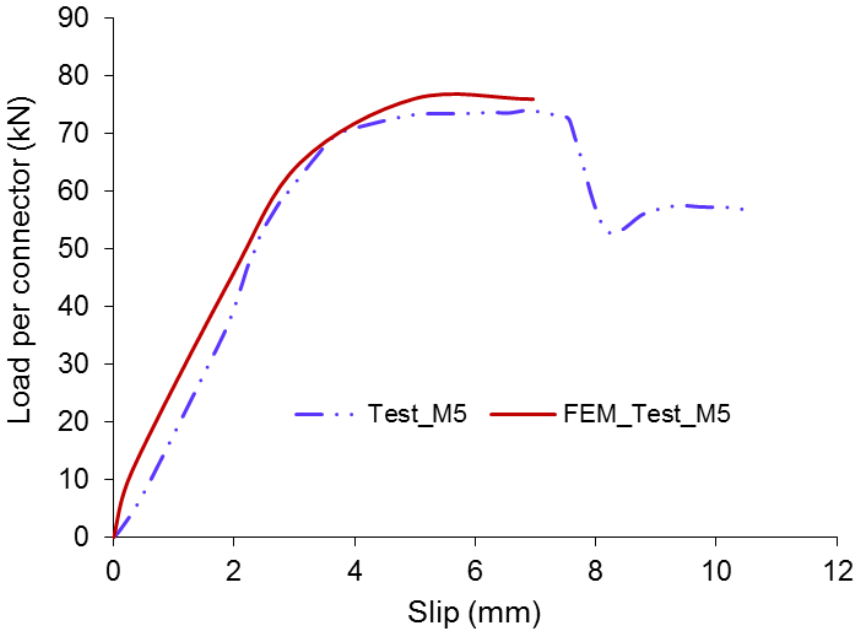

Figure 6-24 Comparison of FE and experiment of M5

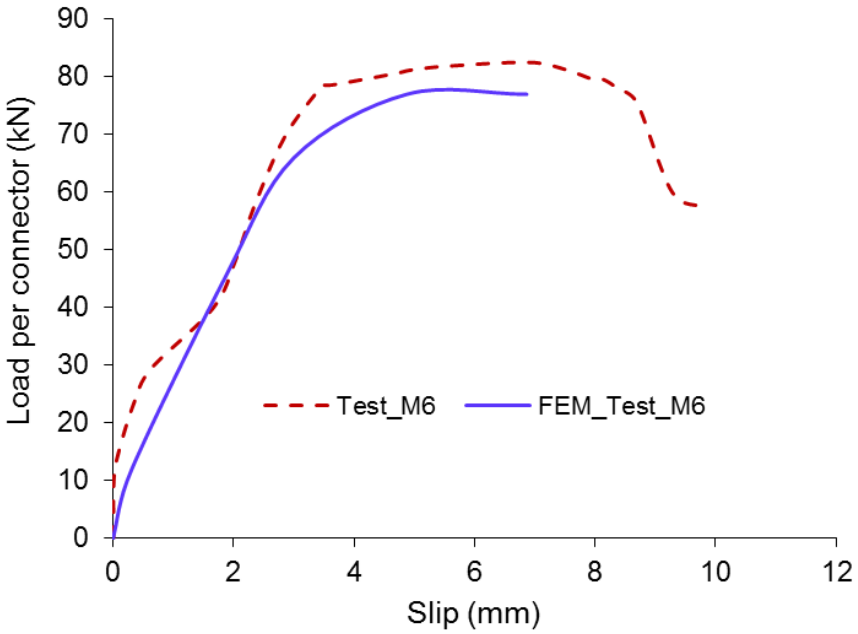

Figure 6-25 Comparison of FE and experiment M6

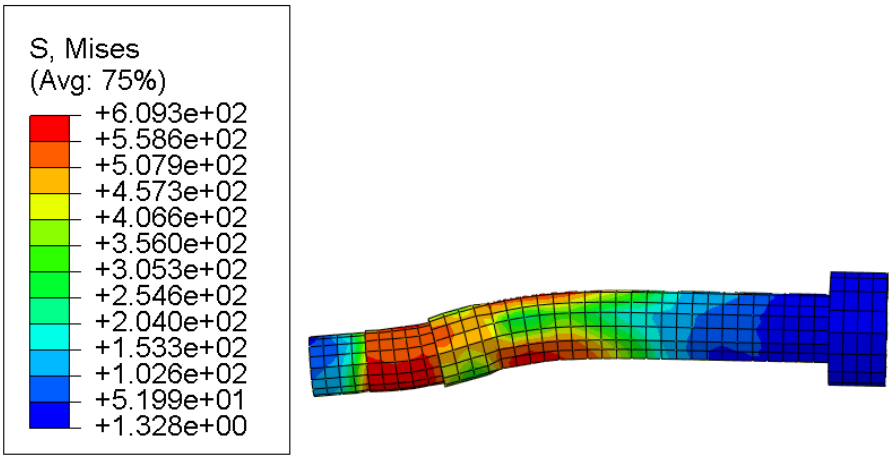

Figure 6-26 Stress contour in demountable shear connector in M6

6.6.4 Test group 4 (M7 and M8)

A demountable shear connector with a shank diameter of 22mm was used for test M7 and the M20 Gr8.8 bolt was used for test specimen M8. The load slip behaviour of the FE model is reasonably close to the experimental tests as shown in Figures 6-27 and 6-28. The initial stiffness was lower in the FE

analysis for both tests, while the ultimate load per connector was 65.6 kN at the slip of 5.6 mm and 64.9kN at the slip 6.9 mm for test M7 and M8 respectively. Where as in the experiment it was 66.3kN at the slip of 3.9 mm and was 64.6 kN at the slip of 5.5 mm for push off test specimen M7 and M8 respectively.

The failure modes were compared with the experimental push off tests as shown in Figures 6-29 and 6-30. The formation of conical failure in the FE model matched push off tested specimens. There was no evidence of connector yielding in the FE model as can be seen in Figure 6-30.

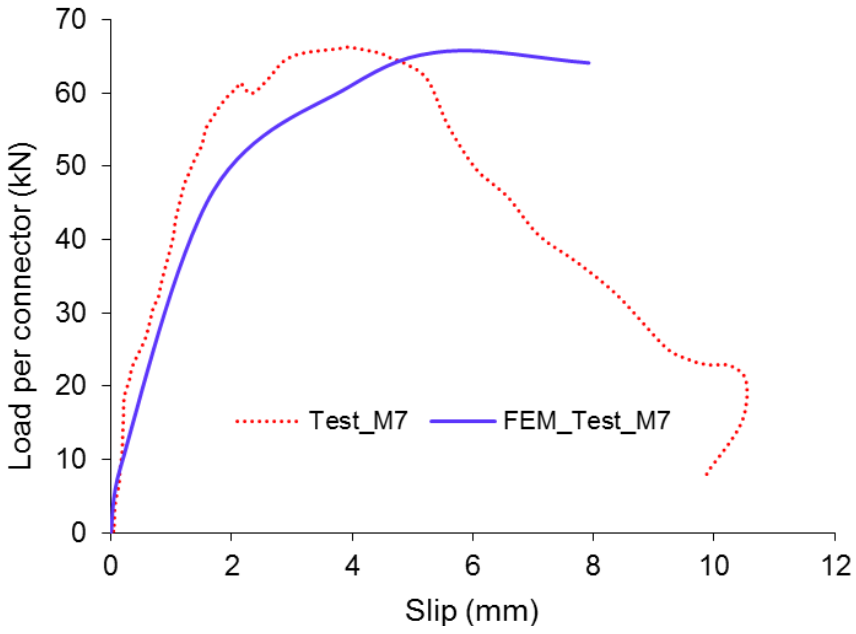

Figure 6-27 Comparison of FE and experiment M7

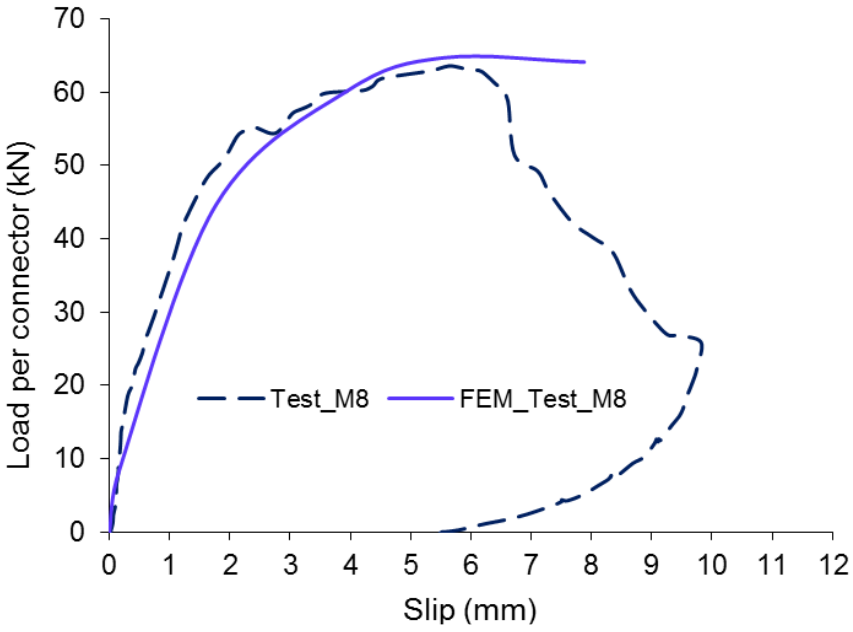

Figure 6-28 Comparison of FE and experiment M8

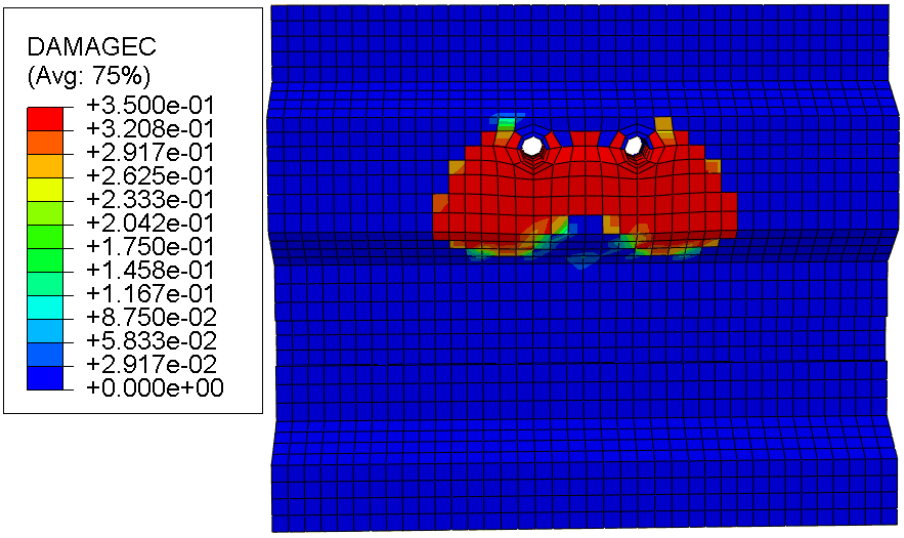

Figure 6-29 Concrete cone failure in FE model of specimen M7

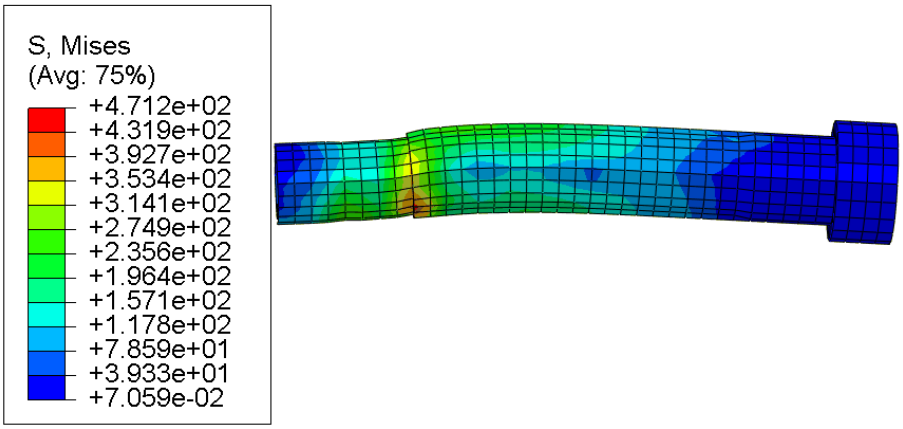

Figure 6-30. Stress contour in demountable shear connector of specimen M7

6.6.5 Test group 5 (M9 M10)

The same FE model was adopted as used in the previous group but with higher concrete strength. The FE model showed very good agreement in terms of ultimate capacity but the stiffness was lower compared to the experimental work in both FE models of M9 and M10 as can be seen in Figures 6-31 and 6-32.

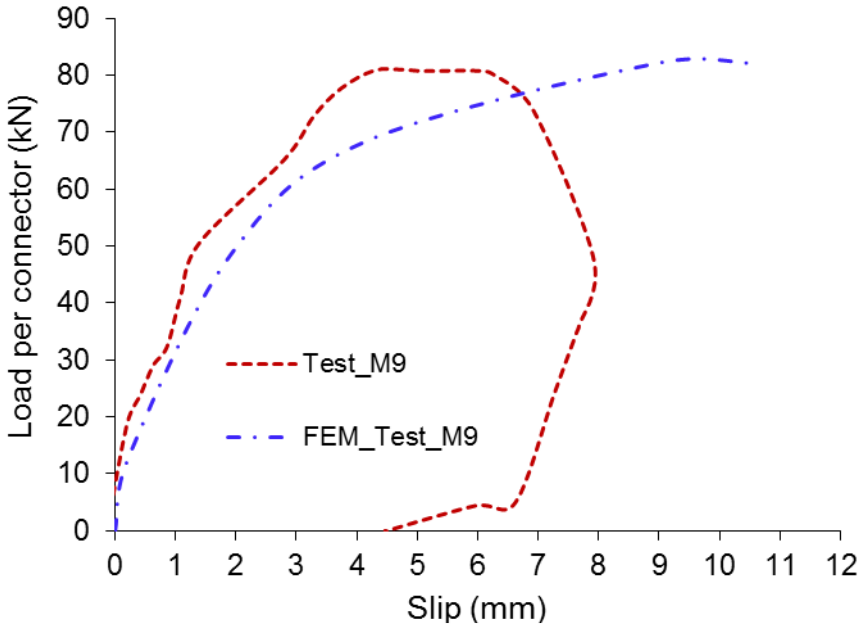

Figure 6-31 Comparison of FE and experiment M9

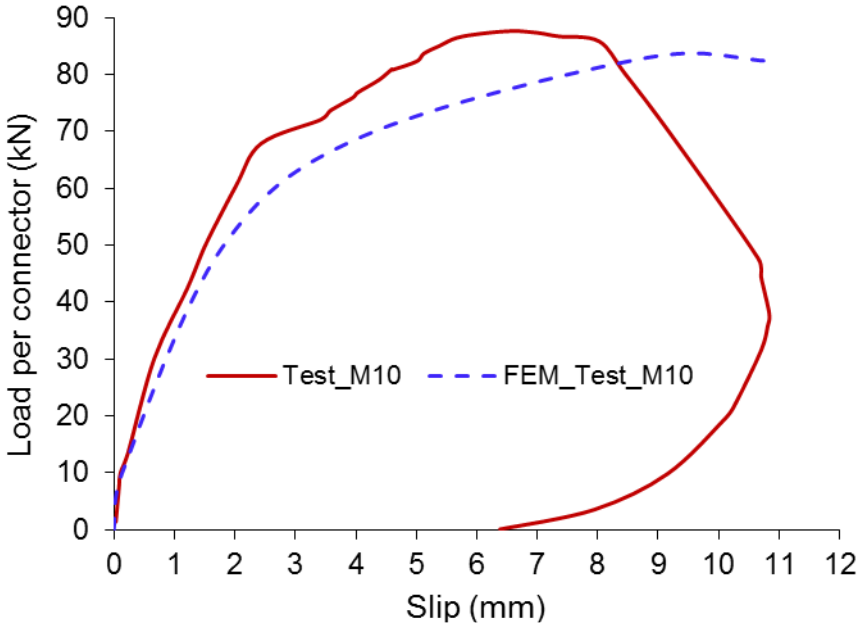

Figure 6-32 Comparison of FE and experiment M10

The failure modes of the experimental push off tests were also compared with the failure modes of the finite element model. In the experiment, the push off specimen failed due to concrete cone failure. The FE model has captured the concrete cone failure as can be seen in Figure 6-33. The concrete damage variable clearly indicates concrete cone failure around the connectors and formed a conical shape. The stress contour plot in Figure 6-34 for the shear connector clearly shows that the connector is not fully yielded.

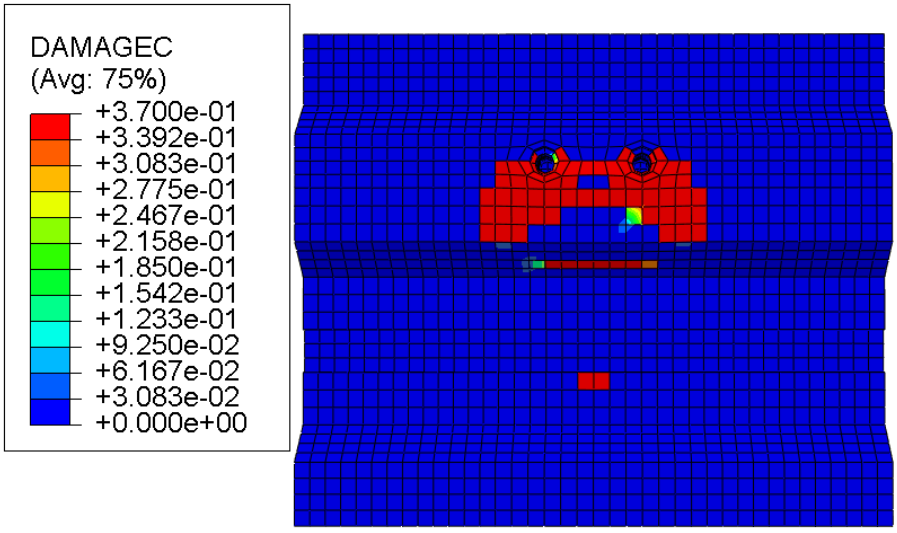

Figure 6-33 Concrete cone failure in specimen M10

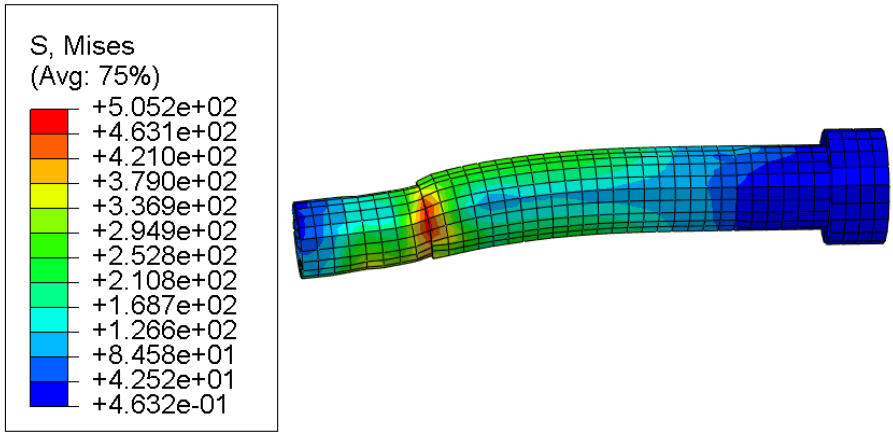

Figure 6-34 Stress contour in demountable shear connectors in specimen M10

6.7 Parametric studies of push off test

Different parameters were used to evaluate the effects on the shear capacity and ductility of the demountable shear connectors. The parameters considered in this study are given in Table 6-5. They include: number of connectors per trough, transverse spacing between pairs of connectors, connector collar diameter, the diameter of the hole in the steel flange and concrete compressive strength. The parametric study was further divided into

five groups as shown in Table 6-6, in which the dimensions of the concrete slab and profiled metal decking were kept constant throughout the FE analysis.

Table 6-5 Parameters used for parametric studies and analysis

Parameters	Range
Number of connectors	1 , 2
Transverse spacing(mm)	80, 100, 120
Collar diameter(mm)	15, 16, 17, 18, 19
Shank diameter (mm)	19
Hole clearance (mm)	0, 1, 2
Concrete strength (MPa)	20,30,40,50

Table 6-6. Details of specimens adopted for parametric studies and results

Group	Specimen	Connector Collar diameter	Concrete Class	Hole clearance	Connector shank diameter	Number of connector	Transverse Spacing	P_{FE} (KN)
Group1	G1-1	17	C20/25	0	19	2	100	61.60
	G1-2	17	C30/37	0	19	2	100	63.63
	G1-3	17	C40/50	0	19	2	100	69.79
	G1-4	17	C50/60	0	19	2	100	71.45
Group2	G2-1	17	C20/25	0	19	1	0	63.38
	G2-2	17	C30/37	0	19	1	0	64.54
	G2-3	17	C40/50	0	19	1	0	72.25
	G2-4	17	C50/60	0	19	1	0	73.93
Group3	G3-1	15	C40/50	0	19	2	100	63.85
	G3-2	16	C40/50	0	19	2	100	64.14
	G3-3	18	C40/50	0	19	2	100	71.25
	G3-4	19	C40/50	0	19	2	100	74.25
Group4	G4-1	17	C40/50	1	19	2	100	69.79
	G4-2	17	C40/50	2	19	2	100	69.79
Group5	G5-1	17	C40/50	0	19	2	60	69.19
	G5-2	17	C40/50	0	19	2	80	69.56
	G5-3	17	C40/50	0	19	2	120	71.96
	G5-4	17	C40/50	0	19	2	150	72.63
	G5-5	17	C40/50	0	19	2	200	73.45
	G5-6	17	C40/50	0	19	2	300	73.94

6.8 FE results and discussion

6.8.1 Effect of number of connectors

Two different sets of connector layouts (a single and pair per trough) were used to assess the effect of connector arrangements on the shear resistance of a shear connection using demountable shear connectors. Figure 6-35 shows a comparison of the shear resistance of the specimen with paired connectors per trough with that of a specimen with a single shear connector per trough. It can be seen that by using single shear connectors in each trough, the shear capacity increases about 4% compared to using paired connectors per trough.

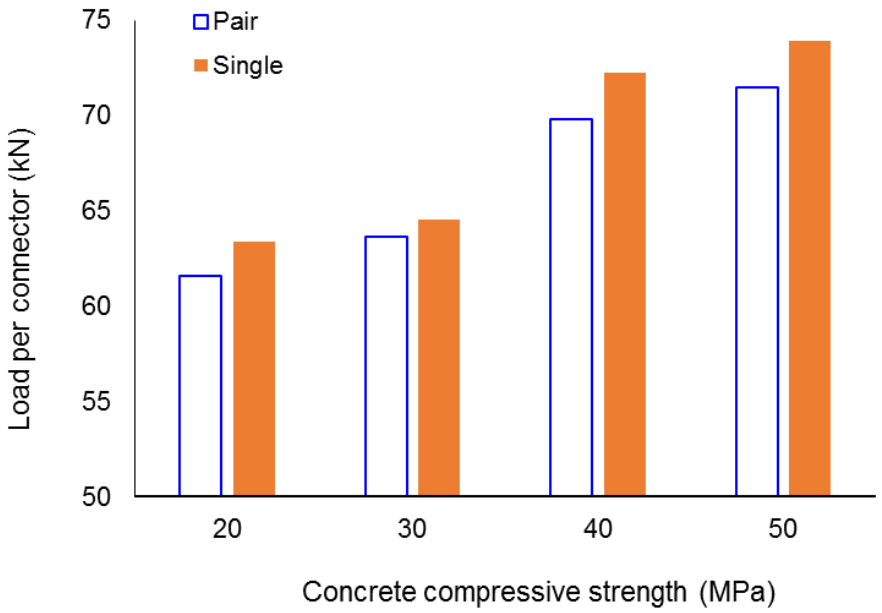

Figure 6-35 Effect of number of connectors per trough

6.8.2 Effect of hole clearance

Figure 6-36 compares the load-slip relationships of the push-off specimens with three different clearance sizes between the connector collar and the pre-drilled holes in the steel flange. In the specimens in which the diameter of the

connector was kept as 17 mm and clearances between the collar and the holes were provided as 0, 1 and 2 mm. As expected, the clearance directly affects the first critical slip. The larger the clearance, the larger is the first critical slip. However, it appears the hole clearance does not have any effect on the ultimate shear resistance.

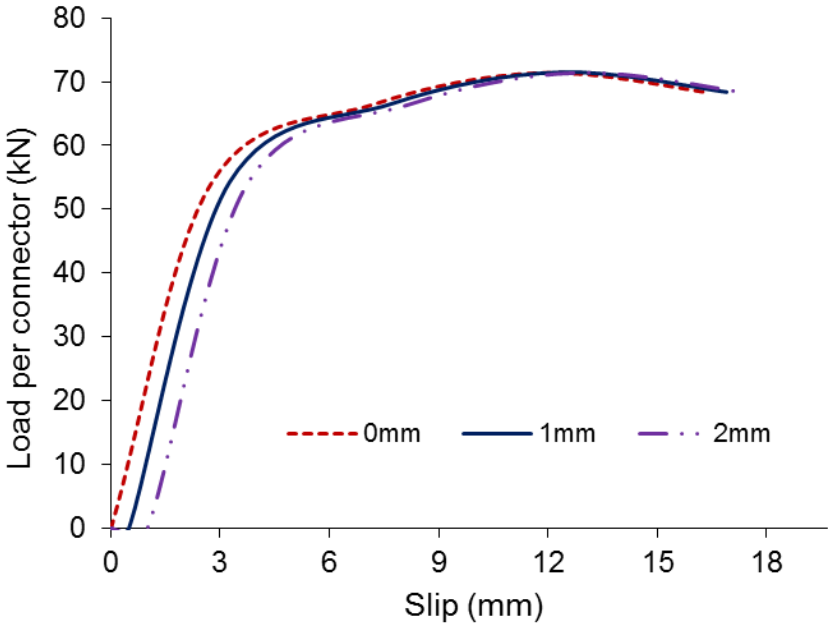

Figure 6-36 Effect of hole clearance

6.8.3 Effect of transverse spacing

It has been observed from the experimental study that the failure mechanism was controlled by either concrete cone failure or a combination of concrete crushing and shearing of connectors. In specimens with paired connectors per trough, the failure zone overlapped compared to single connector specimens. The shear resistance increased slightly with the use of single connectors when compared with the paired connector specimen with the spacing limit of 60-100 mm. It is usually thought that the full shear capacity of an individual connector can be utilized in the paired connector specimen if

the spacing between two connectors is increased significantly. Therefore, the effect of spacing between the connectors was further investigated. The same verified FE model was used to study the effect of the transverse spacing between two connectors in each trough and in a single connector per trough.

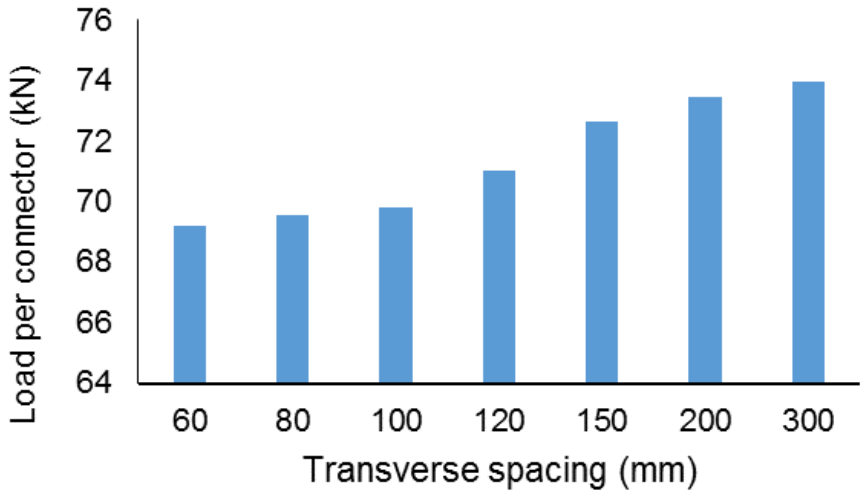

Figure 6-37 Load verses transverse spacing

Six different values for transverse spacing were used in the modelling. The results have been presented in Table 6-6. The FE modelling results indicate that the shear resistance capacity can be increased to about 8% if the spacing between two connectors is increased from 5 times to 16 times the diameter of the connector as can be seen in Figure 6-37. The overlapped compressive damage can be seen in Figures 6-38 to 6-41 with different transverse spacing.

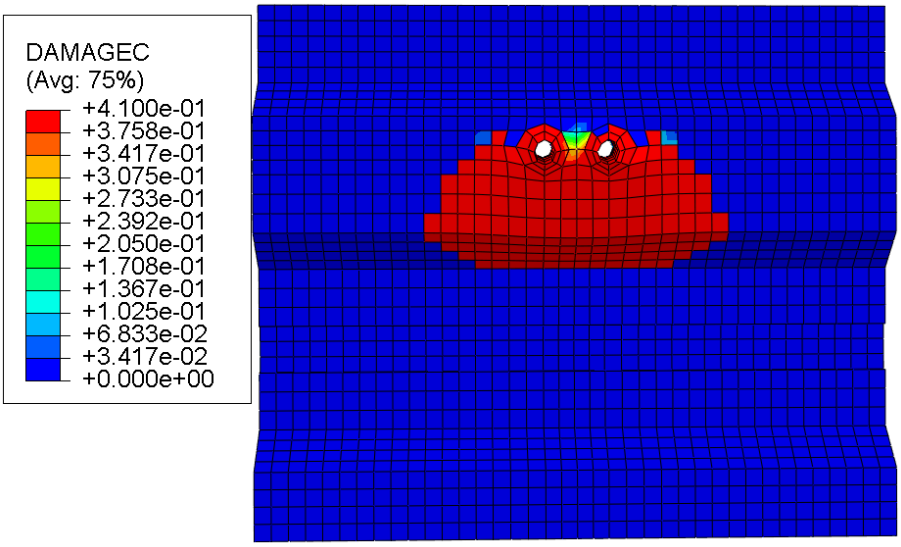

Figure 6-38 Compression damage at the transverse spacing of 60 mm

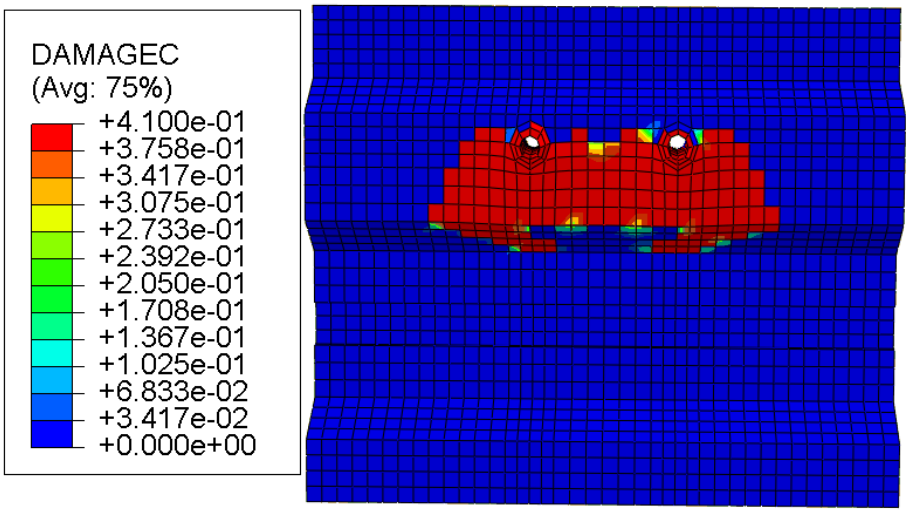

Figure 6-39 transverse spacing 150

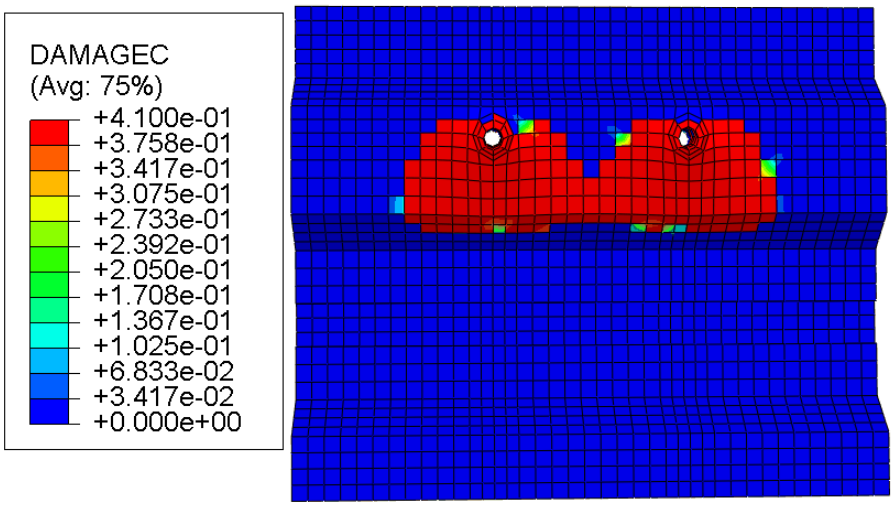

Figure 6-40 Compression damage at 200

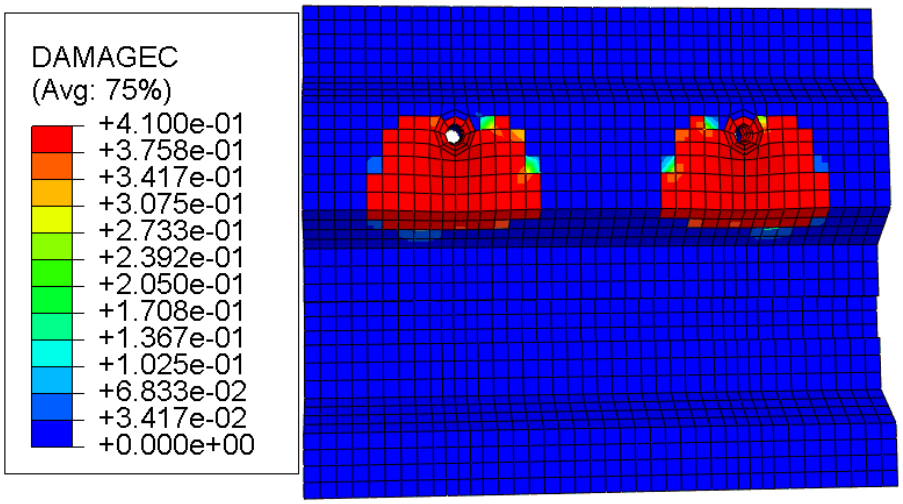

Figure 6-41 Compression damage at 300

6.8.4 Effect of connecter collar

Five different collar diameters were used in the parameter study to analyse the effect of collar diameter on shear resistance of the shear connection. Figure 6-42 presents the effect of collar diameter on the shear capacity of the shear connection. It can be seen that the ultimate shear resistance increases with the increasing of the collar diameter. The shear capacity increased about 6% if the diameter of the collar was increased by about 21%.

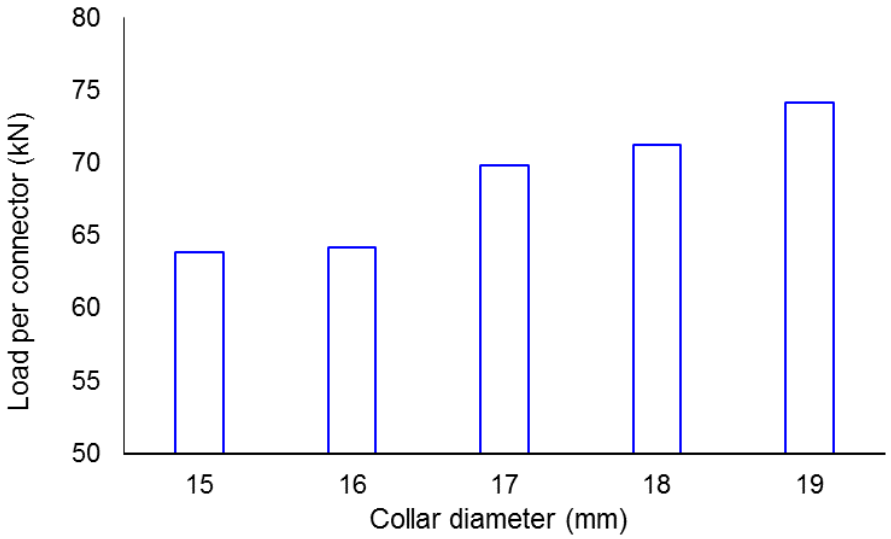

Figure 6-42 Effect of collar diameter

6.8.5 Effect of concrete strength

As shown in Figure 6-35, the strength of concrete significantly affects the shear resistance of the shear connection. It can be seen that the shear resistance increased about 21% when the concrete strength increased from C20/25 to C50/60.

6.9 Composite beam

6.9.1 Finite element model

A three-dimensional finite element model was developed to simulate the structural behaviour of a demountable composite beam using ABAQUS through the explicit technique. The FE model was developed using the same dimensions as the full scale beam test specimen described in Chapter 5. Both geometric and material nonlinearities were considered in the finite element analysis.

The FE model comprises of a concrete slab, profiled metal deck, reinforcement and steel beam. All the parts were modelled separately and assembled together as shown in Figure 6-43 and Figure 6-44.

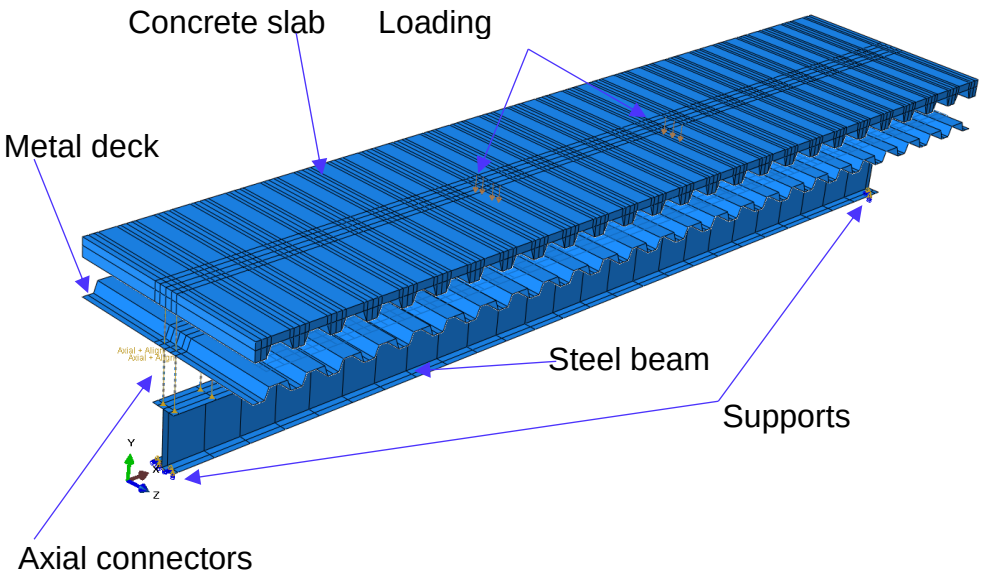

Figure 6-43 3D FE model of DCFS specimen

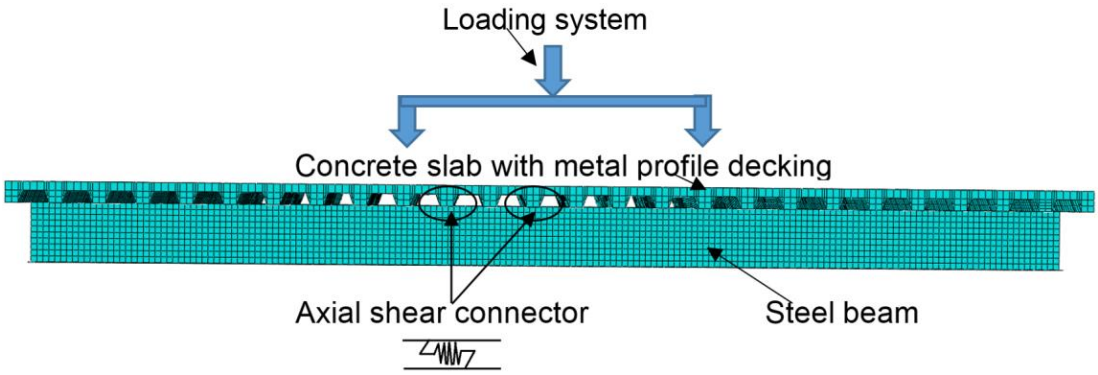

Figure 6-44 FE model of composite beam

The concrete slab was modelled using three dimensional eight node solid element (C3D8R) with reduced integration. Shell element S8R with reduced integration was used for the profiled metal decking and steel beam. The reinforcement mesh was modelled using two node linear three dimensional

truss element T3D2. The demountable shear connectors were modelled using the axial connector option available in the ABAQUS library.

6.9.2 Contact interactions and boundary conditions

The contact between the concrete and metal decking is defined through contact properties. The normal behaviour is defined as hard contact and the tangential behaviour is defined as penalty frictional with a coefficient of 0.40 as used in the push off model. The same interaction property is used for the contact of the steel beam with metal decking. The embedded constrain option was used for the reinforcement bars. In the FE model, the nodes of the steel beam at the supports were restrained from movement along the Y-axis.

6.9.3 Material model

Concrete modelling

The concrete damage plasticity model as described in section 6.3 and available in ABAQUS was used for the concrete slab. This model was successfully used by Qureshi et al. (2011) and Qureshi and Lam (2012) for numerical modelling. The maximum tensile strength of concrete was taken as 10% of the compressive strength of the concrete and the tensile stress cracking model was used for tensile behaviour.

Steel beam and reinforcement

A steel beam with a grade of S355 and yield strength of 410MPa was considered following the mill certificate of the steel beam. The stress-strain relationship was considered as perfect elastic-plastic with a young modulus

of 210GPa and Poisson ratio of 0.3. The reinforcement was also taken as perfect elastic-plastic material with a strength 500MPa.

Shear connector

Shear connectors play an important part in a composite structure as the longitudinal shear forces between the steel beam and composite slab are transferred through the shear connection. The shear connector is modelled using the axial connector element. The effect of the hole in the steel flange and metal profiled deck was ignored in this study. In the FE model, the strength and stiffness of the demountable shear connectors was determined directly from the companion push off tests carried out alongside the DCB specimen test. Therefore, the load-displacement relation as shown in Figure 5-12 was adopted for the modelling of a shear connector, by using the axial connector model option. The axial connector is used between the composite slab nodes and the steel beam flange nodes.

6.9.4 Loading procedure

A two point loading system is used to simulate the experimental test specimen. The load is applied downwards on the top surface of the concrete slab at the same position as used in experimental setup through the velocity control method available in ABAQUS software. The rate of velocity was kept very low to simulate the static condition of loading.

6.9.5 Sensitivity study for mesh and loading rate

Initially different mesh sizes were tried for the concrete slab and the steel beam to achieve the most appropriate results in terms of accuracy and time consumption. Finally, the concrete slab was divided into 200 elements in an x

direction, 12 elements in a Z direction and 3 elements in a y direction for the FE model simulation. Mesh elements were also calibrated for the steel section. Finally 10 elements for web and 4 elements for flanges were chosen.

Three different rates were tried 0.15mm/s, 0.2mm/s and 0.22mm/s to achieve more accurate behaviour. It was found that 0.2mm/s was the most appropriate rate to simulate the experimental work in terms of accuracy and computational time.

6.9.6 Composite beam model verification

The results of the finite element model are verified against the experiment beam test using load deflection behaviour and ultimate load carrying capacity. Table 6-7 compares the total loading carrying capacity of the finite element model of a composite beam with the experimental demountable composite beam test. The ultimate load capacity obtained from the FE analysis is about 3% higher than the experimental value. The comparisons for the load vs mid span deflection and end slip of the finite element and experimental test are made in Figure 6-45 and Figure 6-46. The FE results showed very good agreement with the experimental findings. Failure occurred at the maximum load of 351.99 kN. The mode of failure was yielding of the steel beam as observed in the experiment this was reproduced in the finite element model as presented in Figure 6-47.

Table 6-7. FEM validation result

Test Specimen ID	Concrete cube Strength (Mpa)	Total Load P_{Test} (kN)	P_{FE} (kN)	Deflection (mm)	End slip (mm)	P_{FE} / P_{Test}
DCB	37	340.5	351.9	79.9	7.5	1.03

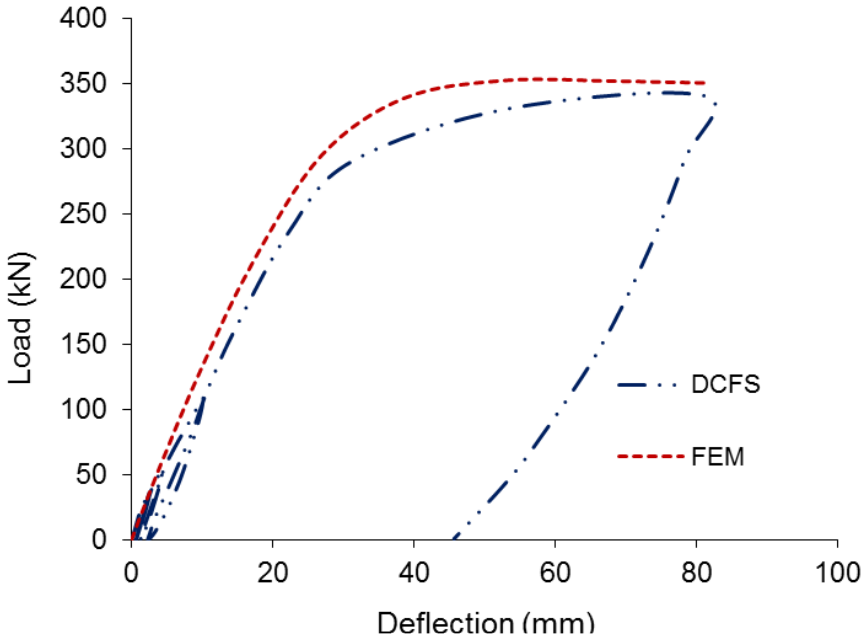

Figure 6-45. Load vs deflection (FE model vs experimental)

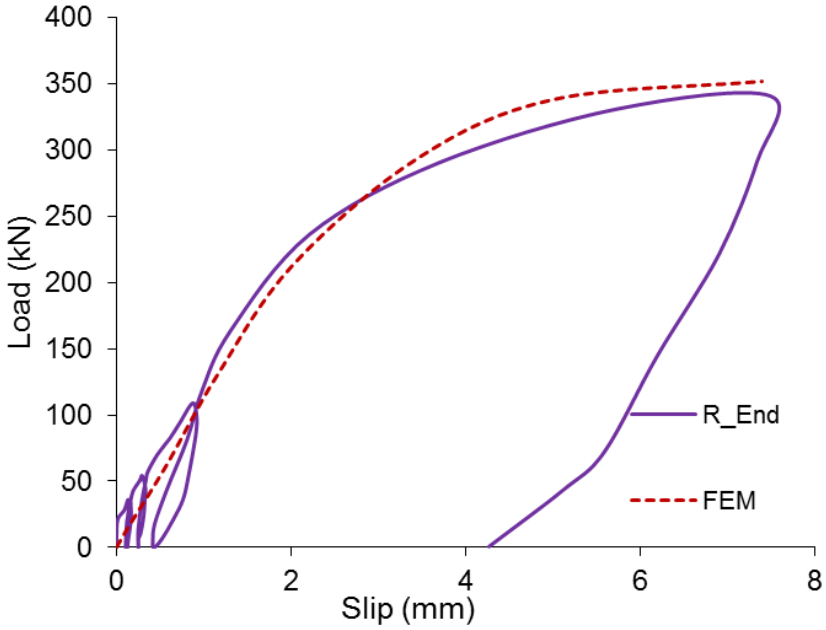

Figure 6-46. Load vs end slip (FE model vs experimental)

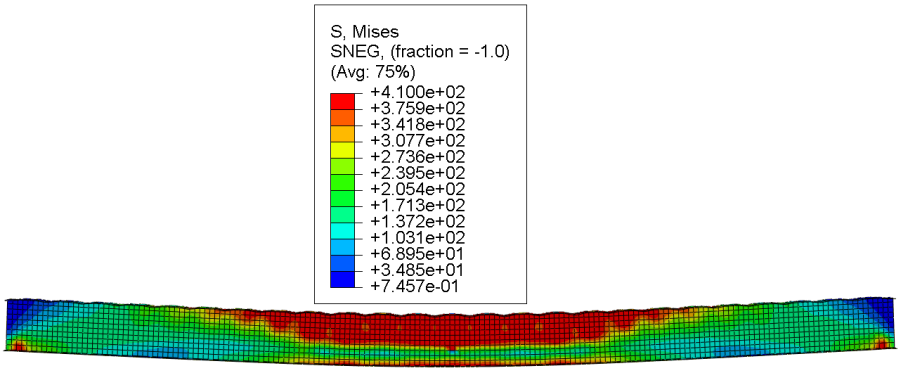

Figure 6-47 Yielding of steel beam

6.10 Parametric studies of composite beam

After having verified the finite element model against the experimental test, the developed FE model was used to study the effect of a number of parameters on the load deflection behaviour of a demountable composite beam. Parametric studies were conducted with variations in: concrete compressive strength, number of connectors per trough, depth of steel beam, transverse spacing between connectors and yield strength of the steel beam. Table 6-9 presents the parameters used for finite element analysis. The dimensions of the concrete slab and profiled metal decking were kept the same throughout the FE analysis.

Table 6-8 Parameters for FE Analysis

Parameters	Range
Number of connectors per trough	1 , 2
Transverse spacing (mm)	40, 80, 115
Beam Depth (mm)	300,360,400,450,500
Yield strength of steel beam(MPa)	310,410,510,610,710
Concrete strength (MPa)	20,30,40,50

6.10.1 Results and discussion

The results of the finite element analysis are presented in table 6-9.

Table 6-9. Results of parametric studies.

Group	Specimen	Connector spacing	Concrete Strength	Number of connector	Beam Depth	Steel beam(fyd)	P_{FE} (kN)
Group 1	G1-1	80	20	2	300	410	340.2
	G1-2	80	30	2	300	410	351.0
	G1-3	80	40	2	300	410	355.8
	G1-4	80	50	2	300	410	358.4
Group 2	G2-1	0	20	1	300	410	338.8
	G2-2	0	30	1	300	410	346.2
	G2-3	0	40	1	300	410	353.2
	G2-4	0	50	1	300	410	356.8
Group 3	G3-1	0	30	1	350	410	441.8
	G3-2	0	30	1	400	410	556.4
	G3-3	0	30	1	450	410	665.8
	G3-4	0	30	1	500	410	762.6
Group 4	G4-1	0	30	1	300	310	268.2
	G4-2	0	30	1	300	510	400.6
	G4-3	0	30	1	300	610	467.2
	G4-4	0	30	1	300	710	527.8
Group5	G5-1	115	30	2	300	410	355.0
	G5-2	40	30	2	300	410	347.8
	G5-3	0	30	0	300	410	281.9

6.10.2 Effect of concrete strength

The strength of concrete affects the load bearing capacity of a composite floor system significantly. Figure 6-48 shows that the load bearing capacity increases about 5% as the concrete cube strength increases from 20Mpa to 50 MPa. The test results also showed that the increase in concrete compressive strength does effect the stiffness of a demountable composite floor system.

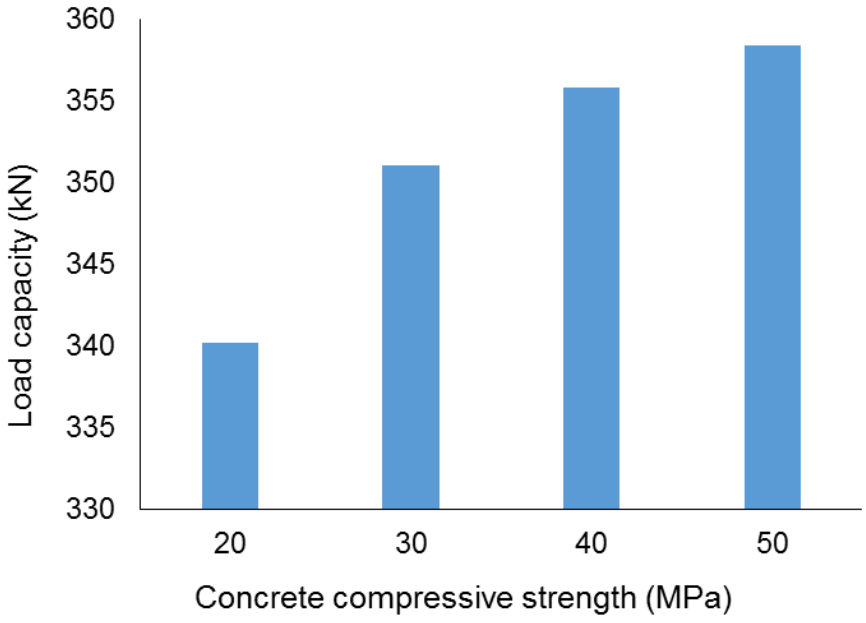

Figure 6-48 Effect of concrete

6.10.3 Effect of steel beam strength

The yield strengths of 310 MPa, 510 MPa, 610 MPa and 710 MPa were used for the steel beam in this parametric study. The yield strength of the steel beam affected the ultimate load bearing capacity of the demountable composite floor system as shown in Figure 6-49. As expected the higher the yield strength, the higher the load carrying capacity of the specimen.

However, it appears that the yield strength does not affect the initial stiffness and the ductility of the composite beam as shown in Figure 6-50.

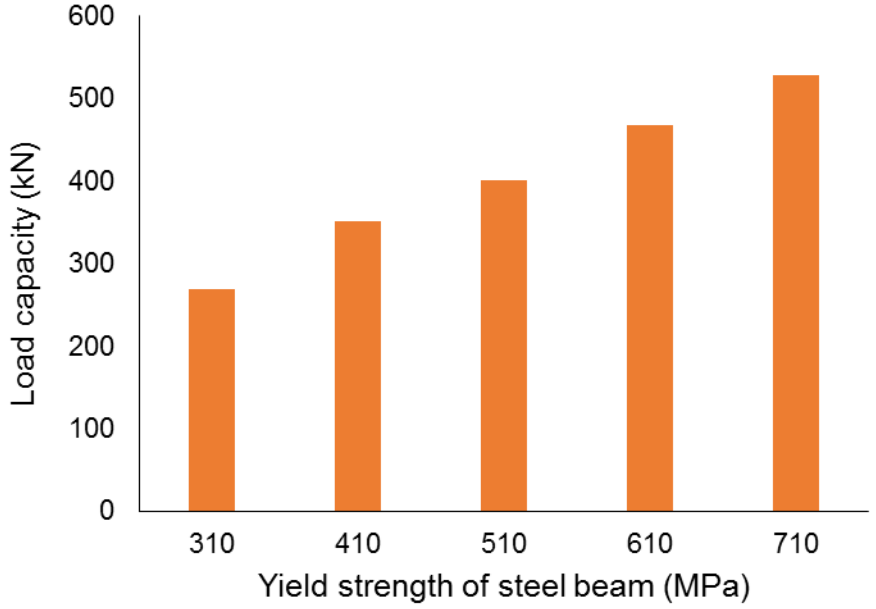

Figure 6-49. Effect of yield strength of steel beam on load capacity

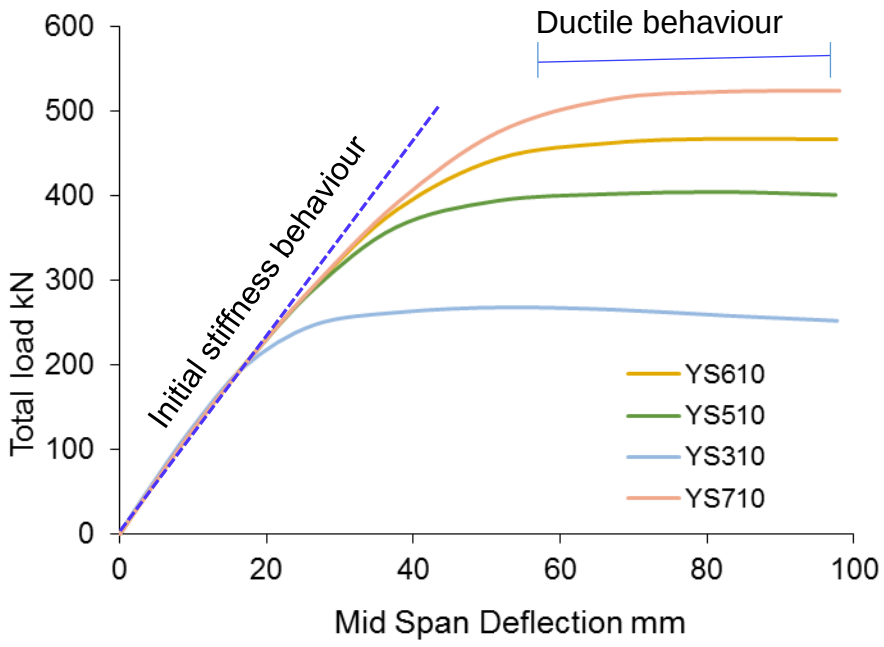

Figure 6-50 Effect of yield stress on initial stiffness

6.10.4 Effect of steel beam depth

A comparison of the effect of the depth of the steel beam is presented in Figure 6-51. It can be seen in Figures 6-51 and 6-52 that the ultimate load carrying capacity and stiffness increased about 78% and 114% respectively with the increase of depth of the steel beam from 300 to 500, but the ductility decreased slightly as shown in Figure 6-53. This indicated that the depth of a steel section has a significant effect on the load bearing capacity and stiffness of the composite beam.

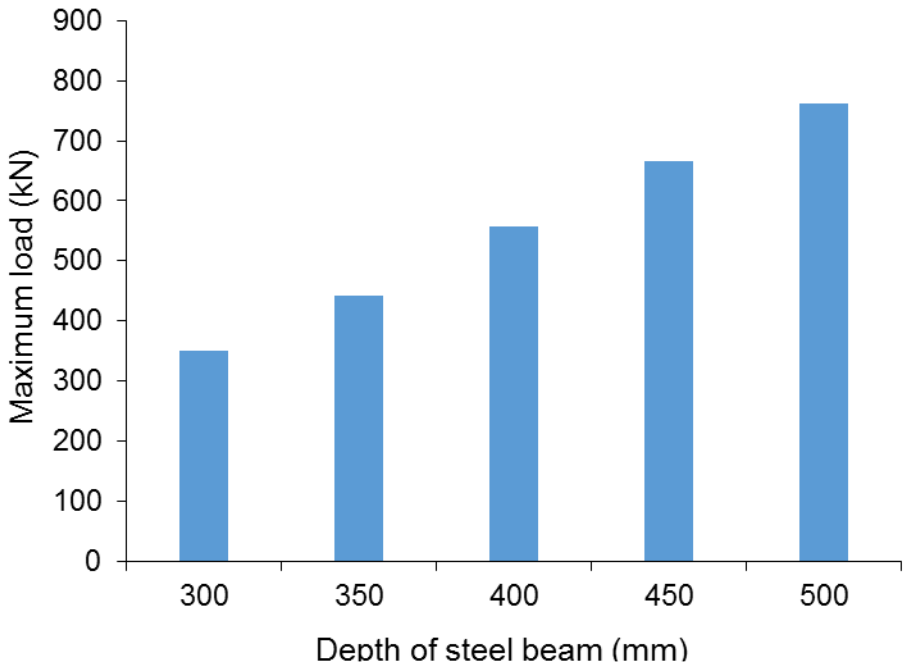

Figure 6-51 Effect of the depth of steel section on composite beam load capacity

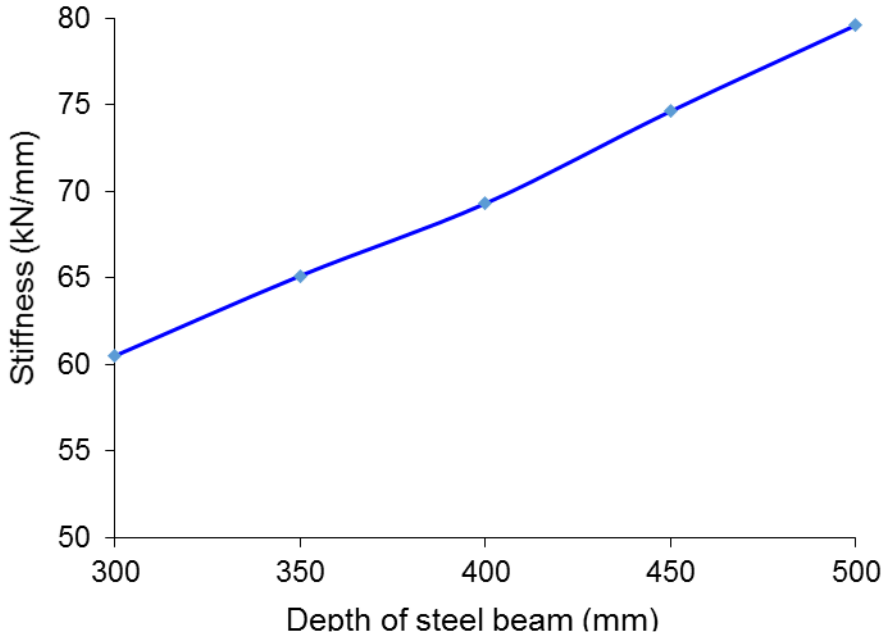

Figure 6-52 Effect of the depth of steel section on the stiffness of the composite beam system

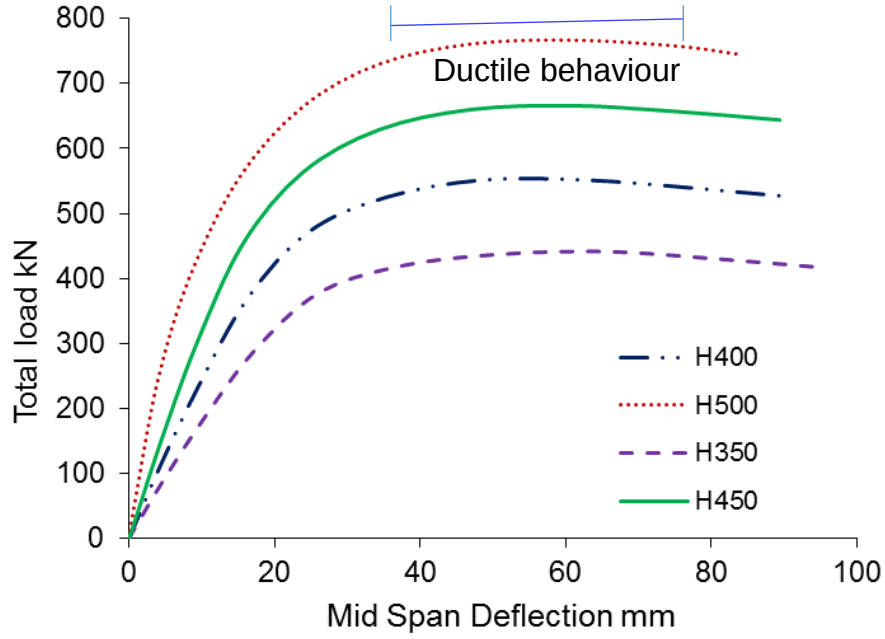

Figure 6-53 Effect of steel section on ductile behaviour

6.10.5 Effect of number of connectors and spacing

The number of shear connectors per trough affected the ultimate moment capacity of the composite beam system as presented in Table 6-9. It can be seen that the ultimate load carrying capacity increased about 25% by using

two shear connectors in each trough compared with using single shear connectors per trough. The parametric studies indicated that the use of shear connectors in composite construction can increase the load bearing capacity of a composite beam about 26% by using paired connectors in each trough

The transverse spacing of 40, 80 and 115 were tried. It was noted that the increase in transverse spacing does not have any significant effect on load carrying capacity.

6.11 Conclusions

Nonlinear finite element models were developed to investigate the behaviour of a demountable shear connector in a composite slab using a metal deck and the structural behaviour of composite beam systems. The following conclusions can be made from the parametric studies.

- The FE analysis indicated that the shear connection capacity can be increased about 8%, if the transverse spacing between two connectors is increased from 5 times to 16 times the diameter of the connector.
- Dynamic Explicit technique can be used to solve the static problem by applying the load slowly and explicit analysis is very efficient for solving discontinuous non-linear and contact problems, so this technique is appropriate for simulation of the push out test with demountable shear connectors.
- Hole clearance did not have any effect on ultimate shear capacity of the shear connection.

- The load bearing capacity can be increased to about 21%, if the compressive strength of concrete is increased from C30/37 to C50/60 strength.
- The finite element model predicted very similar behaviour as observed in the experimental work. FE modelling is an efficient technique used for parametric study.
- The stiffness of a composite beam can be increased to 114%, if the depth of the steel section is increased from 300mm to 500mm
- The experimental and finite element model results show that the demountable composite floor system has a comparable behaviour to non - demountable composite beam system.

Chapter 7
Theoretical comparison of test results

7.1 Introduction

Currently there is no specific assessment method available for demountable shear connectors. The methods available for welded headed shear connectors in Eurocode 4 (2004) and AISC360-10 (2010) are considered in this study. Eurocode 3 (2005) provides an equation for steel connection and ACI 318-08 (2008) provides the equations for anchors in concrete these are also considered for analysing the experimental and finite element results. The equations are summarised in Table 7-1.

Table 7-1 A review of design codes

Codes	Expression	
EC4	$\mathrm{P_{rd,C}} = 0.29\alpha \mathrm{d}^2 \sqrt{\mathrm{f_{ck} E_{cm}}} \,/\, \gamma_\mathrm{v}$	(7-1)
	$\mathrm{P_{rd,S}} = 0.8 \mathrm{f_u} \dfrac{\pi \mathrm{d}^2}{4} \,/\, \gamma_\mathrm{v}$	(7-2)
	$\mathrm{K_t} = \dfrac{0.7}{\sqrt{\mathrm{n_r}}} \dfrac{\mathrm{b_o}}{\mathrm{h_p}} \left[\dfrac{\mathrm{h_{sc}}}{\mathrm{h_p}} - 1 \right] \leq 0.85 \text{ for } \mathrm{n_r} = 1 \text{ and } 0.7 \text{ for } \mathrm{n_r} = 2$	(7-3)
EC3	$F_{v,Rd} = \alpha_v f_{ub} A$	(7-4)
AISC 360-10	$Q_n = 0.5 A_{sa} \sqrt{f_c^{/} E_c} \leq R_g R_p A_{sa} f_u$	(7-5)
ACI 318-08	$P_{Rd,S} = \varphi A_{se} f_{ut}$	(7-6)
	$P_{Rd,C} = k_{cp}\ k \sqrt{f_c^{/}}\ (h_{ef})^{1.5}$	(7-7)

A combination of Eurocode 4 and 3 is used to predict the shear capacity of the demountable shear connectors in this study. The use of these equations is illustrated in Figure 7-1 according to different modes of failure.

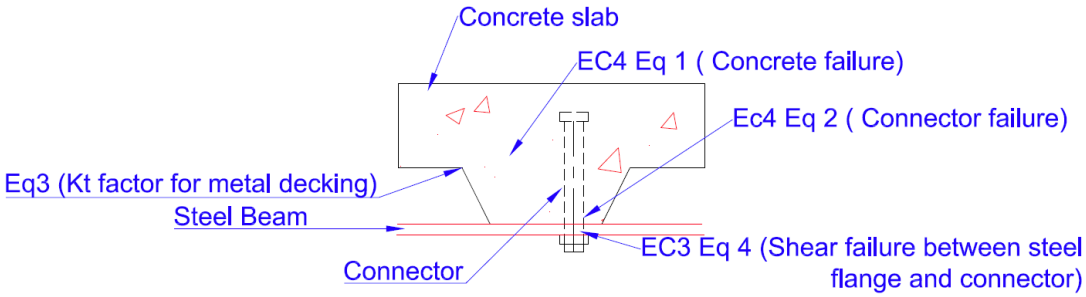

Figure 7-1 Application of EC4 and EC3 on different failure modes

α = $3 \leq \frac{h_{sc}}{d} \leq 4, \alpha = 0.2 \left(\frac{h_{sc}}{d} + 1\right); \frac{h_{sc}}{d} > 4, \alpha = 1.$

d = the diameter of the connector,

f_{ck} = $0.8\, f_{cu}$ is the characteristic cylinder strength of the concrete (MPa).

E_{cm} = $22000 \left(\frac{f_{cm}}{10}\right)^{0.3}$ is the secant modulus of elasticity between 0 and $0.4 f_{cm}$.

f_{cm} = $f_{ck} + 8\ (MPa)$

γ_v = 1 is the partial safety factor

f_u = is the ultimate tensile strength of the shear connector not greater than 500 MPa.

h_p = is deck height,

b_o = is the effective width of a trough

n_r = is the number of stud connectors per trough

h_{sc} = is the overall nominal height of the stud.

A = is the gross cross sectional area of the bolt, when the shear plane passes through the unthreaded part of the connector.

f_{ub} = is the tensile strength of bolt (MPa)

α_v = 0.6 for class Gr. 4.6, 5.6 and 8.8.

A_{sa} = is the cross-sectional area of the steel headed shear stud anchor (mm2),

f'_c = is the specified compressive cylinder strength of concrete (Psi),

E_c = $[0.043\, w_c^{1.5} \sqrt{f_c'}$ (MPa)], is the modulus of elasticity of concrete;

Wc = is the unit weight of concrete slab, 1500 ≤ Wc ≤ 2400 kg/m3.

f_u = is the specified minimum tensile strength of a steel headed stud anchor (MPa).

Rg and Rp are the group (number of studs) and position factors respectively.

Rg = 1.0 for one steel headed stud anchor welded in a steel deck rib with deck oriented perpendicular to the steel shape.

Rg = 0.85 for two steel headed stud anchors welded in a steel deck rib with deck oriented perpendicular to steel shape.

Rp = 0.75 for steel headed anchors welded in a composite slab with the deck oriented perpendicular to the beam and emid-ht ≥ 2 in. (50mm).

Rp = 0.60 for steel headed anchors welded in a composite slab with the deck oriented perpendicular to the beam and emid-ht < 2 in. (50mm).

The abbreviations PRd,C stand for concrete failure mode and PRd,S for connector failure mode.

A_{se} = is the effective cross-sectional area of the anchor for threaded bolts.

f_{ut} = is specific tensile strength of an anchor.

φ = is the strength reduction factor for anchor in concrete equal to 0.65

k_{cp} = is the coefficient for pry-out strength, which is 1.0 for $h_{ef} < 63.5\,mm$ and 2 for $h_{ef} > 63.5\,mm$

h_{ef} = is the effective anchor embedment depth.

k = is the coefficient for concrete breakout tensile strength, which is 24 for cast in anchor and 17 for post install anchor.

7.2 Push off tests

The results obtained from the experimental push off tests are compared with strength prediction methods as provided in Eurocodes 4 and 3, AISC 360-10 and ACI 318-08 to see how well these methods can estimate the shear capacity of demountable shear connectors.

The Eurocodes slightly underestimated the shear resistance of demountable shear connectors regardless of shear connector failure and concrete failure in the specimens with modified reinforcement cages. The AISC 360-10 code

overestimated the shear resistance of demountable shear connectors in both concrete and connector shear failure, except in the case of specimens with high concrete strength, which is about 5% lower than the experimental value of the shear resistance of the demountable connector. The ACI 318-08 method was found to be conservative for high strength concrete and for a single shear connector per trough specimens and slightly overestimated the capacity for lower concrete strength specimens with two connectors per trough.

According to the comparison and analysis, the Eurocodes were found to be more accurate regarding the failure mode prediction than the AISC 360-10 and ACI 318-08. Therefore, a combination of Eurocode 3 and 4 is proposed in this research which can be used to predict the shear resistance of demountable shear connectors with reasonable accuracy. This suggestion is based on the statistical analysis of the experimental and finite element model results as presented in Tables 7-2 and 7-5 in which the coefficient of variance was found to be 17% and 6% for the experimental and finite element model against Eurocodes prediction of shear strength.

It was observed in the experimental results that the shear capacity of the paired connector specimen is about 87% of the single connector specimens. The experimental results show that the shear capacity of specimens with a single connector per trough is about $0.7A_sF_u$, here A_s is the area of a shear connector and F_u is the ultimate strength of the shear connectors. Where as $0.67A_sF_u$ for high concrete strength with a pair of shear connectors specimen.

Table 7-2 Comparison with Eurocode 4 and 3

ID	Experiment		Combine EC4+3				
	P_{Test} (kN/Stud)		P_{Rd} (kN/Stud)				
	Max. Load	Failure	$P_{rd,C}$	$P_{rd,S}$	$F_{v,Rd}$	P_{Rd}	P_{Rd}/P_{Test}
S1	60.0	Concrete	94.9	90.8	68.1	68.1	1.13
S2	44.5	Concrete	91.8	90.8	68.1	68.1	1.5
D1	61.5	Concrete	62.6	90.8	68.1	62.6	1.01
D2	42.2	Concrete	54.6	90.8	68.1	54.6	1.29
M1	69.9	Stud	79.6	90.8	68.1	68.1	0.97
M2	68.2	Stud	76.8	90.8	68.1	68.1	0.99
M3	80.0	Stud	77.8	90.8	68.1	68.1	0.85
M4	79.6	Stud	86.4	90.8	68.1	68.1	0.85
M5	76.1	Stud	93.0	90.8	68.1	68.1	0.89
M6	82.6	Stud	95.6	90.8	68.1	68.1	0.82
M7	66.3	Concrete	59.3	150.8	113.1	59.3	0.89
M8	63.5	Concrete	53.6	209.5	117.6	53.6	0.85
M9	80.9	Concrete	80.2	150.8	113.1	80.2	0.99
M10	87.7	Concrete	81.6	209.5	117.6	80.6	0.93
W1*	61	Concrete	58.9	90.8	68.1	58.9	0.97
Average							1.01
St.Dev.							0.18
COV							17%

W= welded stud, * Ref [Jayas and Hosain, 1988]

Table 7-3 Comparison with AISC 360-10

ID	Experiment		AISC			
	P_{Test} (kN/Stud)		P_{Rd} (kN/Stud)			
	Max. Load	Failure	$Q_{n\,C}$	$Q_{n\,S}$	Q_n	Q_n/P_{Test}
S1	60.0	Concrete	178.0	72.3	72.3	1.20
S2	44.5	Concrete	171.0	72.3	72.3	1.62
D1	61.5	Concrete	107.6	72.3	72.3	1.17
D2	42.2	Concrete	105.1	72.3	72.3	1.71
M1	69.9	Stud	144.2	72.3	72.3	1.03
M2	68.2	Stud	137.9	72.3	72.3	1.07
M3	80.0	Stud	125.8	85.1	85.1	1.06
M4	79.6	Stud	110.6	85.1	85.1	1.06
M5	76.1	Stud	173.8	72.3	72.3	0.95
M6	82.6	Stud	179.4	72.3	72.3	0.87
M7	66.3	Concrete	118.8	120.2	118.8	1.79
M8	63.5	Concrete	86.6	392.2	86.6	1.36
M9	80.9	Concrete	176.4	120.2	120.2	1.48
M10	87.7	Concrete	128.7	392.2	128.7	1.47
W1*	61	Concrete	99.8	72.3	72.3	1.18
Average						1.2
St. Dev.						0.28
COV						23%

W= welded stud, * Ref [Jayas and Hosain, 1988]

Table 7-4 Comparison with ACI318-08

ID	Experiment		ACI			
	P_{Test} (kN/Stud)		P_{Rd}(kN/Stud)			
	Max. Load	Failure	$P_{Rd,C}$	$P_{Rd,S}$	P_{Rd}	P_{Rd}/P_{Test}
S1	60.0	Concrete	427.9	73.8	73.8	1.22
S2	44.5	Concrete	416.6	73.8	73.8	1.65
D1	61.5	Concrete	306.0	73.8	73.8	1.19
D2	42.2	Concrete	273.5	73.8	73.8	1.74
M1	69.9	Stud	371.7	73.8	73.8	1.05
M2	68.2	Stud	360.9	73.8	73.8	1.09
M3	80.0	Stud	311.6	73.8	73.8	0.92
M4	79.6	Stud	339.5	73.8	73.8	0.92
M5	76.1	Stud	421.1	73.8	73.8	0.96
M6	82.6	Stud	430.1	73.8	73.8	0.89
M7	66.3	Concrete	268.8	122.5	122.5	1.84
M8	63.5	Concrete	247.2	399.9	247.2	3.89
M9	80.9	Concrete	425.3	122.5	122.5	1.51
M10	87.7	Concrete	427.2	399.9	399.9	4.56
W1*	61	Concrete	291.1	73.8	73.8	1.2
Average						1.6
						1.06
COV						66%

7.2.1 FE model results against design codes

The capacity of the shear connections obtained from the FE push off model through parametric studies are compared with the design strength equations as provided in Eurocode 4 and Eurocode3.

Table 7-5 Parametric study results

Group	Specimen	P_{FE} (KN)	EC4 + 3			P_{Rd}(KN)	P_{Rd}/P_{FE}
			$P_{rd,C}$(KN)	$P_{rd,S}$(KN)	$F_{v,rd}$(KN)		
Group1	G1-1	68.6	56.7	90.8	68.1	56.7	0.82
	G1-2	69.9	72.7	90.8	68.1	68.1	0.97
	G1-3	71.4	86.9	90.8	68.1	68.1	0.95
	G1-4	73.3	100.0	90.8	68.1	68.1	0.93
Group2	G2-1	69.4	56.7	90.8	68.1	56.7	0.82
	G2-2	72.2	72.7	90.8	68.1	68.1	0.94
	G2-3	73.3	86.9	90.8	68.1	68.1	0.93
	G2-4	73.8	100.0	90.8	68.1	68.1	0.92
Group3	G3-1	64.1	86.9	70.6	53.1	53.1	0.83
	G3-2	67.9	86.9	80.4	60.3	60.3	0.88
	G3-3	73.9	86.9	101.8	76.1	76.1	1.02
	G3-4	74.8	86.9	113.4	85.1	85.1	1.13
Group4	G4-1	71.4	86.9	90.8	68.1	68.1	0.95
	G4-2	71.4	86.9	90.8	68.1	68.1	0.95
Group5	G5-1	69.2	86.9	90.8	68.1	68.1	0.98
	G5-2	69.9	86.9	90.8	68.1	68.1	0.97
	G5-3	72.6	86.9	90.8	68.1	68.1	0.94
	G5-4	73.4	86.9	90.8	68.1	68.1	0.93
	G5-5	73.94	86.9	90.8	68.1	68.1	0.92
	G5-6	74.01	86.9	90.8	68.1	68.1	0.92
Mean							0.95
St. D							0.06
COV							6%

7.3 Composite beam test

7.3.1 Moment capacity

The moment capacity of the composite beam was worked out using rigid plastic theory through rectangular stress blocks for the concrete slab and the steel beam and the interpolation method in accordance with clause 6.2.1.2, EN 1994-1-1 at the mid span of the composite beam. The moment value obtained from the stress block method was about 5% higher than the linear interpolation method. The calculated ultimate moment using the interpolation method was about 6% less than the experimental moment resistance. This indicated the experimental value is very close to the value predicted by the stress block method.

7.3.2 Calculation of moment resistance using stress blocks

The shear capacity of a single shear connector was found to be approximately 39 kN from the push off tests. This value was used to determine the degree of shear connection (η) in the composite beam by using equation 7-8, 7-9 and 7-10.

$$\eta = \frac{N_c}{\min(N_a, N_{c,f})} \tag{7-8}$$

$$N_{c,f} = 0.85 * f_{ck} * B_{eff} * \left(h_s - h_p\right) \tag{7-9}$$

$$N_a = f_y * A_a \tag{7-10}$$

where N_a, is the tensile capacity of the steel section, $N_c (= 10 * 39\ kN)$ is the shear resistance of shear connectors in a shear span and $N_{c,f}$ the capacity of compression force in concrete.

The effect of reinforcement and profiled metal decking was ignored to simplify the calculations. The calculation of the ultimate moment resistance of the composite beam was based on the plastic neutral axis (PNA). The PNA was worked out by balancing the forces in the concrete slab and the steel section. The values of strain (Ɛ) as shown in Figure 7-2 were used to work out the stresses (σ) in the steel top flange and the upper half of the web (Tw) as these parts of the steel section have not yielded. Equations 7-11 and 7-12 were considered to work out the forces in these parts of the steel section. The values of stresses in the bottom half of the web and bottom flange parts were considered fully yielded. The Young modulus (E) of the steel section was assumed to be 210 GPa.

Equation 7-13 presents the forces in the concrete slab due to partial shear connection. The ultimate moment capacity was worked out through equation 7-14 and using the PNA as a centre line of equilibrium.

$$Stress\ (\sigma) = \frac{Force}{Area} \tag{7-11}$$

$$E = \frac{\sigma}{\varepsilon} \tag{7-12}$$

$$\mathrm{F_c} = \eta * (\mathrm{h_s} - \mathrm{h_p}) * \mathrm{b_{eff}} * \mathrm{f_{ck}} \tag{7-13}$$

$$\mathrm{M_u} = \mathrm{Fc} * \left(\frac{\mathrm{hs}}{2} + \mathrm{tf} + \mathrm{Tw1}\right) + \mathrm{FTf} * \left(\frac{\mathrm{tf}}{2} + \mathrm{Tw1}\right) + \mathrm{FTw1} * \left(\frac{\mathrm{Tw1}}{2}\right) + \mathrm{FTw2} * \left(\frac{\mathrm{Tw2}}{2}\right) + \mathrm{FBw} * \left(\mathrm{Tw2} + \frac{\mathrm{Bw}}{2}\right) + \mathrm{FBf} * \left(\frac{\mathrm{tf}}{2} + \mathrm{Tw2} + \mathrm{Bw}\right) \quad (7\text{-}14)$$

where $\mathrm{M_u}$ is the ultimate moment capacity Fc is the force in concrete Beff is the effective width of concrete FTf, ($\mathrm{FTw1}$ and $\mathrm{FTw2}$), FBw and FBf are the forces in the steel top flange, top web (Tw), bottom web (Bw) and bottom flange respectively. The height of the upper half of the web and bottom half of the web is represented by Tw and Bw respectively. $\mathrm{Tw1}$ is the height of the web part from PNA to the top flange, $\mathrm{Tw2}$ is the height of the web from PNA to the centre line (CL) of the steel beam Bw is the height of the web from the centre line of the steel beam to the bottom flange. The thickness of the flange and the web is tf and tw respectively.

7.3.3 Calculation of moment resistance using interpolation method

The moment resistance of the composite floor system was worked out using equation 7-15, 7-16 and 7-17.

$$M_{Rd} = M_{Pl,a,Rd} + \left(M_{Pl,Rd} - M_{Pl,a,Rd}\right) * \eta \quad (7\text{-}15)$$

$$M_{Pl,a,Rd} = N_a \left(h_a + \frac{h_a}{2} - \frac{N_a}{N_{c,f}} \frac{h_s - h_p}{2}\right) \quad (7\text{-}16)$$

$$M_{Pl,a,Rd} = f_y * W_{Ply} \quad (7\text{-}17)$$

where M_{Rd} is moment resistance of composite beam at partial shear connection, $M_{Pl,a,Rd}$ is moment capacity of steel beam, $M_{Pl,Rd}$ is moment capacity at full shear connection and η is degree of shear connection.

The variables, h_a, h_s and h_p represent the height of the steel section, thickness of the concrete slab and he height of the profiled metal decking, respectively.

The comparison of the present study by using the block stress method and interpolation method is shown in Table 7-6. The prediction of moment capacities from both methods is conservative compared to the experimental results. Both methods could be applicable for the design of a demountable composite floor system.

The moment value obtained from the stress block method is about 5% higher than the linear interpolation method. The calculated ultimate moment using the interpolation method is about 7% less than the experimental moment resistance. This indicated the experimental ultimate moment value is very close to the value predicted by the stress block method and it could be used for this type of composite construction.

Table 7-6 Comparison of ultimate moment capacity

Method	Experimental (M_{u_exp})	Block stress method (M_u)	interpolation method (M_{Rd})	M_{u_exp}/ M_u	M_{u_exp}/M_{Rd}
Ultimate moment (kNm)	323.50	317.80	302.28	1.01	1.07

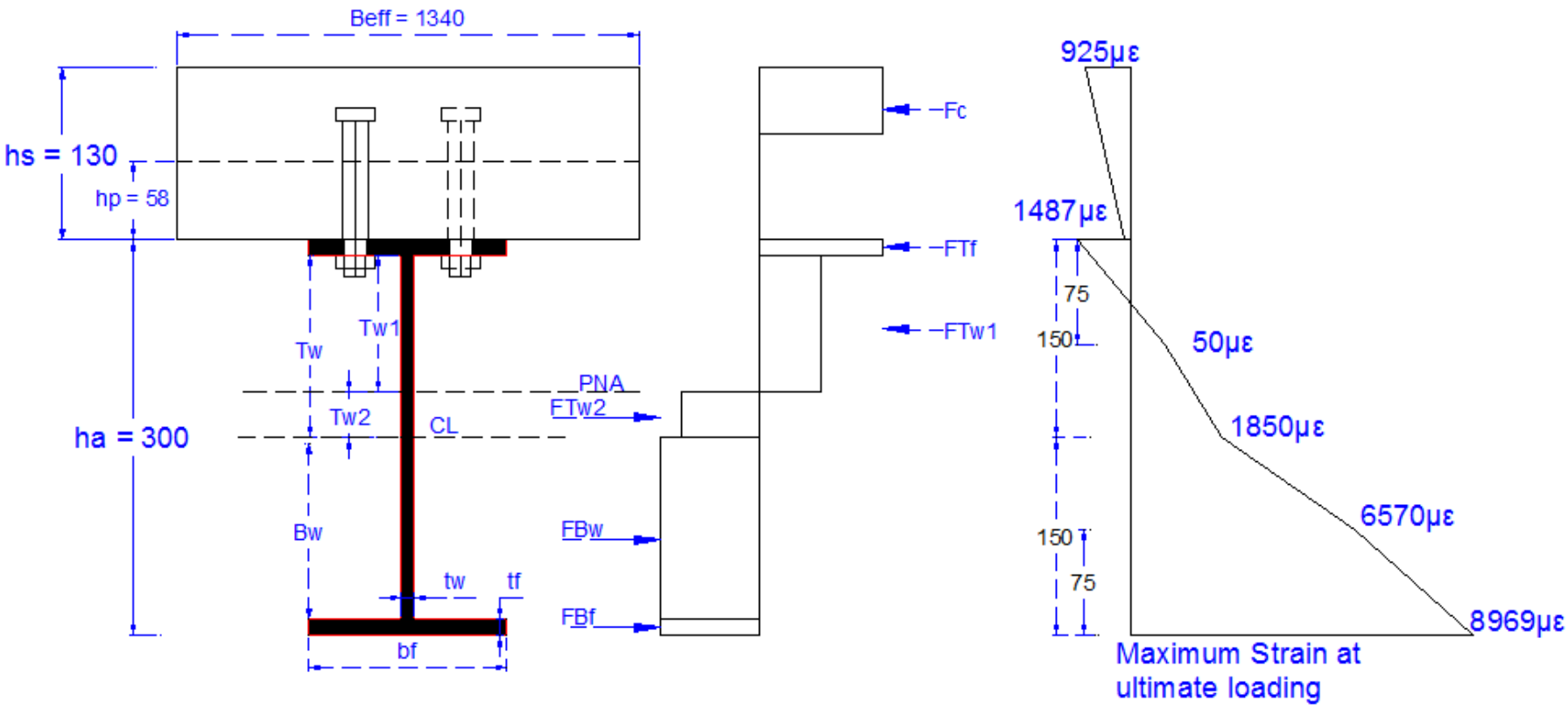

Figure 7-2 Rectangular stress block calculation model for ultimate moment capacity

7.4 Load deflection analysis

A second moment of area of the composite beam is needed for the calculation of the deflection of the composite beam. The second moment of area (I_a) of the steel beam (IPE 300) is found to be 79.98x10^6 mm^4. The second moment of area of the composite section is worked out using equation 7-18 with a modular ration (α_e) of 6 and is found to be 326.08x10^6 mm ^{4}. The vertical deflection (δ) of a composite floor system under two point loading is worked out using equation 7-19.

$$I_{comp} = I_a + \frac{B_e\,(\,h_s - h_p)^3}{12\alpha_e} + \frac{AB_e\,(h_s - h_p)(\,h_a + h_s + h_p)^2}{4[\,A\alpha_e + B_e\,(h_s - h_p)]} \qquad (7\text{-}18)$$

$$\delta = \frac{P_t\, a(3l^2 - 4\,a^2)}{24EI_{comp}} \qquad (7\text{-}19)$$

where B_e is the effective width of the slab and A is the area of the steel section, l is the span of the composite floor span and a is the distance of the point load from the end support.

The deflection of a composite beam is also calculated using BS 5950-3.1:1990 + A1:2010 (British Standard 2010), which provides a method as shown in equation 7-20 for predicting the deflection of a composite beam with partial shear connections in a propped construction for welded shear connectors.

$$\delta = \delta_c + 0.5(1 - \frac{N_a}{N_P})(\delta_s - \delta_c) \qquad (7\text{-}20)$$

$$\delta_c = \frac{P_t\ a(3l^2 - 4\ a^2)}{24EI_{comp}} \quad (7\text{-}21)$$

$$\delta_s = \frac{P_t\ a(3l^2 - 4\ a^2)}{24EI_a} \quad (7\text{-}22)$$

δ_s is the deflection for the steel beam acting alone, N_a is actual number of shear connectors between an intermediate point and the adjacent support and N_p is the number of shear connectors for a positive moment.

The predicted deflection (δ) values of equation 7-19 and 7-20 are presented in Table 7-7. The predicted deflection by equation 7-20 is about 4%, higher and 7% lower than the actual experimental value at 1, 1.5 and 3.0 times the working load respectively. This shows that the equation provided by BS 5950-3.1 could be adopted for demountable composite beams to predict the deflection.

Table 7-7.Comparison of predicted deflection with experimental results

Loading cycle	Pt (kN)	δ Deflection predicted by eq 7-19 (mm)	δ Deflection predicted by eq 7-20 (mm)	δ actual(mm)	δ Deflection predicted by eq 7-19 / δ actual	δ Deflection predicted by eq 7-20 / δ actual
C1-4	18.12	1.39	2.71	2.6	0.53	1.04
C5	27.20	2.09	4.07	3.8	0.55	1.07
C6	54.50	4.19	8.17	8.8	0.48	0.93

7.5 Conclusions

The following conclusions are drawn from analytical analysis.

- A combination of Eurocode 3 and 4 could be used to predict the shear capacity of demountable shear connectors accurately.

- The AISC and ACI codes may be used to assess the shear capacity of demountable shear connectors for connector failure mode.
- The reduction factor Rg in AISC 360-10 is only appropriate for paired demountable shear connector specimens.
- The experimental results show that the shear capacity of specimens with a single connector per trough is about $0.7A_sF_u$.
- The ultimate moment capacity of the demountable composite beam predicted by plastic theory is very close to the experimental results, only about 1% lower than experimental value.
- The experimental deflection of the DCB specimen at 3 times the working load is just 7% higher than the prediction of the deflection equation.
- BS 5950-3.1 could be adopted for demountable composite beams to predict the deflection.

Chapter 8
Conclusions and future work

8.1 Summary

The behaviour of demountable shear connectors in composite structures was investigated in this thesis. Two main methods of investigation, experimental and finite element model were used in this research. Experimental work was conducted using push off technique as explained in chapter 3 and full scale composite beam test which is presented in chapter 5. The finite element analysis was also carried out for deeper understanding of the composite structures using demountable shear connectors in chapter 6.

The experimental part includes the construction and testing of 16 push off tests with demountable shear connectors. The main parameters investigated were the type of reinforcement, type of demountable shear connectors, diameter of connectors, number of connectors in each trough of profiled metal decking and concrete compressive strength. The experimental observation focused on the mode of failures, slip and capacity of shear connection.

Two full scale composite beam tests were also conducted, one with welded shear connectors and the other with demountable shear connectors. The focus of the full scale testing was to carry out a direct comparison between welded and demountable shear connectors in full scale composite beams. The other reason was to evaluate the structural behaviour, moment capacity, deflection, end slips, strain distribution in steel beam and failure modes.

The numerical simulation was also adopted in this research to evaluate the effect of different parameters on the shear capacity, ductility, stiffness and ultimate moment of demountable composite structures. A three dimensional nonlinear finite element model was developed using ABAQUS 6.12 package. The proposed model was validated against the experimental results of the push off tests and composite beam test in the present research.

Finally, a theoretical analysis was carried out to evaluate the available design methods in chapter 7 against experimental and finite element model results. The main aim was to evaluate the applicability of using the available design methods for the prediction of shear capacity, moment capacity and deflection of demountable composite structures.

The main aim of this chapter is to summarize the principal findings of the research carried out in this study and provide a number of recommendations and suggestions for future work.

8.2 Conclusions

The behaviour of demountable shear connectors in composite structures with profiled metal decking have been investigated through experimental and numerical study. The experimental and finite element model results show that the demountable composite beam has a comparable behaviour to non - demountable composite beam system. The following conclusions can be drawn from experimental push off tests.

- The demountable shear connections have high ductility and similar shear capacity and behaviour compared with their equivalent welded shear connectors although the initial stiffness is slightly lower.

- The shear connector arrangement affects the shear connection's behaviour. Connections with a single connector per trough allows the development of full shear resistance of the connector, but specimens with two connectors per trough provides better ductility.
- Concrete strength affects the behaviour of the demountable shear connectors. It appears that the ultimate shear resistance increases with the increase in concrete strength, however the connector's ductility decreases.
- Similar to the welded shear connectors, demountable shear connectors have two main failure modes: connector fracture and concrete crushing.
- The experimental results showed that a combination of Eurocode 3 and 4 could be used to predict the shear capacity of demountable shear connectors accurately. The AISC and ACI codes may be used to assess the shear capacity of demountable shear connectors for connector failure mode. The reduction factor Rg in AISC 360-10 is only appropriate for paired demountable shear connector specimens.
- The experimental results show that the shear capacity of specimens with a single connector per trough is about $0.7A_sF_u$.
- The use of modified reinforcement improves the splitting resistance of a concrete slab and overcomes the possibility of premature failure of the concrete slabs. Therefore, it is recommended to use this for all push-off tests.
- The demountable headed shear connectors have a good potential to be used as an environmental friendly alternative to the welded

headed studs in profiled metal deck composite slabs, which will allow the steel beam to be reused after dismantling.

Full-scale composite beam systems using demountable shear connectors and conventional welded shear connectors were tested to compare the load bearing capacity and deconstructability. The following conclusions may be made from full scale beam test.

- The structural behaviour of the demountable composite floor system was very similar to the composite beam system with conventional welded shear connectors. However, the demountable composite beam showed higher ductility although the initial stiffness was lower.
- The deflection of the DCB specimen at 3 times the normal working load was about span/500 and without any yielding of the steel beam section.
- The ultimate moment capacity of the demountable composite floor predicted by plastic theory is very close to the experimental results, only about 1% lower than the experimental value.
- British standard BS 5950-3.1 could be used for the prediction of the deflection for demountable composite structures.
- Composite beams with demountable shear connectors can be demounted and reused successfully under service loading.

Numerical modelling was also conducted and following conclusions are drawn from finite element modelling.

- The FE analysis indicated that the shear connection capacity in push off tests can be increased about 8%, if the transverse spacing

between two connectors is increased 5 times to 16 times the diameter of the connector.

- Dynamic Explicit technique can be used to solve the static problem by applying the load slowly and explicit analysis is very efficient for solving discontinuous non-linear and contact problems, so this technique is appropriate for simulation of the push out test with demountable shear connectors.
- Hole clearance did not have any effect on ultimate shear capacity of the shear connection.
- The load bearing capacity can be increased to about 21%, if the compressive strength of concrete is increased from C30/37 to C50/60 strength.
- The finite element model predicted very similar behaviour as observed in the experimental work.
- The stiffness of a composite beam can be increased to 114%, if the depth of the steel section is increased from 300mm to 500mm

8.3 Proposed future work

Based on the results obtained from this study, the following recommendations are proposed for future work.

1. The scope of the research conducted in this study is limited to push tests and one beam test with 70 and 60 mm deep profiled metal decking respectively. The recent availability of profiled metal decks as high as 146 mm in the market makes it necessary to conduct some experimental studies involving very deep trapezoidal profiled sheeting and check the shear

resistance of demountable connectors in deep decks against available design code provisions.

2. The experimental data is limited for double connectors in the favourable position. It is suggested that some push tests should be conducted to take into account the effect of the position of the connector within a rib, thickness of the profile metal decking, lightweight concrete, higher number of shear connectors in a rib and larger shear connector spacing.

3. The composite beam tests and companion push tests using different decking profiles 50 mm, 80 mm and 146 mm should be conducted to understand the behaviour of the demountable shear connectors in a beam and a push test, to identify the factors that lead to discrepancy in the results of composite beams and push tests.

4. The finite element model developed in this study can be extended to take into account the lightweight concrete, different sizes of shear connectors, different available profiled metal decking, effect of waveform reinforcement embedded in the concrete slab and fibre reinforced concrete, and parallel sheeting.

5. The experimental data is limited to perpendicular orientation of profiled metal decking. Therefore, composite beam and push test should be conducted using the parallel orientation of profiled metal decking.

6. The long term effect on the relaxation of torque (nut) should be investigated using different types of nut.

7. The optimum torque should be investigated using different torque values in push tests and beam tests.

Reference

ABAQUS. (2012) User's Manual. Version 6.12. Providence, RI, USA: DS SIMULIA Corp, 2012.

ACI 318-08. (2008) Building code requirements for structural concrete, American Concrete Institute, USA.

AISC 360-10. (2010) Specification for Structural Steel Buildings. American Institute of Steel Construction. Chicago, USA.

Akinade, O.O et al. (2016) Design for Deconstruction (DFD): Critial success factors for diverting end-of-life waste from landfills. *Waste Management* 60, p. 3-13. ISSN 0956-053X

Allwood, JM. Cullen, JM and Milford, RL. (2010) Options for Achieving a 50% Cut in Industrial Carbon Emissions by 2050. *Environmental Science and Technology 44, p. 1888–1894.*

Ataei A and Bradford MA. (2014) Finite element analysis of sustainable and deconstructable semi-rigid beam to column composite joints. In *5th ICCM2014. 2014, Structures*, Cambridge, England. p. 585-590.

Ataei A. Bradford MA and Liu X (2016) Experimental study of composite beams having a precast geo polymer concrete slab and deconstructable bolted shear connectors. *Engineering Structures*, V 114 p. 1-13

BS EN ISO 6892-1 (2009): (2009) Metallic materials-tensile testing-Part1: Method of test at ambient temperature.

BS 5950-3.1: 1990 + A1:2010: (2010) Structural use of steelwork in building. British Standards Institution. London

BS EN 1991-1-1: Eurocode 1. 2002. Actions on structures: Part 1-1., in General actions –Densities, self-weight, imposed loads for buildings. London: British Standards Institution.

BS EN 1994-1-1: Eurocode 4. 2004. Design of composite steel and concrete structures: Part 1-1., in General rules and rules for buildings. London: British Standards Institution.

BS EN 1992-1-1: Eurocode 2. 2004. Design of concrete structures: Part 1-1: General rules and rules for buildings. London: British Standards Institution.

BS EN 1993-1-3: Eurocode 3. 2006. Design of steel structures: Part 1-3: General rules and rules for buildings. London: British Standards Institution.

BS EN 1993-1-8: Eurocode 3. 2005. Design of steel structures. Part 1-8: Design of joints. Brussels Belgium: European Committee for standardization (CEN).

Chen Xu, Kunitomo Sugiura, Chong Wu and Qingtian Su. 2012. Parametric static analysis on group studs with typical push out tests. *Journal of Constructional Steel Research*, 72 p.84-96

Dai X., Lam D. and Saveri E. 2015. Effect of Concrete Strength and Stud Collar Size to Shear Capacity of Demountable Shear Connectors. *Journal of Structural Engineering.* **141**(11).

Dallam LN. 1968. High Strength Bolt Shear Connectors - Pushout Tests. *ACI Journal*, Proceeding (No.9): p. 767-769.

Dedic DJ. and Klaiber WF. 1984. High Strength Bolts as Shear Connectors In Rehabilitation Work. *Concrete International*. 6(7): p. 41-46.

Ellobody E. and Lam D. 2002. Modelling of headed stud in steel precast composite beams. *Steel and Composite Structures*. 2(5): P355-378

Ellobody E. and Young B. 2006. Performance of shear connection in composite beams with profiled steel sheeting. *Journal of Constructional Steel Research*. 62(7), pp. 682-694.

Ellobody E. Young B. and Lam D. 2006. Behaviour of normal and high strength concrete-filled compact steel tube circular stub columns. *Journal of Constructional Steel Research,* 62(7), pp.707-715.

Fisher, J.W. 1970. Design of Composite Beams wit h Formed Metal Deck. *Engineering Journal, AISC,* **7**(3), pp.88-96.

Grant, J.A., Fisher, J.W. and Slutter, R.G. 1977. Composite Beams with Formed Steel Deck. *Engineering Journal, AISC*, **14**(1), pp.24-43.

Hawkins N. 1987**.** Strength in shear and tension of cast in place anchor bolts. *Anchorage to Concrete, SP-103. American Concrete Institute*, Detroit, MI pp. 233-55.

Hawkins, N.M. and Mitchell, D. 1984. Seismic Response of Composite Shear Connections. *Journal of Structural Engineering, ASCE,* **110**(9), pp.2120-2136.

Hegger J. and Goralski C. 2006. Structural behaviour of partially concrete encased composite sections with high strength concrete. *Composite Construction in Steel and Concrete*. p. 346-355

Henderson I., Mirza O., Zhu X. and Uy B. 2012. Dynamic assessment of composite structures with different shear connection system. ASCCS 2012

Tenth International Conference on Steel -Concrete Composite and Hybrid Structures. Singapore.

Hicks, SJ. 2009. Strength and ductility of headed stud connectors welded in modern profiled steel sheeting. *Structural Engineering international*. 19(4): pp. 415-419.

Jayas BS. and Hosain MU. 1988. Behaviour of Headed Studs in Composite Beams: Push-Out Tests. *Canadian Journal of Civil Engineering*, 15(2), pp.240-253.

Kwon G. Engelhardt MD and Klingner R. 2010. Behaviour of post-installed shear connectors under static and fatigue loading. Journal of *Constructional Steel Research*. 66(4): pp. 532-41

Lam D. and Ellobody E. 2005. Behaviour of Headed Stud Shear Connectors in Composite Beam. *Journal of Structural Engineering*, ASCE. 131(1): pp. 96-108.

Lam D. and Saveri E. 2012. Shear Capacity of Demountable Shear Connectors. *Proceeding of 10th International Conference on Advances in Steel Concrete Composite and Hybrid Structures*. Singapore.

Lee M. and Bradford MA. 2013. Sustainable composite beam behaviour with deconstructable bolted shear connectors. *Proceeding of the Composite Construction in Steel and Concrete* VII.

Marshall WT, Nelson HM and Banerjee HK. 1971. An experimental study of the use of high strength friction grip bolts as shear connectors in composite beam. *Journal of Structural Engineering*. 49(4): pp. 171-178

Mirza O., Uy B. and N. Patel. 2010. Behaviour and strength of Shear Connectors Utilising Blind Bolting. *Proceeding of 4th International Conference on Steel and Composite Structures*. Singapore.

Mottram JT. and Johnson RP. 1990. Push tests on studs welded through profiled steel sheeting. *Journal of Structural Engineering*. 68(10): p. 187-193.

Moynihan MC. and Allwood J. 2014. Viability and performance of demountable composite connectors. *Journal of Constructional Steel Research*. 99: pp. 47-56.

Ollgaard JG., Slutter RG. and Fisher JW. 1971. Shear strength of stud connectors in lightweight and normal concrete. *Engineering Journal-American Institute of Steel Construction*, AISC. 8(2): p. 55-&.64.

O.Mirza and B.Uy, 2010. Effect of the combination of axial and shear loading on the behaviour of headed stud steel anchors. *Engineering Structures*, 32, p. 93-105

Pallares L. and Hajjar JF. 2010. Headed steel stud anchors in composite structures. Part I: Shear. *Journal of Constructional Steel Research*. 66(2): pp. 198–212.

Pathirana S., Mirza O., Zhu X. and Uy B. 2012. Experimental study on the behaviour of composite steel concrete beams using blind bolts. *Tenth International Conference on Steel -Concrete Composite and Hybrid Structures.* Singapore.

Pathirana S., Mirza O., Zhu X. and Uy B. 2016. Flexural behaviour of composite steel concrete beams utilising blind bolt shear connectors. *Engineering Structures*, 114 p.181-194

Pavlović M., Marković Z., Veljković M. and BuĎevac D. 2013. Bolted shear connectors vs. headed studs behaviour in push-out tests. *Journal of Constructional Steel Research*, 2013. **88**(0): p. 134-149.

Pavlović M., Spremić M., Marković Z., and Veljković M. 2013. Headed shear studs versus high-strength bolts in prefabricated composite decks. *Proceedings of the 2013 Composite Construction in Steel and Concrete* VII.

Qureshi J. and Lam D. 2012. Behaviour of Headed Shear Stud in Composite Beams with Profiled Metal Decking. *Advances in Structural Engineering*. 15(9): pp. 1547-1558.

Qureshi J., Lam D. and Ye J. 2011. Effect of shear connector spacing and layout on the shear connector capacity in composite beams. *Journal of Constructional Steel Research.* 67(4): pp. 706-719.

Qureshi J., Lam D. and Ye J. 2011. The influence of profiled sheeting thickness and shear connector's position on strength and ductility of headed shear connector. *Engineering Structures*. 33(5): pp. 1643-1656.

Rowe M. and Bradford MA. 2012. Partial shear interaction in deconstruct able steel-concrete composite beams with bolted shear connectors. *Proceedings of Design, Fabrication and Economy of Metal Structures Conference*. pp. 585-590

Shariati M., Ramli Sulong NH., Suhatril M., Shariati A., Arabnejad Khanouki MM. and Sinaei H. 2012. Behaviour of C-shaped angle shear connectors under monotonic and fully reversed cyclic loading: An experimental study. *Materials & Design*. 41(0): pp. 67-73.

Schaap BA. 2004. Methods to develop composite action in non-composite bridge floor systems: Part I. MSc thesis. The University of Texas at Austin. pp. 280.

Appendix A: (The publications from the PhD research)

Journal

N. Rehman, D. Lam, X. Dai and A.F. Ashour. “Experimental study on demountable shear connectors in composite slabs with profiled decking,” Journal of Constructional Steel Research, volume.122, July 2016, pages 178-189.

N. Rehman, D. Lam, X. Dai and A.F. Ashour. “Testing of composite beam with demountable shear connectors,” Journal of Structures and Buildings (ICE) (In Press)

D. Lam, X. Dai, A.F. Ashour and N. Rehman. “Recent research on composite beams with demountable shear connectors,” Steel Construction, volume.10, May 2017, pages 125-134. ISSN 1867-0520

Conferences

D. Lam, X. Dai, A.F. Ashour and N. Rehman. “Behaviour of demountable shear connectors in composite beams with profiled metal decking,” 8th international conference on advances in steel structures, LISBON, Portugal, July 22-24, 2015.

N. Rehman, D. Lam, X. Dai and A.F. Ashour. “Behaviour of demountable shear connectors in composite beams,” Young Researcher Conference 2015, London 4th April 2015.

N. Rehman, D. Lam, X. Dai and A.F. Ashour. “Deconstructable composite floor system with metal profiled decking,” Young Researcher Conference 2016, London 6th April 2016.

Appendix B: (Calculations)

Degree of shear connection

$\eta = \frac{N_c}{\min(N_a, N_{c,f})}$ $\eta = \frac{N_c}{\min(N_a, N_{c,f})} = \frac{10 * 39}{2205.8} = 0.18$ = 18% degree of shear connection	(7-8)
$N_{c,f} = f_{ck} * B_{eff} * (h_s - h_p)$ = 29*1340*(130 – 58)*10^{-3} = 2797.9 kN	(7-9)
$N_a = f_y * A_a$ = 410 * 5380* 10^{-3} = 2205.8 kN	(7-10)

Calculation for moment using stress block method

$Stress\ (\sigma) = \frac{Force}{Area}$	(7-11)
$E = \frac{\sigma}{\varepsilon}$	(7-12)
$F_c = \eta * (h_s - h_p) * b_{eff} * f_{ck}$ = 0.18 * (72) * 1340 * 29 = 503.6kN Forces in top flange of steel beam. $FTf = Stress * Area = (Young\ modulus * strain) * Area$ $= (210\ 000) * (1487) * (10.7 * 150)10^{-9}$ = 501.2 kN Forces in upper half upper half of the web of steel beam $FTw1 = Stress * \frac{1}{2} Area = (Young\ modulus * strain) * \frac{1}{2} Area$ $= (210\ 000) * (50) * (7.1 * 139.3/2)10^{-9}$ = 5.2 kN $FTw2 = Stress * \frac{1}{2} Area = (Young\ modulus * strain) * \frac{1}{2} Area$ $= (210\ 000) * (1850) * (7.1 * 139.3/2)10^{-9}$ = 192.1 kN In the bottom half of the steel beam. The Yield strength of 410MPa is	(7-13)

used as steel is fully yielded.

Forces in bottom of the web.

$$\text{FBw} = \text{Yield Stress} * \text{Area} = 410 * (7.1 * 139.3)10^{-3}$$

= 405.5 kN

Forces in bottom flange

$$\text{FBf} = \text{Yield Stress} * \text{Area} = 410 * (10.7 * 150)10^{-3}$$

= 658.05kN

Balancing the forces along the central line of steel beam to work out the PNA

503.6+501.2+5.2 + 192.1 = 405.5 + 658.05

1202.1 = 1063.55

The difference in forces at centre line is 138.55 kN. So half of 138.55 kN force is needed to add in bottom half of steel beam. Which is 69.3kN.

Force = 69.3kN

Stress at the middle of steel web is 388.5MPa. Height of the PNA from central line can be determined using following equation

Area = Force / Stress

Height * width = Force / Stress

Height = Force / (Width * Stress)

= 69.3 / (7.1 * 388.5)*10^3

= 25.0 mm

Above the centre line of steel beam. Now taking the moment at neutral axis.

$M_u = Fc * \left(\frac{hs - hp}{2} + hp + tf + Tw1\right) + FTf * \left(\frac{tf}{2} + Tw1\right) + FTw1 * \left(\frac{Tw1}{2}\right)$ $+ FTw2 * \left(\frac{Tw2}{2}\right) + FBw * \left(Tw2 + \frac{Bw}{2}\right) + FBf$ $* \left(\frac{tf}{2} + Tw2 + Bw\right)$ = [503.6*(199.9)+501.2*(119.55)+5.2*(79.375)+192.1*(22.275)+192.1*(12.55) +405.5*(94.75) +658*(169.75)]*10^{-3} = 317.8 kNm	(7-14)

$M_{Rd} = M_{Pl,a,Rd} + \left(M_{Pl,Rd} - M_{Pl,a,Rd}\right) * \eta$ =246.8 + (555.0 – 246.8) x 0.18 = 302.28 kNm	(7-15)
$M_{Pl,Rd} = N_a \left(h_s + \frac{h_a}{2} - \frac{N_a}{N_{c,f}} \frac{h_s - h_p}{2}\right)$ $2205.8 \left(130 + \frac{300}{2} - \frac{2205.8}{2797.9} \frac{130 - 58}{2}\right)$ = 555.0 kNm	(7-16)
$M_{Pl,a,Rd} = f_y * W_{Ply}$ = 410 x 602 x10^{-3}	(7-17)

= 246.8 kNm	

Calculations for deflection are shown below.

$I_{comp} = I_a + \frac{B_e\,(\,h_s - h_p)^3}{12\alpha_e} + \frac{AB_e\,(h_s - h_p)(\,h_a + h_s + h_p)^2}{4[\,A\alpha_e + B_e\,(h_s - h_p)]}$ $79.98\,x10^6 + \frac{1340\,(\,130 - 58)^3}{12x6}$ $+ \frac{5380x1340\,(130 - 58)(\,300 + 130 + 58)^2}{4[\,5380\,x\,6 + 1340\,(130 - 58)]}$ =79.98x10^6 + 246.95x10^6 = 326.9x10^{6}mm^4	(7-18)
$\delta = \frac{P_t\,a(3l^2 - 4\,a^2)}{24EI_{comp}}$ $\frac{18.12x10^3x1900(3x5200^2 - 4x1900^2)}{24x210000x326.9x10^6}$ = 1.39 mm	(7-19)

and 2.09 mm or the point load of 27.2kN 4.19 mm for the point load of 54.5 kN	

$\delta = \delta_c + 0.5(1 - \frac{N_C}{N_t})(\delta_s - \delta_c)$ NC are the number of connectors in the shear span and Nt is total number of connectors = 1.39 +[0.5 *(1- 10 / 26)*(5.69-1.39)] = 2.71 mm for the point load of 18.12 kN and = 2.09 +[0.5 *(1- 10 / 26)*(8.55-2.09)] = 4.07mm for the point load of 27.2 kN = 4.19 +[0.5 *(1- 10 / 26)*(17.12-4.19)] = 8.17mm for 54.50 kN $\delta_c = \frac{P_t\, a(3l^2 - 4\,a^2)}{24EI_{comp}}$ $\frac{18.12x10^3x1900(3x5200^2 - 4x1900^2)}{24x210000x326.9x10^6}$ =1.39mm And	(7-20) (7-21)

2.09 mm for the point load of 27.2 kN 4.19 mm for 54.50 kN	
$\delta_s = \frac{P_t\, a(3l^2 - 4\, a^2)}{24EI_a} = \frac{18.12x10^3x1900(3x5200^2 - \ 4x1900^2)}{24x210000x79.98x10^6}$ = 5.69 mm And is 8.55 mm for the point load of 27.2 kN is 17.12 mm for the point load of 54.5 kN	(7-22)

Back Calculations for degree of shear connection

The experimental moment capacity of the specimen was 323.5kNm

$M_{Rd} = M_{Pl,a,Rd} + \left(M_{Pl,Rd} - M_{Pl,a,Rd}\right) * \eta$
$M_{Pl,Rd} = N_a \left(h_s + \frac{h_a}{2} - \frac{N_a}{N_{c,f}} \frac{h_s - h_p}{2}\right)$ $M_{Pl,Rd} = 2205.8 \left(130 + \frac{300}{2} - \frac{2205.8}{2378.2} \frac{130 - 58}{2}\right)$ $M_{Pl,Rd}$ = 544 kNm
$M_{Pl,a,Rd} = f_y * W_{Ply}$ = 410 x 602 x10^{-3} = 246.8 kNm
$M_{Rd} = 32.5\ kNm$ $\eta = ?$

$M_{Rd} = M_{Pl,a,Rd} + \left(M_{Pl,Rd} - M_{Pl,a,Rd}\right) * \eta$

323.5 = 246.8 + (544 - 246.8) * η

$\eta = \frac{323.5 - 246.8}{544 - 246.8} = 0.26 = 26\%$

Back calculation for stud capacity

$\eta = \frac{N_c}{\min(N_a, N_{c,f})}$
$N_{c,f} = 0.85 * f_{ck} * B_{eff} * (h_s - h_p)$ = 0.85 * 29*1340*(130 – 58)*10^{-3} = 2378.2 kN
$N_a = f_y * A_a$ = 410 * 5380* 10^{-3} = 2205.8 kN

$$\eta = \frac{N_c}{\min(N_a, N_{c,f})}$$

$$N_c = \frac{\eta * \min(N_a, N_{c,f})}{1}$$

$N_c = \eta * N_a$ = 0.26 * 2205.6 = 573.456 kN

Divide by 10 (Number of shear connectors in shear span)

So Stud capacity is 57.3